

**Evaluation of Oxidative Behavior of Polyolefin
Geosynthetics Utilizing Accelerated Aging Tests
Based on Temperature and Pressure**

A Thesis

Submitted to the Faculty

of

Drexel University

by

Mengjia Li

in partial fulfillment of the
requirements for the degree

of

Doctor of Philosophy

April 2005

Dedications

To my family with love.

Acknowledgments

I would like to express my sincere appreciation to the people who have assisted me in the last four years.

First and foremost, I would like to thank my advisor Dr. Y. Grace Hsuan for her valued guidance, advice, and support through the course of this research. She provided me the insight into not only the research projects but also other academic matters, which is invaluable to the rest of my life. I also wish to extend my deep gratitude to Dr. Robert Koerner for his precious advices and instructions. Special thanks are given to Dr. George Koerner for the experimental help in Geosynthetic Research Institute.

I would also like to express my sincere thanks to my colleague, Mr. Jingyu Zhang, Mr. Songtao Liao, and Mr. Lei Lou and other graduate students, for their tremendous help in my experiments and a lot of good discussions. I sincerely thank all other faculty members, staffs, and fellow graduate students in the Department of Civil, Architectural and Environmental Engineering for making my graduate life in Drexel most enjoyable and rewarding.

Finally, I would like to take the chance to thank my family, for their full-heart supports during my Ph.D. study, especially in my hard times.

Table of Contents

List of Tables	vii
List of Figures.....	ix
Abstract.....	xiii
Chapter 1. Background and Literature Review.....	1
1.1 Background.....	1
1.2 Literature Review	4
1.2.1 Accelerating Polyolefin Oxidation with Elevated Temperature Incubation	5
1.2.2 Limitations of Temperature Acceleration Method.....	8
1.2.3 Antioxidant Lifetime Prediction with Temperature Acceleration Method	10
1.2.4 Accelerating Polyolefin Oxidation with Oxygen Pressure Incubation	12
1.3 Objectives	14
Chapter 2. Test Materials, Incubation Apparatus and Procedures, and Evaluation Methods	16
2.1 Test Materials	16
2.2 Incubation Plan	18
2.3 Incubation Apparatus and Procedures	21
2.3.1 Forced Air Ovens.....	21
2.3.2 High Pressure Cells.....	22
2.3.3 Low Pressure Cells	24
2.3.4 Water Baths.....	26
2.4 Degradation Evaluation Test Methods	26
Chapter 3. Antioxidant Depletion of Polypropylene Slit Film Geotextiles under Temperature, Pressure and Water Environments	29
3.1 Introduction.....	29

3.2 Antioxidant Depletion in Elevated Temperatures and High Pressures Incubation (Series I).....	33
3.2.1 Test Results.....	33
3.2.2 Antioxidant Lifetime Prediction	39
3.2.3 Discussion	46
3.3 Antioxidant Depletion in Elevated Temperatures and Low Pressure Incubation (Series II)	51
3.3.1 Test Results.....	51
3.3.2 Discussion	53
3.4 Antioxidant Depletion in Elevated Temperature and Water Environment (Series IV).....	56
3.5 Conclusions.....	58
Chapter 4. Antioxidant Depletion of High Density Polyethylene Geogrids under Temperature, Pressure and Water Environments	61
4.1 Introduction.....	61
4.2 Antioxidant Depletion in Elevated Temperature Aging at Atmospheric Pressure (Series III).....	64
4.2.1 Test Results.....	64
4.2.2 Antioxidant Lifetime Predictions Based on Oven-Aging Data	66
4.3 Antioxidant Depletion in Elevated Temperatures and High Pressures (Series I)	72
4.3.1 Test Results.....	72
4.3.2 Effect of oxygen pressure on OIT.....	74
4.3.3 Antioxidant Lifetime Prediction Based on Aging Data in Elevated Temperatures and High Pressures.....	76
4.3.4 Discussion	80
4.4 Antioxidant Depletion in Elevated Temperature and Water Environment.....	84
4.5 Conclusions.....	87

Chapter 5. Oxidative Behaviors of Polypropylene Nonwoven Geotextiles under Temperature, Pressure and Water Environments	90
5.1 Introduction.....	90
5.2 Oxidative Behaviors in Elevated Temperatures and High Pressures (Series I)	93
5.2.1 Depletion of Antioxidants	93
5.2.2 Tensile Property	96
5.2.3 Discussion – Oxidative Degradation of GT-nw.....	98
5.3 Antioxidant Depletion in Elevated Temperature and Water Environment (Series IV).....	101
5.4 Conclusions.....	104
Chapter 6. Service Lifetime Prediction of Polypropylene Slit Film Geotextiles Utilizing an Accelerated Aging Test Based on Temperature and Pressure	106
6.1 Introduction.....	106
6.2 Experimental – Enhanced Elevated Temperatures & High Pressures (Series I)	111
6.3 Results and Data Analysis	112
6.3.1 Establishing of Stage C Straight Lines and Calculation of Relevant Parameters.....	112
6.3.2 Discussion of Enhanced Pressure and Temperature Effects on AO Depletion and Polyolefin Oxidation Reactions.....	118
6.3.3 Prediction of GT-sf Stage C Half-life at Service Condition	124
6.4 Conclusions.....	134
Chapter 7. Closing Conclusions and Future Study.....	137
7.1 Summary and Conclusions	137
7.2 Future Study.....	142
List of References.....	144
Appendix A. List of Symbols	149
Vita	151

List of Tables

1.1 Expected lifetimes (in years) for various geosynthetics applications	3
2.1 Selected polyolefin-based geosynthetic products	16
2.2 Properties of as-received slit film woven geotextile, GT-sf	17
2.3 Properties of the as-received HDPE geogrid GG-1 and GG-2	17
2.4 Properties of as-received slit film woven geotextile GT-nw	18
2.5 Incubation condition series used in this research program	20
2.6 Sample size for evaluation test for 95% probability level	28
3.1 High pressure incubation environments for aging GT-sf geotextiles	32
3.2 Low pressure incubation environments for aging GT-sf geotextiles.....	33
3.3 Reaction rate constant k (month ⁻¹) under different incubation conditions	38
3.4 Values of constants obtained from calculation of Eq. (3-9)	42
3.5 Predicted lifetime of the antioxidant at different temperatures	45
3.6 Predicted lifetime of the antioxidant at different pressures	45
3.7 Acceleration factor to reach 15% OIT retained using Eq. (3-8)	46
3.8 Rate constant k predicted values vs. measured values	56
4.1 The different environments in two oven-aging incubation series.....	63
4.2 Data used to obtain antioxidant depletion reaction rates	77
4.3 Test data used to obtain four constants in Eq. (4-6)	79
5.1 High Pressure Incubation environments for aging GT-nw geotextiles.....	92
6.1 Incubation Conditions.....	111
6.2 Stage C oxidation rate R_C (%/day).....	116

6.3 Stage C half-life $t_{C-50\%}$ (days)	116
6.4 Stage A/B time for zero property change t_{AO} (days).....	116
6.5 Critical OIT%.....	117
6.6 Pressure shift factors to $P_{ref} = 0.02$ MPa for aging data at high incubation pressures.....	132
7.1 Service lifetime estimation of the four materials based on temperature/pressure incubation test data (unit: years)	138

List of Figures

1.1 Three conceptual stages of polyolefin oxidative degradation.....	2
2.1 Experimental settings inside the oven incubation devices.....	22
2.2 High pressure cells: incubated samples and pressurization system	23
2.3 High pressure cells in incubation ovens.....	23
2.4 Low pressure cells: pressurization system.....	25
2.5 Low pressure cells: incubated samples with fix frames.....	25
2.6 Typical thermal graph illustrating the obtaining of the HP-OIT value.....	27
3.1 Changes in GT-sf properties over time at 55°C under 6.3 MPa air pressure.....	35
3.2 Changes in GT-sf HP-OIT retained over time at 65°C under various pressures ..	35
3.3 Changes in GT-sf MI retained over time at 65°C under various pressures	36
3.4 Changes in GT-sf tensile strength retained over time at 65°C under various pressures.....	36
3.5 GT-sf HP-OIT response under the same oxygen partial pressure at 35°C and 65°C	37
3.6 Arrhenius plots at three constant pressures.....	39
3.7 Activation energy against oxygen pressure	40
3.8 Constant “A” in Eq. 9 plotting against oxygen pressure	41
3.9 The effects of the reaction rate constant in terms of temperature and pressure...	42
3.10 HP-OIT data fitted with model predicted curves of Eq. (3-10) at 65°C	43
3.11 The response surface of antioxidant lifetime in terms of temperature and pressure	44
3.12 Relationship between reaction rate and oxygen pressure	48

3.13 Changes in GT-sf HP-OIT retained over time at 105°C under low pressures	52
3.14 GT-sf HP-OIT response under the same oxygen partial pressure	53
3.15 Exponential trend curves – OIT% vs. time in pure nitrogen	55
3.16 Exponential trend curves – OIT% vs. time in low partial oxygen pressures	55
3.17 Comparisons of antioxidant depletion behaviors of GT-sf in water environment and regular oven aging.....	57
3.18 Comparisons of antioxidant depletion behaviors of GT-sf in water environments and high-pressure oven aging	57
4.1 Dimensions of single-rib geogrid specimen	63
4.2 Changes in material properties versus time for GG-1 at 75°C.....	65
4.3 Changes in material properties versus time for GG-2 at 75°C.....	66
4.4 OIT retained value versus incubation time for GG-1 in Series III at five different oven temperatures	68
4.5 Arrhenius plot of antioxidant reaction rate of GG-1.....	69
4.6 Changes in OIT value versus incubation time for GG-2 in Series III oven aging	71
4.7 Arrhenius plot of the OIT depletion rate of GG-2	71
4.8 Test results for GG-1 specimens aged at 65°C and 6.3MPa oxygen.....	73
4.9 OIT response of GG-1 at same oxygen partial pressure at 35°C & 65°C.....	75
4.10 OIT response curves of GG-1 at different temperatures and oxygen pressures .	75
4.11 Re-plotting Region II of the OIT curves in Figure 4.10	76
4.12 $\ln(R_{OA})$ versus oxygen pressure at 65°C for GG-1	77
4.13 Relationship among $t_{5\%OIT}$, temperature and pressure for GG-1.....	80
4.14 Comparisons of antioxidant depletion behaviors of GG-1 in water environment and regular oven aging.....	86

4.15 Comparisons of antioxidant depletion behaviors of GG-1 in water environments and high-pressure oven aging	86
5.1 Changes in HP-OIT of GT-nw over time in 1-atm circulating air oven at different temperatures	95
5.2 Changes in HP-OIT of GT-nw over time under 6.3 MPa air pressures at different temperatures	95
5.3 Changes in HP-OIT of GT-nw over time at 65°C under different oxygen pressures	96
5.4 GT-nw tensile strength vs. time at 65°C under different pressures	97
5.5 GT-nw tensile elongation vs. time at 65°C under various pressures	98
5.6 Changes in GT-nw properties over time at 65°C under 6.3 MPa oxygen pressure	100
5.7 Changes in HP-OIT of GT-nw in water environments at different temperatures	101
5.8 Changes in GT-nw HP-OIT at 45°C with different aging conditions.....	103
5.9 Changes in GT-nw HP-OIT at 55°C with different aging conditions.....	103
5.10 Changes in GT-nw HP-OIT at 65°C with different aging conditions.....	104
6.1 Typical oxidative degradation curves of PP yarn geotextiles.....	110
6.2 Tensile property changes with the incubation time in 1.3MPa incubation.....	113
6.3 Stage C degradation straight lines in 1.3MPa incubation	113
6.4 GT-sf degradation curves in 105°C, 1.3MPa oxygen incubation	114
6.5 AO Depletion Activation Energy Change for GT-sf in 6.3MPa oxygen incubation	119
6.6 Arrhenius Plots for R_C vs. $1/T$ at different oxygen pressures	122
6.7 R_C vs. Oxygen Pressure at different temperatures	124
6.8 Stage C straight lines plotted against Stage C Age $t' = t - \text{DIT}$ (Linear Coordinate Scale).....	127

6.9 Stage C straight lines plotted against Stage C Age $t' = t-DIT$ (Semi-Log Coordinate Scale).....	128
6.10 Stage C Master Curve Generated by Two-Step TTS Method (For 1.3 MPa oxygen incubation data).....	130
6.11 Stage C Master Curves at reference temperature 10°C for various incubation oxygen pressures.....	130
6.12 Stage C Master Curves at Service Condition.....	132

Abstract

Evaluation of Oxidative Behavior of Polyolefin Geosynthetics Utilizing Accelerated Aging Tests Based on Temperature and Pressure

Mengjia Li

Hsuan, Y. G., Ph.D

Polyolefin geosynthetics are susceptible to oxidation, which eventually leads to the reduction in their engineering properties. In the application of polyolefin geosynthetics, a major issue is an estimate of the materials durability (i.e. service lifetime) under various aging conditions. Antioxidant packages are added to the polyolefin products to extend the induction time, during which antioxidants are gradually depleted and polymer oxidation reactions are prevented.

In this PhD study, an improved laboratory accelerating aging method under elevated and high pressure environments was applied to evaluate the combined effect of temperature and pressure on the depletion of the antioxidants and the oxidation of polymers. Four types of commercial polyolefin geosynthetic materials selected for aging tests included HDPE geogrid, polypropylene woven and nonwoven geotextiles. A total of 33 different temperature/pressure aging conditions were used, with the incubation duration up to 24 months. The applied oven temperature ranged from 35°C to 105°C and the partial oxygen pressure ranged from 0.005 MPa to 6.3 MPa.

Using the Oxidative Induction Time (OIT) test, the antioxidant depletion, which is correlated to the decrease of the OIT value, was found to follow apparent first-order decay. The OIT data also showed that, the antioxidant depletion rate

increased with temperature according to the Arrhenius equation, while under constant temperatures, the rate increased exponentially with the partial pressure of oxygen. A modified Arrhenius model was developed to fit the antioxidant depletion rate as a function of temperature and pressure and to predict the antioxidant lifetime under various field conditions.

This study has developed new temperature/pressure incubation aging test method with lifetime prediction models. Using this new technique, the antioxidant lifetime prediction results are close to regular temperature aging data while the aging duration can be reduced considerably. Using the enhanced aging pressure and temperature with this aging method plus a new analytical methodology utilizing time-temperature-superposition and time-pressure-superposition techniques, the post-antioxidant lifetime (Stage C) of the materials can also be predicted and so a total lifetime for different polyolefin geosynthetics can be evaluated quantitatively.

Chapter 1. Background and Literature Review

1.1 Background

Polyolefins, the most widely used commercial polymers, are a class of organic materials prepared by the polymerization of olefins (hydrocarbons containing one double bond per molecule), especially ethylene and propylene. In the geosynthetic industry, polyolefin denotes synthetic products composed of at least 85 percent by weight of polyethylene (PE) or polypropylene (PP).

The use of polyolefin geosynthetics has been steadily increasing in different areas of civil engineering applications in recent years. The required long service lives of many structures greatly challenge the longevity of the polyolefin geosynthetics, and the endurance properties of this material are always of much concern to civil engineers.

Polymeric materials undergo the adverse effects of an oxidation reaction that can occur at any stage in the life cycle of a polymer. Researchers (Grassie and Scott, 1985; Billingham and Calvert, 1980) have shown that during both processing and service, polyolefins are susceptible to oxidative degradation, which eventually leads to an engineering property reduction caused by polymer chain scission. Oxidation of polyolefins is an auto-accelerating reaction, i.e. the rate accelerates until reaching a constant rate. The antioxidant (AO) is added to delay the onset of oxidation. For a

properly stabilized polyolefin geosynthetic product, the oxidation process normally includes three stages (Fig 1.):

Stage A: antioxidant depletion period; no property changes take place

Stage B: the induction time of oxidation with slow property changes

Stage C: oxidative degradation period with significant property changes

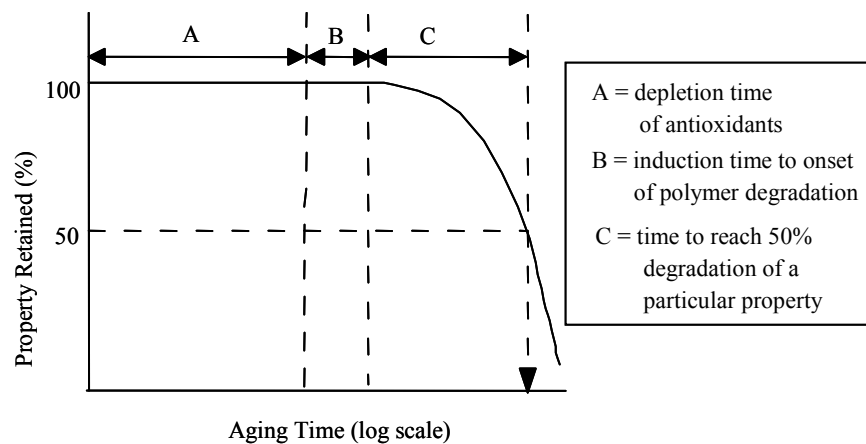


Figure 1.1 Three conceptual stages of polyolefin oxidative degradation (Hsuan and Koerner, 1998)

The service lifetime (half-life) of geosynthetics is often defined as the time it takes to reach 50% of the original properties, e.g. tensile strength at failure or tensile elongation at failure. The typical required lifetimes for various geosynthetics' structure systems are listed in Table 1.1.

While the best way to illustrate the service lifetime of materials is by the case history, the oldest geogrid reinforced retaining wall is about 25 years, and the first

generation of modern landfill lined with geomembranes and geotextiles is about 30 years old. The lifetime assessment of similar products cannot be demonstrated by a case history. Therefore, it is necessary to assess their durability by acceleration tests and to predict the oxidative behavior of the geosynthetics at service conditions.

Table 1.1 Expected lifetimes (in years) for various geosynthetics applications

Geosynthetics-Type	Roads/Drains	Walls/Slopes	Dams/Tunnels	Landfills*
Geotextile/Geogrid	50-100	75-100	100-200	30-1,000
Geomembrane/GCL	N/A	N/A	100-200	30-1,000
Geonet/Geocomposite	N/A	N/A	100-200	30-1,000

*Even to thousands of years for containment of radioactive waste (Koerner, 1998)

In general, the rate of chemical reaction is governed by three parameters, as shown in Equation (1-1) (Morrison and Boyd, 1992):

$$\text{Rate of reaction} = \text{collision frequency} * \text{energy factor} * \text{probability factor} \quad (1-1)$$

The collision frequency depends upon the density of particles (i.e., concentration or pressure of the gas reactant involved in the reaction) and the particle's moving speed (which depends on the temperature). The energy factor is mainly contributed by the temperature. The probability factor is similar for oxidation reactions under different environmental conditions. Thus, regarding the acceleration effects, temperature has the greatest influence, followed by pressure (or concentration).

In this study, the laboratory aging test was designed to utilize both pressure and/or temperature to accelerate the oxidation rate. Incubation environments included pressure/temperature, temperature only and temperature/water. Selected commercial polyolefin geosynthetics were evaluated for their oxidation processes. The incubation durations varied from two days to seven years depending on the incubation condition. Samples were retrieved at various time intervals and evaluated by a number of tests for their physical, chemical and mechanical properties. Test data from each of the incubation environments were compared to identify the individual and combined effects of pressure, temperature and water. In addition, analytical models were developed for extrapolating test data from these accelerated aging conditions to site-specific ambient temperature and pressure conditions and to predict the antioxidant lifetime and the materials service lifetime.

1.2 Literature Review

There is significant amount of publication relating to the aging and degradation of synthetic polymers. There is a Journal dedicated to this area (Polymer Degradation and Stability, by Elsevier). The literature review of this thesis focuses on the oxidative degradation of polyolefins.

1.2.1 Accelerating Polyolefin Oxidation with Elevated Temperature Incubation

The most common approach to accelerating the chemical reactions behind polyolefin oxidative degradation is temperature aging. Specimens are incubated at several elevated temperatures and the degradation is monitored through changes in their physical, chemical or mechanical properties. The data from accelerated temperature aging tests are extrapolated to site temperature by using the Arrhenius equation, which is based on the exponential temperature dependence of the rate of the chemical reaction, i.e.

$$\text{Rate of Reaction} = A \exp\left(-\frac{E_a}{RT}\right) \quad (1-2)$$

Where,

E_a = the Arrhenius activation energy

R = the ideal gas constant, 8.31 kJ/mol-K

T = the absolute temperature (K)

A = the pre-exponential factor, usually considered as a constant

The oxidative degradation process of polyolefins involves a series of chemical reactions which include antioxidant depletion reactions, followed by autoxidation of the polymer; each of these reactions is assumed to follow Arrhenius behavior (Grassie and Scott, 1985). Kinetic analysis of these reactions results in a steady-state rate expression with an Arrhenius temperature dependence, where E_a represents the effective activation energy for the combined reactions underlying the degradation

(Gillen *et al.*, 1996). It is assumed that this combined effective activation energy remains unchanged throughout the temperature range under analysis, such that a linear relationship exists between the logarithm of the half-life (time to 50% material property change), and the inverse of absolute temperature. Most importantly, the linear relationship is assumed extending to the service conditions to be predicted; thus, it can be used for the lifetime prediction of the material's behavior. Koerner *et al.* (1993) proposed a general "Arrhenius model" to predict the mechanical, physical and chemical degradation behaviors of polymeric geosynthetic materials used in long-term applications such as landfill liners and covers, surface impoundments, retaining wall and slope reinforcement, etc. The predicted lifetimes of polyolefin geosynthetic products, including HDPE geomembranes, HDPE geogrids, and woven and nonwoven polypropylene geotextiles, have been reported to be from tens to hundreds of years (Hsuan *et al.*, 1997, 1998, 1999; Salman *et al.*, 1999; Sangam and Row, 2002; and Mueller *et al.*, 2002, 2003).

Another model that has been used to analyze data from temperature acceleration tests is the time-temperature superposition (TTS) method. Ferry (1980) indicated that there is a direct equivalency between time and temperature. This implies that the time over which the degradation process occurs can be reduced by conducting the test at elevated temperatures. The resulting data from elevated temperature tests can then be shifted to lower temperatures to establish a master curve of the material property of interest. A shift factor (a_T) will be established with respect to a reference temperature, and a shift factor (a_T) will be established with respect to each test temperature. There are two models to correlate the shift

factor with temperature. The first model is the Williams-Landel-Ferry (WLF) equation (Ferry, 1980):

$$a_T = \exp \left[\frac{-C_1(T - T_{ref})}{C_2 + (T - T_{ref})} \right] \quad (1-3)$$

Where C_1 and C_2 are constants, T_{ref} is the reference temperature (in K), T is the experimental temperature (in K), and a_T is the shift factor.

The other model commonly used is the Arrhenius equation (Ferry, 1980):

$$a_T = \exp \left[\frac{E_a}{R} \left(\frac{1}{T_{ref}} - \frac{1}{T} \right) \right] \quad (1-4)$$

Where E_a is the reaction activation energy and gas constant $R = 8.31$ kJ/mol-K, T_{ref} is the reference temperature (in K), T is the experimental temperature (in K), and a_T is the shift factor.

The Arrhenius model is more appropriate for polyolefin geosynthetics due to the fact that WLF equation is typically used to describe the time/temperature behavior of polymers near the glass transition temperature T_g region. For polyolefin materials of geosynthetics, this T_g is typically well below 0°C.

Once the series of the temperature shift factor a_T is determined, it can be used to normalize data obtained at various temperatures to a single reference temperature by the relationship,

$$t_{T_{ref}} = a_T t_T \quad (1-5)$$

where, $t_{T_{ref}}$ denotes the aging time at reference temperature T_{ref} , and t_T is the aging time at experimental temperature T . (Ferry, 1980)

By applying the TTS methods to a polyolefin cable material, Gillen and Clough (1989 and 1991) demonstrated that certain degradation property obtained at short times and high temperatures can effectively predict property at long times and low temperatures.

1.2.2 Limitations of Temperature Acceleration Method

As indicated by Koerner *et al.*, (1993), the application of the aforementioned degradation prediction methods are based on a tacit assumption that the activation energy, ' E_a ' remains constant within the interested temperature range; thus, the reaction rate can be extrapolated to the lower in-situ temperature. However, this assumption may not be applicable to all polyolefin materials according to reported experimental results.

Therefore, the temperature acceleration aging has certain limitations. Caution should be taken when extrapolating high temperature results to lower ambient temperatures. Too high temperatures should not be applied in aging tests. Selecting the appropriate temperature range should be based on the properties of specific

materials in the study and the previous testing database on similar products. Furthermore, Bright (1993) pointed out that a very small error in E_a value will lead to a huge error in the extrapolation of kinetic rate predictions at service temperatures due to the exponential function.

Kramer (1986) performed a temperature aging study of a crosslinked PE in a temperature range from 120°C to 240°C. The plot of the degradation data showed curvature at 150°C, so straight line extrapolations from short-term experiments at elevated temperatures to low temperatures are not valid. Achimsky (1997) used infra-red (IR) spectrophotometry to monitor the oxidative degradation of an isotactic PP in an oven-aging test with a temperature range from 50°C to 150°C. The Arrhenius plot of the onset of oxidation, t_i , displays a slope change at about 80°C, indicating that a transition of the oxidation kinetic of the material might have taken place. Gugumus (1999) also reported that the Arrhenius plots of the failure times for unstabilized PP films show a marked downward curvature at temperatures around 80°C and that antioxidant-stabilized PP films show a similar curvature in the Arrhenius plot at temperature higher than 80°C.

For geosynthetic materials, Elias, et al., (1999) indicates that HDPE geomembranes should not be incubated at temperatures higher than 95°C, above which the polymer structure would be altered and the activation energy, E_a , of oxidation would change accordingly. The maximum recommended incubation temperature for HDPE is 85°C. Salman *et al.* (1998) observed microstructural

changes in a (PP) geotextile at temperatures as low as 50°C in air. These observations imply that incubation at elevated temperatures could result in the development of some processes other than thermo-oxidative reactions.

1.2.3 Antioxidant Lifetime Prediction with Temperature Acceleration Method

As shown in Figure 1.1, Stage A – the AO Depletion Stage takes up a very large portion of the total polymer oxidative degradation process. So, it is very important to monitor and evaluate the AO lifetime of the materials with the proper approaches. The Oxidative Induction Time (OIT) test is widely used to monitor the remaining active antioxidant amount in the polymer. The OIT value represents the required time for the geosynthetics specimen to start to be oxidized at a certain temperature and oxygen pressure condition.

Blaine *et al.* (1997) and Horrocks *et al.* (1997) reviewed and summarized a number of successful applications of the St-OIT and HP-OIT test in determining the oxidative damage and/or the effectiveness of the antioxidant package in polyolefin materials. Gary (1990) showed that the both OIT values increase monotonically with the antioxidant concentration for a given formulation. Therefore, it is possible to approximate OIT as a linear function of the concentration of the antioxidant.

Arrhenius-based methods are often used in antioxidant lifetime prediction based on the high-temperature OIT data (Ling *et al.*, 1997). However, the antioxidant

depletion mechanism could change with the increasing temperature. It is reported by Woo *et al.* (1997) that the activation energy for antioxidant depletion increases significantly after the OIT test temperature is above a critical level, at around 210°C. The reason might be the strong volatilization of the additives within the polymer at this high temperature.

For PP and low density polyethylene (LDPE) cable, Ding (2001) reported that the Arrhenius activation energy of the antioxidant depletion reaction in oven-aging does not remain constant over the temperature range from 30°C to 90°C but changes with the temperature following a monotonic increasing curved trend. Therefore, for these two cable materials, the antioxidant lifetime predictions based on straight-line extrapolations from high temperatures could lead to grossly optimistic results under ambient conditions.

From the antioxidant package point of view, the potential for volatilization and/or solubility must be considered. It has been demonstrated that thiosynergistic antioxidants are vulnerable to volatilization at temperatures higher than 65°C (Hsuan and Guan, 1998).

Therefore, depending on the properties of the product and its antioxidant package, the upper incubation temperature may be as low as 50°C to 65°C in order to properly simulate in-situ oxidation degradation. Using such low temperatures, however, will substantially decrease the acceleration effect. As indicated in equation

1-2, in order to compensate for low temperatures, the pressure (or concentration) of oxygen could be used to increase the oxidation rate.

1.2.4 Accelerating Polyolefin Oxidation with Oxygen Pressure Incubation

Data on the pressure effect of stabilized polyolefin products, however, are very limited. Salman *et al.* (1998) performed a limited number of tests on stabilized PP geotextiles and HDPE geogrids, using high oxygen pressures. They found that the degradation had been greatly accelerated. Boss and Chien (1966) demonstrated that at a given temperature, the rate of oxidation of unstabilized PP is directly proportional to the oxygen concentration. Vink (2000) also obtained a linear relationship between oxidation and pressure in the temperature range from 50°C to 90°C, using an unstabilized PP film, as shown in Equation 1-6.

$$\rho = K \cdot C_o \quad (1-6)$$

Where,

$\rho = d[O_2]/dt$, the oxidation rate, defined as the oxygen amount absorbed during unit time for unit mass of sample

C_o = the oxygen concentration, i.e. the partial oxygen pressure

K = a constant which is dependent on the initial oxidation reaction rate, oxygen diffusion coefficient and sample thickness

This linear relationship is only valid at oxygen concentrations below ambient air condition. Gillen and Clough (1991) and Gillen *et al.* (1999) developed a general

solution for the basic autoxidation scheme of polymers. Considering diffusion-limited situations, the analytical results of this model show a linear oxygen pressure dependence of the oxidation rate at the lower pressure level, while the slope of the curve (oxidation rate vs. pressure) decreases monotonically with increasing pressure levels until it eventually approaches zero, i.e. the oxidation rate is insensitive to the oxygen concentration.

Diffusion-limited oxidation occurs whenever the rate of oxygen consumption within the material is greater than the rate at which it can be resupplied by diffusion from the surrounding air atmosphere (Gillen *et al.*, 1996). Billingham (1980) demonstrated that the oxygen-diffusion rate controlling of oxidation for thick samples changes to reaction-rate controlling in the thin samples. Oxygen diffusion is expected to be unimportant in the thermal oxidation of any polyolefin at the temperature of common use because the oxidation rate is relatively low. At the elevated temperatures used for accelerated aging, diffusion is unlikely to be important for any commercial film or fibre sample, but may be significant for thick films and bulk polymer.

By the analysis of the thermo-oxidative degradation of LDPE in air and in oxygen, Budrugaac (1994, 2001) observed that the temperature dependence of the degradation rate constant follows the Arrhenius model as shown in Equation (1-7). By varying the oxygen partial pressure (from 0.2 to 10 atm), the pre-exponential

factor A in Equation (1-7) correlates to the oxygen partial pressure (P) according to a power-law relationship:

$$A = A_0 P^\delta \quad (1-7)$$

Where A_0 and δ are material constants

The published data indicate that OIT values are also strongly dependent on the oxygen pressure; the OIT values were greatly shortened by the oxygen pressure, due to a higher oxidation reaction rate (Ezrin, 2003; Blaine *et al.*, 1997; Truttmann *et al.*, 1997; Rosa *et al.*, 2000). By varying the pressure and temperature in OIT test conditions, Tikuisis (1992) found an exponential relationship between OIT results and testing pressure at temperatures above the melting point of the HDPE geomembrane.

1.3 Objectives

Due to the afore-discussed complexity of the polyolefin oxidation induced by elevated temperature and high oxygen partial pressure, it is necessary to perform a systematic study with new designs of experimental methodology so as to accomplish a more comprehensive evaluation. The overall objectives of this PhD research are:

- To assess the acceleration effects of elevated temperature and/or pressure incubation environments on the oxidative reactions of four types of commercial polyolefin geosynthetic products.
- To monitor the oxidative behaviors of the test materials under various incubation conditions by using a number of physical, thermal, and mechanical tests to develop the degradation trend curves over the aging time.
- To qualitatively discuss the other factors influencing the long-term oxidation mechanism, e.g. antioxidant volatilization by high temperature and flowing air in the oven, antioxidant extraction by water exposure, etc., and to compare their effects with those of pressure and temperature aging tests.
- To establish the analytical model to predict antioxidant lifetime (Stage A in the oxidative degradation process) as a function of pressure and temperature.
- To establish an analytical model to predict the total service half-lives, i.e. the time to reach 50% loss in tensile mechanical properties at service conditions.
- To explore the possibility of developing the temperature and pressure incubation testing standard for accelerated degradation of commercial polyolefin geosynthetic products, and to evaluate the reliability of the new test method with respect to predictions under in-service conditions

Chapter 2. Test Materials, Incubation Apparatus and Procedures, and Evaluation Methods

2.1 Test Materials

Four types of polyolefin geosynthetic products were selected for this research program. The product and resin types are listed in Table 2.1 with a code designated to each of them.

Table 2.1 Selected polyolefin-based geosynthetic products

Product Code	Type	Resin
GT-sf	Slit film woven geotextile	Polypropylene (PP)
GG-1	Uniaxial geogrid	high density polyethylene (HDPE)
GG-2	Uniaxial geogrid	high density polyethylene (HDPE)
GT-nw	Needle-punched nonwoven geotextile	Polypropylene (PP)

GT-sf – This is a PP slit film woven geotextile. In the study, only filaments from the weft direction of the geotextile were used. The fiber was stabilized with proprietary antioxidant packages; however, the manufacturer did indicate that the antioxidant package contained the hindered amine light stabilizer (HALS). The as-received properties of the filament are shown in Table 2.2.

GG-1 and GG-2 – two types of unidirectional HDPE geogrids, were evaluated by temperature aging, while only GG-1 was assessed by temperature/pressure and water immersion aging. These two geogrids were stabilized with proprietary antioxidant

packages, which were not provided by the manufacturer. The as-received properties of the geogrids are listed in Table 2.3.

Table 2.2 – Properties of as-received slit film woven geotextile, GT-sf

Test Method		Mean Value	Standard Deviation
Density (kg/m ³) – ASTM D792		901	--
Thickness (mm)		0.95	0.008
Melt Flow Index (g/10 min) – ASTM D1238		5.63	0.27
Single Filament Tensile Test – ASTM 3822	Break strength (N)	48	5.0
	Break elongation (%)	16.5	5.5
HP-OIT (min) – ASTM D5885		118.3	10.1

Note: The physical, mechanical, and thermal properties listed in the table are based on the results of 5 to 10 replicates of the as-received material in each test.

Table 2.3 – Properties of the as-received HDPE geogrid GG-1 and GG-2

Test Method	GG-1		GG-2	
	Mean Value	Standard Deviation	Mean Value	Standard Deviation
Unit Weight (g/m ²) ASTM D5261	826	--	655	--
Density (kg/m ³) ASTM D792	949	--	957	--
Standard OIT (min) ASTM D 3895	136	7.2	40	4.25
MI (g/10 min) ASTM D1238	0.11	--	0.08	--
Tensile Strength (kN) ASTM D 6637	1.94	0.15	2.40	0.05
Tensile Elongation (%) ASTM D 6637	23.0	0.75	17.7	0.83

Note: The physical, mechanical, and thermal properties listed in the table are based on the results of 5 to 10 replicates of the as-received material in each test.

GT-nw – the polypropylene needle-punched nonwoven geotextile, with an additive package that includes HALS, was evaluated for temperature/pressure aging and water immersion aging. The incubation specimens for GT-nw were 2 inch by 8 inch strips.

Table 2.4 shows the as-received properties of this product.

Table 2.4 – Properties of as-received slit film woven geotextile GT-nw

Test Method		Mean Value	Standard Deviation
Unit Weight (g/m ²) – ASTM D5261		335	--
Melt Flow Index (g/10min) – ASTM D1238		10.4	0.32
50 mm Strip Tensile Test	Break strength (N)	234	14
	Break elongation (%)	64	5.6
HP-OIT (min) - ASTM D5885		74.4	14.1

Note: The physical, mechanical, and thermal properties listed in the table are based on the results of 5 to 10 replicates of the as-received material in each test.

2.2 Incubation Plan

Four incubation series were used in this research program. The temperature and pressure used in each incubation series are described in Table 2.5.

In Series I, high pressure/temperature aging, six temperatures from 35°C to 105°C, and five oxygen partial pressures [P_o] ranging from 0.02 to 6.3MPa were used. Specially-designed high pressure cells were used for all pressure incubations except the 0.02MPa oxygen partial pressure, for which specimens were directly exposed to the ambient condition inside the forced air oven. The incubation temperatures from 35°C to 65°C were used for GT-sf, GT-nw, and GG-1 for the purpose of assessing

antioxidant depletion behaviors, which will be discussed in the Chapters 3 to 5, whereas the aging tests at 85°C and 105°C were carried out only on the GT-sf samples to achieve polymer degradation in a reasonable testing time span so as to validate the lifetime prediction model over a wide range of elevated temperatures (Chapter 3).

Series II, low pressure/high temperature aging, is a continuation of the Series I incubation; it includes two elevated temperatures at 95°C and 105°C together with seven oxygen pressures. The seven $[P_{O_2}]$ levels were either below or just above the $[P_{O_2}]$ in air (0.02Mpa). Low-pressure cells specially-designed with a gas mix system were utilized to create stagnant N₂/O₂ environments with an appropriate fraction of oxygen gas. The total pressure inside the cell was maintained at one atmosphere, i.e. 0.1MPa. The cell gas was refreshed three times a week to ensure that the desired level of oxygen concentration was maintained. The relative high temperature used in this series of incubation was to compensate for the decelerating effect attributed to lowering the oxygen partial pressure. It should be noted that incubation temperatures used in this series are near the upper range for the oven-aging of polyolefin materials. Only the GT-sf was evaluated in this series.

Table 2.5 Incubation condition series used in this research program

Incubation Series	Duration	Temperature (°C)	Partial Oxygen Pressure (MPa)	Incubated Materials			
				GT-sf	GT-nw	GG-1	GG-2
I High-pressure /Temperature aging	Up to 2 years	35	0.02 (in air), 0.44, 0.74, 1.03, 1.30	X	X	X	N/A
		45	0.02 (in air), 1.30, 6.30	X	X	X	N/A
		55	0.02 (in air), 1.30, 6.30	X	X	X	N/A
		65	0.02 (in air), 1.30, 2.80, 4.90, 6.30	X	X	X	N/A
		85	0.02 (in air), 1.30, 2.80, 4.90, 6.30	X	N/A	N/A	N/A
		105	0.02 (in air), 1.30, 2.80, 4.90, 6.30	X	N/A	N/A	N/A
II Low-pressure /Temperature aging	Up to 100 days	105	0 (In pure N ₂), 0.005, 0.01, 0.015, 0.02, 0.05, 0.1	X	N/A	N/A	N/A
		95	0 (In pure N ₂)	X	N/A	N/A	N/A
III Temperature aging	Up to 7 years	55	0.02 (in air)	N/A	N/A	X	X
		65	0.02 (in air)	N/A	N/A	X	X
		75	0.02 (in air)	N/A	N/A	X	X
IV Water- immersed aging	1 year	45	In water	X	X	X	N/A
		55	In water	X	X	X	N/A
		65	In water	X	X	X	N/A

Note: For 0.02 MPa oxygen partial pressure condition, samples were placed directly in ovens. For oxygen pressure levels higher than 0.02 MPa, samples were incubated in high pressure stainless steel cells, while for oxygen pressure levels lower than 0.02 MPa, specially designed low pressure cells were used.

Series III, temperature aging, utilized forced air ovens at three elevation temperatures: 55°C, 65°C, and 75°C. Results from this series served as references to those from Series I in the assessment of the effect of $[P_o]$ on antioxidant depletion. The two geogrid samples, GG-1 and GG-2, were exposed to this series of incubation conditions.

Series IV, water immersion aging, was designed to assess the interaction between antioxidants and water. In addition to thermo-oxidation, the antioxidants can also be depleted via extraction by the surrounding liquids (such as water) and by hydrolysis. In this incubation series, GT-sf, GT-nw and GG-1 samples were evaluated at three elevation temperatures: 45°C, 55°C and 65°C.

2.3 Incubation Apparatus and Procedures

The focus of this research was to establish a new acceleration aging method using both elevated temperature and oxygen pressure. The incubation equipment for Series I, II, and III included forced air ovens and two types of pressure cells for high and low pressure incubation. The details of the two pressure cells will be described in the following sections. For Series IV, water baths were used.

2.3.1 Forced Air Ovens

Forced air ovens were used in Series I, II, and III to provide temperature acceleration. In Series III, the oven incubation procedure was performed according to

the ASTM D5721. The geogrid specimens were fixed in positions with 25mm spacing in between, as can be seen in Figure 2.1. No pretensions were applied to the specimens. Oven ventilation was controlled to provide sufficient fresh air intake, while the oven temperatures were maintained at the desired temperature, $\pm 0.5^{\circ}\text{C}$.



Figure 2.1 Experimental settings inside the oven incubation devices

2.3.2 High Pressure Cells

The pressure environments were created using either air or oxygen gas. Test specimens were placed inside the pressure cell. Air or oxygen gas was gradually introduced into the cell until it reached the desired level of pressure at room temperature. The pressure cell assembly, incubation specimens, and pressurized system are shown in Figure 2.2. The pressurized cells were then placed in different ovens that were set at the desired incubation temperatures, as shown in Figure 2.3. The cell was kept closed during the incubation. The pressure was monitored using the

gas gauge attached to the cell. If the pressure decreased by more than 0.1 MPa, the gas inside the cell was refreshed.

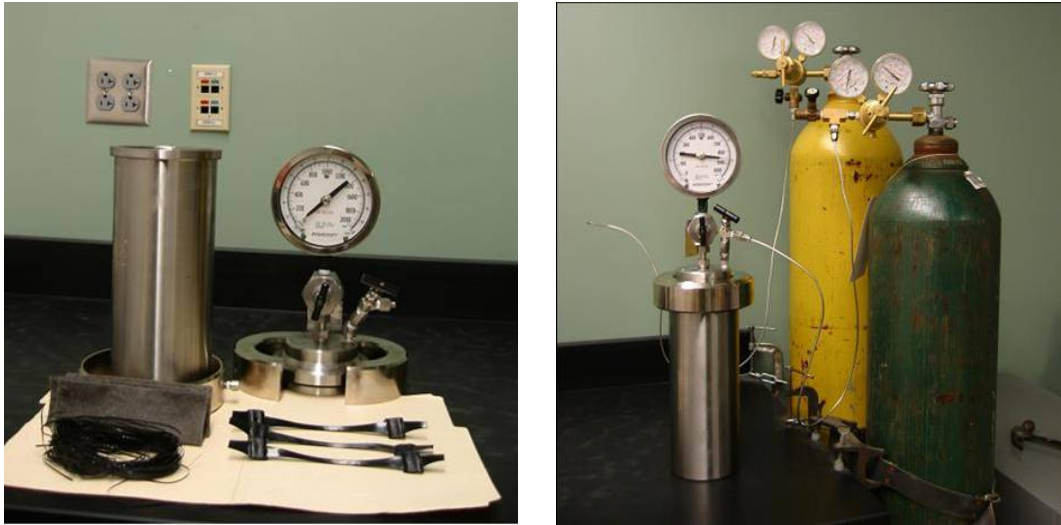


Figure 2.2 High pressure cells: incubated samples and pressurization system



Figure 2.3 High pressure cells in incubation ovens

2.3.3 Low Pressure Cells

”Low pressure” refers to low oxygen partial pressure inside the incubation cells. The uniqueness of the low pressure cell set up is not in the pressure cell, but in the gas mixing system. Since the levels of oxygen pressure used in the incubation were below those in the atmosphere, 0.02 MPa oxygen partial pressure, specially mixed gases consisting of different fractions of oxygen and nitrogen were created using a gas proportioner, as shown in Fig. 2.4.

The pressure cell was vacuumed to a level of 800 mbar for 3 minutes to remove the air. Subsequently, an appropriately mixed oxygen/nitrogen gas was introduced to the cell until the pressure reached 1 atm. The vacuum/pressure procedure was repeated twice to assure that air inside the cell was fully replaced by the mixed gas. Once the appropriate gas mixture was achieved, cells were placed in ovens set at desired temperatures.

Note that the pressure inside a cell increased with temperature; thus, the actual incubation pressure is higher than 1 atm. The cell pressure was monitored by the pressure gauge. The gas was refreshed three times a week to ensure that the oxygen level remained consistent. Regarding the specimen’s configuration, the filaments were fixed by binder clips along a copper wire frame to avoid being sucked out by the vacuum, Fig 2.5.



Figure 2.4 Low pressure cells: pressurization system



Figure 2.5 Low pressure cells: incubated samples with fix frames

2.3.4 Water Baths

Water bath incubation is designed to simulate the geosynthetics in field which are exposed to the water. All specimens, geogrid rips, GT-sf filaments, and GT-nw strips were fully immersed in water baths that were maintained at testing temperatures $\pm 3^{\circ}\text{C}$.

2.4 Degradation Evaluation Test Methods

The incubated samples were retrieved at different time intervals for testing to monitor changes in their material properties. The tests used to assess the material properties were as follows:

- *Oxidative Induction Time (OIT)*

The OIT value is an indicator of the amount of remaining active antioxidant in a test specimen; lower OIT values indicate a lesser amount of antioxidant. The standard OIT (Std-OIT) test was performed according to ASTM D3895 using a differential scanning calorimeter (DSC) with a standard test cell. The Std-OIT is the required time for a specimen to be oxidized at a temperature of 200°C and 35kPa oxygen with a flow rate of 50 ml/min. A schematic thermal curve is shown in Figure 2.6(a).

The high-pressure oxidative induction time (HP-OIT) test is conducted at an isothermal temperature of 150°C with 3.5MPa oxygen, as shown in Figure 2.6(b). The HP-OIT test was specifically designed to measure the amount of antioxidant in a package that contains HALS. The HALS antioxidants have boiling points around 150°C; thus, they are not suitable for evaluation using the Std-OIT test, which is conducted at an isothermal temperature of 200°C. The HALS antioxidants would be artificially depleted at such a high testing temperature, giving a false indication in the amount of antioxidant present in the test specimen (Hsuan and Guan, 1998).

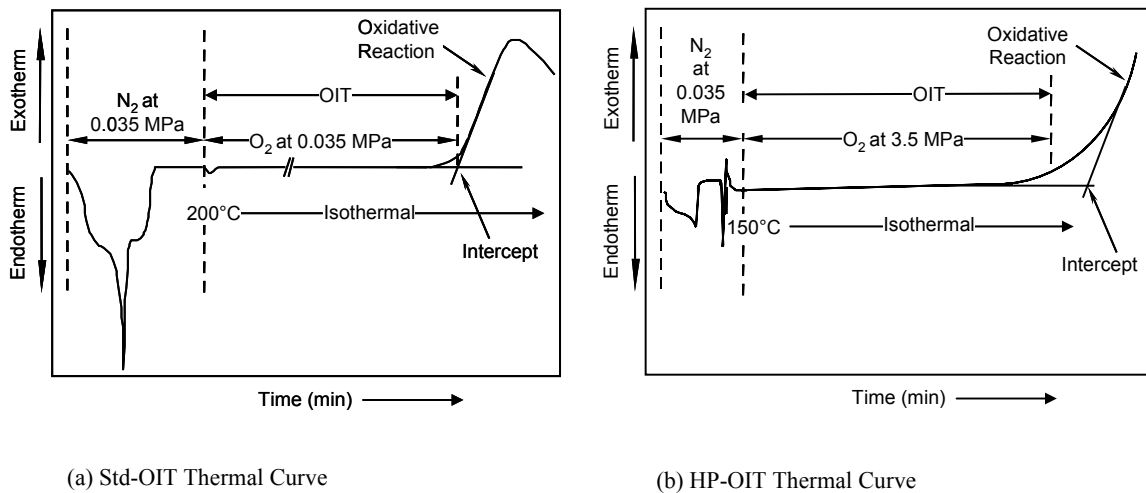


Figure 2.6 Typical thermal graph illustrating the obtaining of the HP-OIT value

- *Tensile tests*

In general, oxidative degradation results in chain scission that leads to embrittlement of the material, particularly in the tensile breaking elongation. Thus, tensile properties were used to detect the onset of oxidation degradation. For GG-1 and GG-2, the single rib tensile properties were measured according to the ASTM D 6637. Five replicates were tested for each sample. For GT-sf, the filament tensile test

was performed according to the ASTM D3822, and eight replicates were tested. The tensile properties of GT-nw were evaluated using the 50 mm wide strip tensile test, and five replicates were tested.

- *Melt Flow Index (MI) test*

Melt index (MI) is a qualitative method used to assess the molecular weight of polymer. For the same material, a decrease in MI value indicates crosslinking in the polymer, while an increase suggests chain scission. The MI test was performed according to ASTM D1238 at 190°C/2.16kg for GG-1 and GG-2, and 230°C/2.16kg for GT-sf and GT-nw.

The average standard deviation of OIT and tensile property test results of as-received test materials are listed in Table 2.2, Table 2.3, and Table 2.4. The number of specimens to be tested for each aged sample group was determined using Student's t Distribution following the procedures required by ASTM D 4595. Thus, the test results will reach a statistical significance that one can expect a 90% probability level that any test result is not more than 5% above or below the true average value. The sample size are listed in the Table 2.6

Table 2.6 – Sample size for evaluation test for 95% probability level

Test Method	GT-sf	GG-1 & GG-2	GT-nw
Melt Flow Index	N/A	N/A	N/A
Tensile Properties	8	5	5
OIT	4	3-5	6

Note: Melt Index test need large amount of material for single reading so only one test can be perform for each sample group due to the limited incubation cell space.

Chapter 3. Antioxidant Depletion of Polypropylene Slit Film Geotextiles under Temperature, Pressure and Water Environments

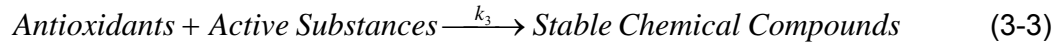
3.1 Introduction

Polypropylene (PP) slit film geotextiles are regularly used in separation and reinforcement applications in which service lifetimes of 30 to 100 years are required. For the long-term degradation of PP geotextiles, the concern is over oxidation degradation.

The antioxidant package, which includes both the type and amount of antioxidants, is critical to the longevity of polypropylene (**PP**) geotextiles, since the lifetime of the antioxidants makes up a significant portion of the polymer, as shown in Figure 1.1 in Chapter 1. In order to assess the lifetime of PP geotextiles, the depletion of the antioxidant should first be evaluated.

Polypropylene is susceptible to oxidation through a series of free radical reactions, as shown in Eqs. (3-1) and (3-2). The result of these oxidation reactions is chain scission (i.e., breaking of polymer chains), leading to a decrease in molecular weight and a subsequent decrease in mechanical properties.





where RH is polypropylene; $R\bullet$ and $H\bullet$ are free radicals; $ROO\bullet$, $RO\bullet$ and $OH\bullet$ are oxygenated free radicals; k_1 , k_2 and k_3 are reaction rate constants.

Antioxidants are added to PP geotextiles to protect the polymer from oxidation and to prolong the onset of oxidation. Until the antioxidants are essentially depleted, the mechanical properties remain unchanged (Hsuan and Guan, 1998). The function of the antioxidants is to convert active substances such as free radicals and active alkyl peroxides to stable molecules, preventing them from reacting with the polymer.

In the sequence of chemical reactions from Eq. (3-1) to Eq. (3-3), the reaction rate of Eq. (3-3) must be quicker than that of Eq. (3-2) to prevent accumulation of free radicals. Once the oxygenated free radicals are formed via Eq. (3-2), they are rapidly converted to stable compounds by the antioxidants. It is assumed that the formation rate of oxygenated free radicals is equal to the depletion rate of antioxidants, which is monitored throughout the incubation period.

In some preceding papers, the depletion mechanism of antioxidants in HDPE geomembranes has been studied; the antioxidant lifetimes of these products were reported to be from decades up to hundreds of years, depending on the material formulation and service conditions (Row and Sangam, 2002; Hsuan and Koerner, 1998; Mueller and Jacob, 2003). Mueller *et al.* (2003) reported that similar oxidative

resistance characteristics existed in nonwoven PP geotextiles. However, compared with HDPE geomembranes, the antioxidant lifetime in nonwoven PP geotextiles was much shorter because they are less stable, and the PP geotextiles showed a rapid reduction in mechanical properties after the oxidative degradation began.

In this chapter, the depletion of antioxidants in PP slit film geotextiles (GT-sf) in three different incubation conditions is evaluated and discussed. The three incubation conditions are briefly described as follows:

(a) Elevated temperatures and high oxygen partial pressures

The specific incubation conditions are showed in Table 3.1, and they are a part of the Series I incubation conditions in Table 2.5. (The test results of GT-sf at elevated temperatures of 85°C and 105°C will be presented in Chapter 6.) The incubation conditions involved four temperatures and four partial oxygen pressures. It should be noted that the pressure cell of 6.3 MPa air (equal to a partial oxygen pressure of 1.3 MPa) was also included in each of the temperatures so that data could be compared with that of the 1.3 MPa pure oxygen incubation. The incubation duration ranged from one to two years.

(b) Elevated temperatures and low oxygen partial pressures

The specific incubation conditions are shown in Table 3.2, and they are also listed in Series II in Table 2.5. The nitrogen and oxygen gas mixtures were introduced and maintained in low pressure cells. The partial oxygen pressures

[P_{O_2}] are kept at levels from 0 to 0.1 MPa. In most conditions, oxygen concentrations within the cells are below the oxygen level in the air, i.e. 0.02 MPa [P_{O_2}]. With the enhanced temperature conditions used, the aging durations of this series were up to 3 months.

(c) Elevated water temperature

The incubation conditions are those listed in Series IV in Table 2.5. Specimens were immersed in water at temperatures of 45°, 55° and 65°C. The aging times were up to 12 months.

Table 3.1 – High Pressure Incubation environments for aging GT-sf geotextiles

	Oven Temperature (°C)			
	35	45	55	65
Incubation Pressure (MPa)	0.1 air 6.3 air 1.3 O ₂ -- -- --	0.1 air 6.3 air -- -- -- 6.3 O ₂	0.1 air 6.3 air -- -- -- 6.3 O ₂	0.1 air 6.3 air 1.3 O ₂ 2.8 O ₂ 4.9 O ₂ 6.3 O ₂
Incubation Duration (months)	24	24	24	12

Note: 0.1 MPa air means samples were placed in ovens directly without using the pressure cells since 1atm = 0.1MPa.

Table 3.2 – Low Pressure Incubation environments for aging GT-sf geotextiles

	Oven Temperature (°C)	
	95	105
Incubation Pressure	1 atm (100% N ₂ , 0% O ₂) – 0 MPa [P_{O_2}]	1atm (100% N ₂ , 0% O ₂) – 0 MPa [P_{O_2}]
	--	1atm (95% N ₂ , 5% O ₂) – 0.005 MPa [P_{O_2}]
	--	1atm (90% N ₂ , 10% O ₂) – 0.01 MPa [P_{O_2}]
	--	1atm (85% N ₂ , 15% O ₂) – 0.015 MPa [P_{O_2}]
	--	1atm (50% N ₂ , 50% O ₂) – 0.05 MPa [P_{O_2}]
	--	2atm (75% N ₂ , 25% O ₂) – 0.05 MPa [P_{O_2}]
	--	1atm (0% N ₂ , 100% O ₂) – 0.1 MPa [P_{O_2}]
Incubation Duration (months)	Up to 3 months	

3.2 Antioxidant Depletion in Elevated Temperatures and High Pressures Incubation (Series I)

3.2.1 Test Results

Evaluation of Material Properties for Incubated Specimens

The tensile properties, MI and OIT of incubated specimens were evaluated at different retrieval times. The changes in each material property are presented in percent retained, which is calculated according to Equation (3-4).

$$\% \text{ retained} = \frac{\text{test value of incubated specimen at a specific time}}{\text{test value of as received specimen}} * 100 \quad (3-4)$$

For tensile properties, there was a large scattering in the tensile elongation which could be caused by the slipping during the tensile test. Thus, the tensile strength is used to assess the oxidation degradation of the GT-sf.

After 24 months of incubation, there were no significant changes in the MI and tensile properties for specimens incubated in 6.3 MPa air at all four temperatures. However, a gradual decrease of HP-OIT was observed. Figure 3.1 shows the changes of material properties with incubation time at 55°C.

In contrast, substantial changes in both MI and tensile properties were measured in incubation conditions of 4.9 and 6.3 MPa oxygen pressure at temperatures of 55° and 65°C. The HP-OIT decreased much faster than in those in the air environments. The changes of HP-OIT, MI, and tensile strength over time at 65°C in different oxygen pressures are shown in Figures 3.2, 3.3, and 3.4. For specimens incubated in oxygen pressures of 2.8, 4.9 and 6.3 MPa, the MI started to increase and the tensile strength began to decrease when the HP-OIT dropped to approximately 15% retained, indicating the onset of oxidation degradation. It appears that MI and tensile strength have similar sensitivity in response to the oxidation degradation of PP tape yarns. After 3 months of incubation in 6.3 MPa oxygen at 65°C, the filaments were completely cracked.

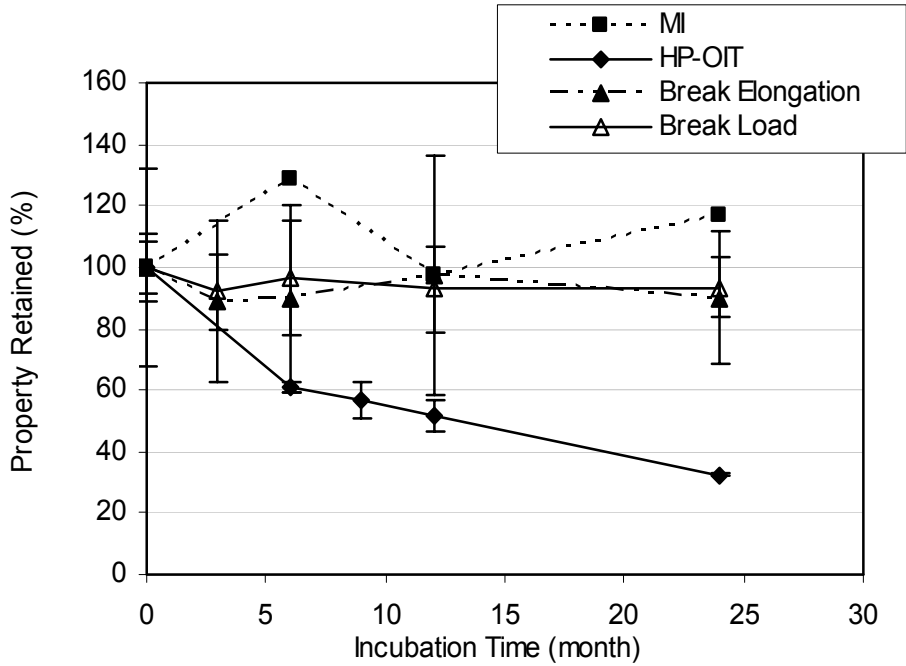


Figure 3.1 Changes in GT-sf properties over time at 55°C under 6.3 MPa air pressure

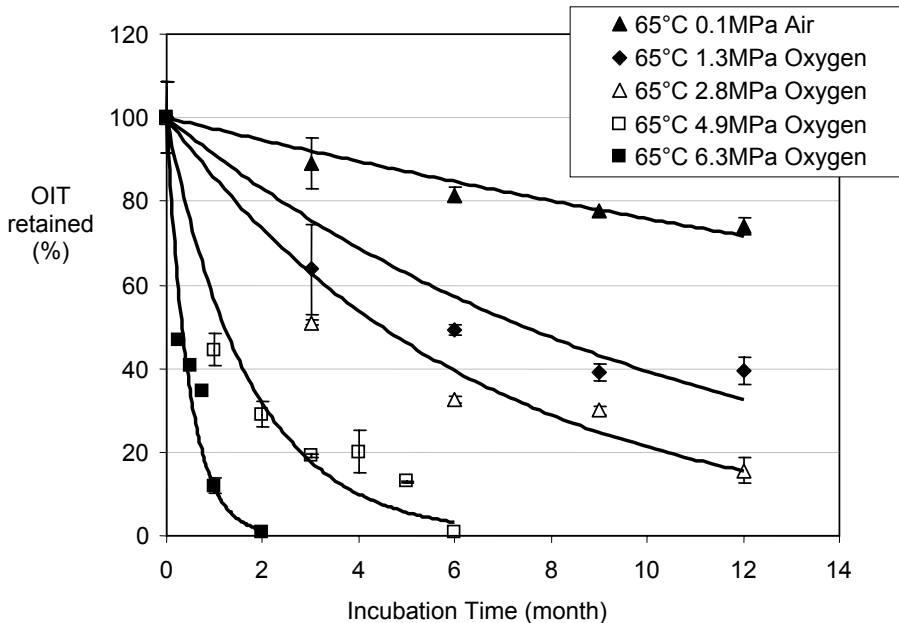


Figure 3.2 – Changes in GT-sf HP-OIT retained over time at 65°C under various pressures

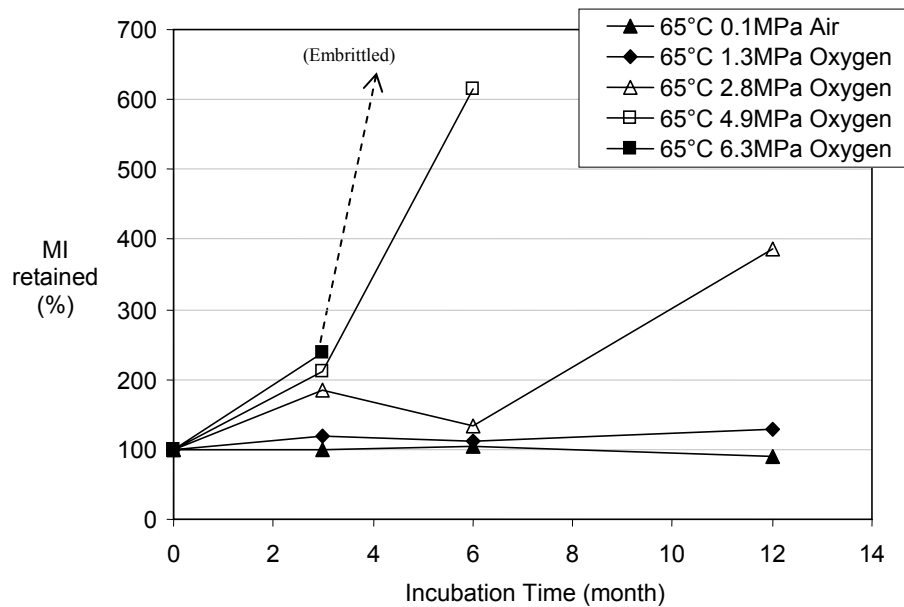


Figure 3.3 – Changes in GT-sf MI retained over time at 65°C under various pressures

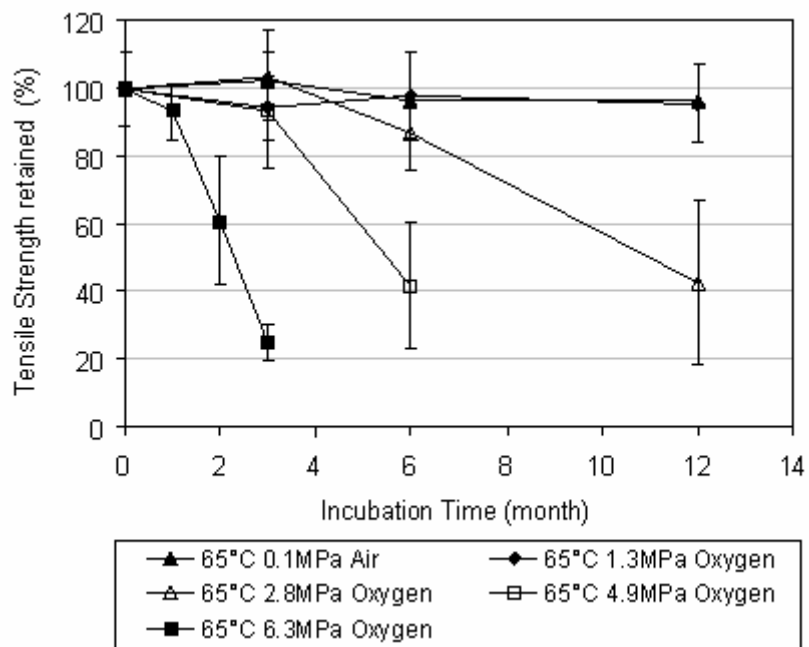


Figure 3.4 – Changes in GT-sf tensile strength retained over time at 65°C under various pressures

Evaluation of the Oxygen Partial Pressure

Boss and Chien (1966) found that the oxidation rates of PP were very similar in both air and oxygen when the same oxygen partial pressures were used. On the contrary, Vink and Fontijn (2000) showed that the half-life of a PP geotextile is shorter in pure oxygen pressure than in corresponding air pressure at the same oxygen partial pressure. In this study, data obtained from 1.3 MPa oxygen pressure was compared with those obtained from 6.3 MPa air pressure, which contained 1.3 MPa oxygen partial pressure. Figure 3.5 shows that the HP-OIT data under these two pressures are very similar at incubation temperatures of 35° and 65°C. The results indicate that the depletion of antioxidants is controlled by the oxygen partial pressure and is not affected by the magnitude of the total pressure. Thus, in the data analysis all air pressure values are converted to oxygen partial pressure [P_{O_2}] by multiplying by a factor of 0.21.

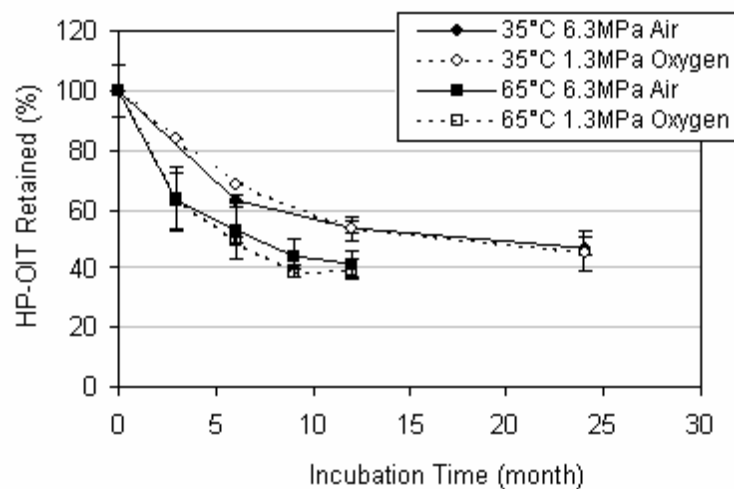


Figure 3.5 – GT-sf HP-OIT response under the same oxygen partial pressure at 35°C and 65°C

Antioxidant Depletion with Incubation Time

Antioxidant depletion was measured by the HP-OIT test at different incubation durations. As shown in Figure 3.2, the HP-OIT retained decreases exponentially with incubation time, according to Eq. (3-5). The equation indicates a first order reaction for the depletion of antioxidants. Similar HP-OIT response curves were also obtained at 45° and 55°C under different oxygen pressures.

$$\ln(OIT\%) = -kt \quad (3-5)$$

where $OIT\%$ is HP-OIT percent retained after incubation time t , t is incubation time (months), and k is a reaction rate constant which is a function of the incubation temperature and oxygen partial pressure.

Table 3.3 shows the rate constant values and the corresponding least squares coefficient (R^2) by fitting the data at each incubation condition with an exponential equation. At 35°C, however, the depletion of antioxidants proceeded relatively slowly; the HP-OIT retained were still above 50% in the majority of the incubation conditions after 24 months. Subsequently the HP-OIT retained exhibited a poor exponential relationship with incubation time, as indicated by the low R^2 values.

Table 3.3 – Reaction rate constant k (month⁻¹) under different incubation conditions

Temperature		35°C		45°C		55°C		65°C	
Rate coefficient		k	R^2	k	R^2	k	R^2	k	R^2
Oxygen Partial Pressure (Mpa)	0.02	0.0034	-0.34	0.0126	0.98	0.0211	0.95	0.0277	0.94
	1.3	0.0208	0.41	0.0348	0.55	0.0513	0.9	0.0945	0.95
	2.8	NA	NA	N/A	N/A	N/A	N/A	0.1553	0.94
	4.9	NA	NA	N/A	N/A	N/A	N/A	0.4522	0.85
	6.3	NA	NA	0.3733	0.96	0.6478	0.85	1.9044	0.89

Note N/A = not available (these conditions were not included in the test program)

3.2.2 Antioxidant Lifetime Prediction

Effects of Temperature and Oxygen Pressure on Antioxidant Depletion

Under constant pressure, the reaction rate constant (k) in Eq. (3-5) increases with temperature (T) according to the Arrhenius equation, which is expressed in Eq. (3-6). Figure 3.6 shows the Arrhenius plots for three oxygen pressures (0.02, 1.3 and 6.3 MPa) at temperatures of 45°C, 55°C and 65°C.

$$k = A \exp(-E / RT) \quad (3-6)$$

where k is the reaction rate constant, E is the activation energy (kJ/mol), R is the universal gas constant (J/mol-K), T is the incubation temperature (K) and A is a material constant.

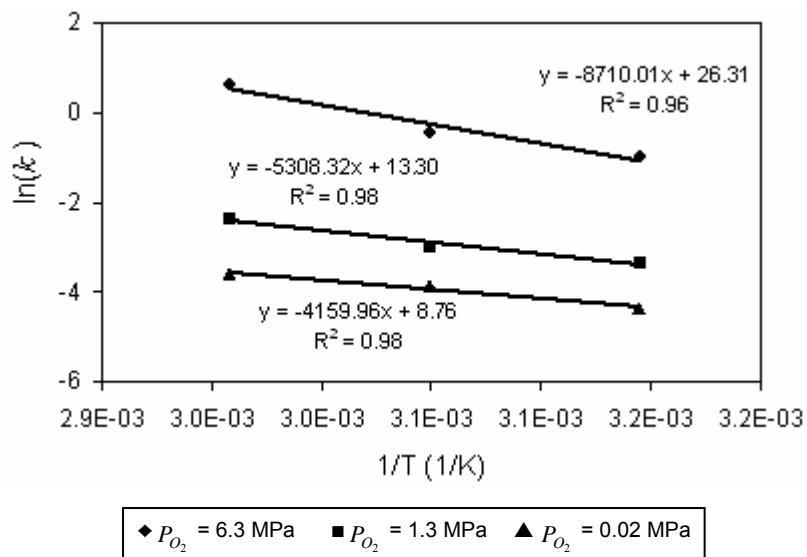


Figure 3.6 – Arrhenius plots at three constant pressures

The slope of the lines, which is proportional to the activation energy (E) of the reaction and the “A” value, vary with oxygen pressure. The relationship between (E) and oxygen pressure is found to be linear, as shown in Figure 3.7 and Eq. (3-7). On the other hand, the constant “A” is exponentially related to the pressure, as shown in Figure 3.8 and Eq. (3-8).

$$E = E_{ao} + \alpha P_{O_2} \quad (3-7)$$

where E is activation energy, E_{ao} is a constant and corresponds to the activation energy at 1 atmosphere and α is a constant, P_{O_2} is oxygen partial pressure.

$$A = C \exp(\beta P_{O_2}) \quad (3-8)$$

where A is a pressure dependent constant, P_{O_2} is oxygen partial pressure, and C and β are constants.

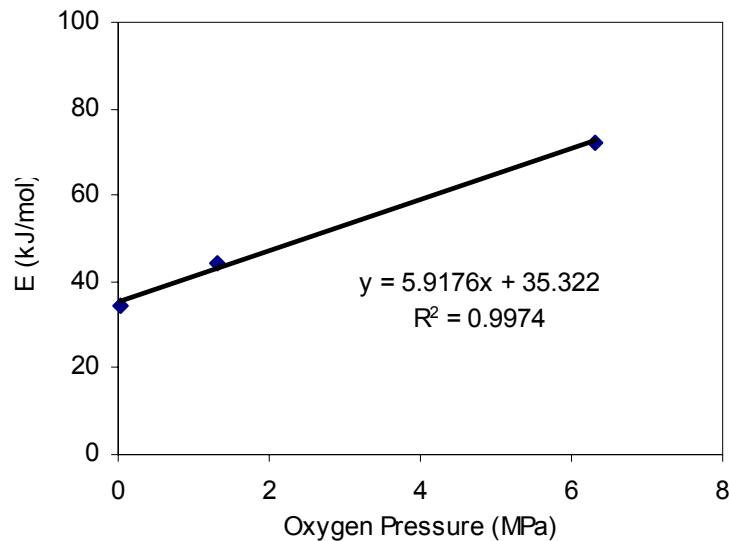


Figure 3.7 – Activation energy against oxygen pressure

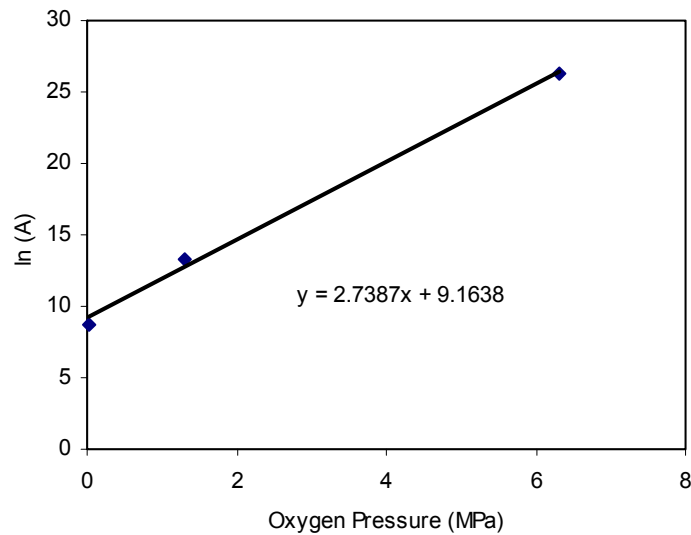


Figure 3.8 – Constant “A” in Eq. 9 plotting against oxygen pressure

Based on the above analysis, the relationship of reaction rate constant (k) in terms of temperature and pressure can be established by substituting Eqs. (3-7) and (3-8) into Eq. (3-6), resulting in Eq. (3-9).

$$k = C \cdot \exp \left[-\frac{E_{ao} + \alpha P_{O_2}}{RT} + \beta P_{O_2} \right] \quad (3-9)$$

A least squares multi-variable regression analysis is applied to calculate the four constants in Eq. (3-9) by using data shown in Table 3.3 at temperatures 45°, 55° and 65°C and five pressure levels. The four computed constants are given in Table

3.4. Figure 3.9 shows the response surface of (k) in terms of temperature and pressure.

Table 3.4 – Values of constants obtained from calculation of Eq. (3-9)

Constant	Value
E_{ao}	32.8 kJ/mol
C	3705.2 month ⁻¹
α	4.70 m ³ /mol
β	2.284 MPa ⁻¹

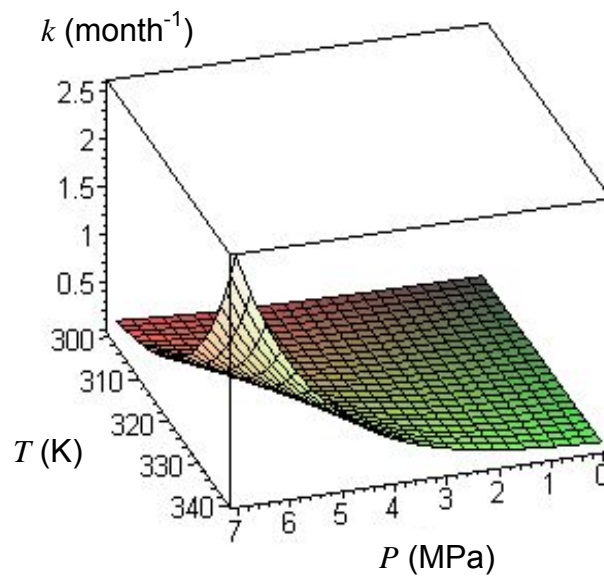


Figure 3.9 – The effects of the reaction rate constant in terms of temperature and pressure

Modified Arrhenius Model Predicting Antioxidant Lifetime

The depletion of antioxidants in terms of temperature and pressure is expressed in Eq. (3-10), which results from the substitution of Eq. (3-9) into Eq. (3-5). The resulting lifetime of the antioxidants is then given in Eq. (3-11).

$$\ln(HP - OIT\%) = -C \cdot \exp\left[-\frac{E_{ao} + \alpha P_{O_2}}{RT} + \beta P_{O_2}\right] * t \quad (3-10)$$

Figure 3.10 shows the 65°C HP-OIT data fitted with Eq. (3-10), using the four computed constant values from Table 3.4. The correlation between the data and the prediction line is very good. Similar correlation (not shown) is also observed at 45° and 55°C.

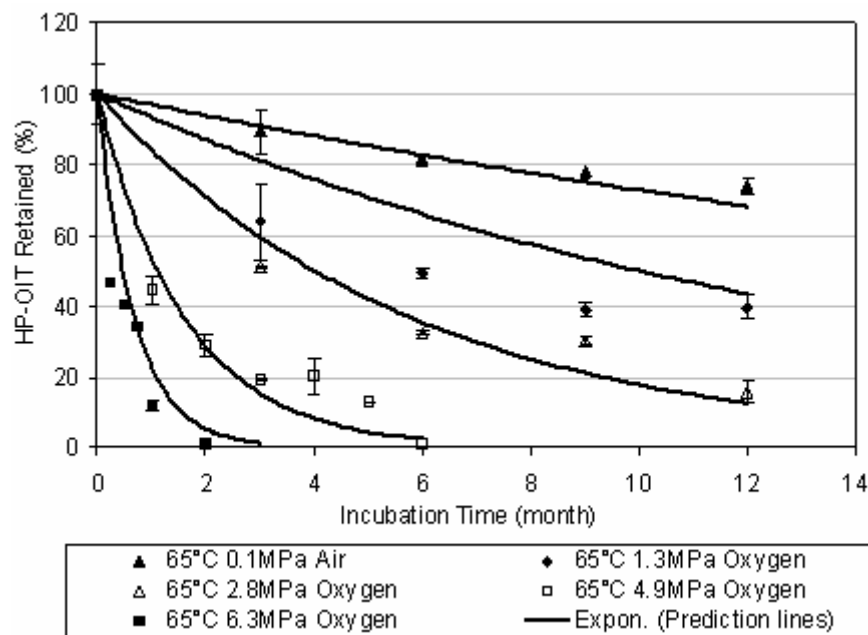


Figure 3.10 – HP-OIT data fitted with model predicted curves of Eq. (3-10) at 65°C

As indicated in Section 3.2.1, the oxidation of the PP filament began when the HP-OIT value decreased to 15% retained. Therefore, the effective lifetime of the antioxidants in this particular PP filament is the time to reach 15% of the HP-OIT value of unaged material, and is expressed in Eq. (3-11).

$$t = \frac{\ln(15\%)}{-C \cdot \exp\left[-\frac{E_{ao} + \alpha P_{O_2}}{RT} + \beta P_{O_2}\right]} \quad (3-11)$$

The response surface of the antioxidant lifetime in terms of temperature and pressure is shown in Figure 3.11. Table 3.5 shows the predicted lifetimes at temperatures ranging from 5° to 35°C under 1 atmosphere of air pressure (0.02 MPa oxygen pressure). However, the predicted antioxidant lifetimes are almost the same when oxygen percentage decreases from 20% to 5%, as shown in Table 3.6.

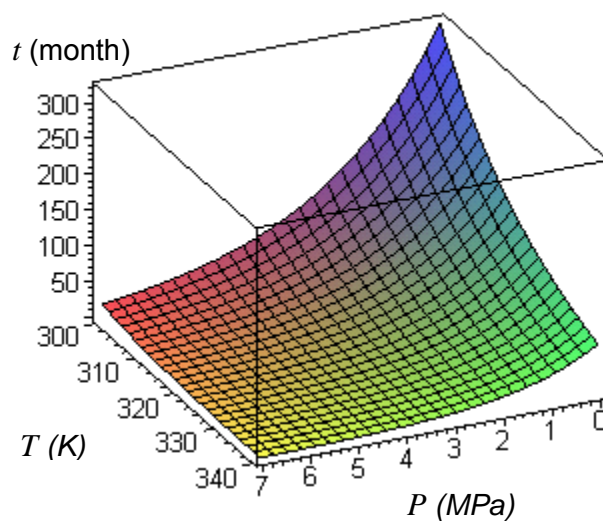


Figure 3.11 – The response surface of antioxidant lifetime in terms of temperature and pressure

Based on Eq. (3-11), the acceleration factors induced by elevated temperature and high oxygen partial pressure can be calculated. For the antioxidant package of this particular PP filament, the predicted lifetime at ambient site condition ($0.02 P_{O_2}$ and 10°C) is found to be 580 months (48 years). The acceleration factor, based on the ratio of lifetime ($\frac{t_{site}}{t_{test}}$) at different incubation temperatures and $[P_{O_2}]$, is shown in Table 3.7. Under incubation conditions of 65°C and $6 \text{ MPa } P_{O_2}$, the duration to reach the 15% critical HP-OIT value will be only 1.6 months, with an acceleration factor of 373.

Table 3.5 – Predicted lifetime of the antioxidant at different temperatures

Temperature ($^\circ\text{C}$)	Oxygen Pressure (MPa)	Lifetime of antioxidants (months/years)
5	0.02	747/62
15	0.02	456/38
25	0.02	287/24
35	0.02	187/16

Table 3.6 – Predicted lifetime of the antioxidant at different pressures

Oxygen Partial Pressure (MPa)	Temperature ($^\circ\text{C}$)	Lifetime of antioxidants (months/years)
0.005 (5% oxygen)	10	585/48.8
0.01 (10% oxygen)	10	583/48.7
0.015 (15% oxygen)	10	582/48.6
0.02 (20% oxygen)	10	581/48.4

Table 3.7 – Acceleration factor to reach 15% OIT retained using Eq. (3-8)

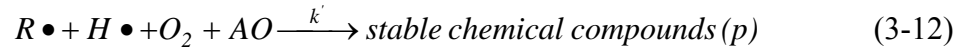
P_{O_2} (MPa)	Predicted Lifetime at 0.02 P_{O_2} and 10°C	Incubation Temperature		
		45°C	55°C	65°C
0.02	580 months	4.7	6.8	9.7
2		13	21	33
4		35	63	110
6		95	192	373

3.2.3 Discussion

The antioxidant depletion of this particular PP filament at elevated temperatures under high oxygen pressure from 0.02 to 6.3 MPa was evaluated using the HP-OIT test. The kinetics of the antioxidant depletion mechanisms and the lifetime of antioxidants in terms of temperature and oxygen pressure are discussed in this section.

Kinetics of Antioxidant Depletion Mechanisms

The chemical interactions between antioxidants, oxygen, and free radicals are expressed by Eq. (3-1) to (3-3). The formation of oxygenated free radicals ($FO\bullet$) controls the antioxidant (AO) depletion, since the reaction rate of antioxidant depletion is faster than that of free radical generation reaction, in order to prevent accumulation of free radicals in the polymer. The overall reaction can be summarized into a single equation, Eq. (3-12).



According to chemical kinetics (Atkins, 1986), the product of a chemical reaction is proportional to the concentrations of reactants. Eq. (3-13) can be derived based on Eq. (3-12).

$$\frac{-d[AO]}{dt} = \frac{-d[O_2]}{dt} = \frac{-d[R\bullet, H\bullet]}{dt} = \frac{d[p]}{dt} = k' [AO][O_2][R\bullet, H\bullet] \quad (3-13)$$

where $[AO]$, $[O_2]$, $[R\bullet, H\bullet]$, and $[p]$ represent the concentrations of antioxidants, oxygen, active free radicals, and reaction products, respectively, and k' is the rate constant.

For a given incubation condition (i.e., constant pressure and temperature), both oxygen and free radical concentration are in excess and considered to be constants throughout the incubation duration. Eq. (3-13) can also be expressed as Eqs. (3-14) and (3-15). Thus, the depletion rate of antioxidants can be used to determine the kinetic mechanism of the reactions.

$$\frac{-d[AO]}{dt} = k[AO] \quad (3-14)$$

$$\ln\left(\frac{(AO)_t}{(AO)_0}\right) = \ln(OIT\%) = -kt \quad (3-15)$$

where $k = k' [O_2] [R\bullet, H\bullet]$.

At constant temperature, the $[O_2]$ in the polymer is proportional to the oxygen partial pressure in the surrounding gas (Incropera and DeWitt, 2002). At constant oxygen pressure, the $[R\bullet, H\bullet]$ increases with temperature. Thus, the k is temperature and pressure dependent.

The reaction rate of Eq. (3-9) can be governed by either a rate controlling or a diffusion limiting mechanism. In this study, the rate constant is found to be exponentially related to the oxygen partial pressure at constant temperature, as shown in Figure 3.12. Eq. (3-10) is subsequently obtained. A similar equation was also deduced by Tikuisis *et al.* (1992). They determined the HP-OIT value of a high density polyethylene geomembrane under pressures ranging from 0.7 to 5.6 MPa at isothermal temperatures of 150° to 200°C.

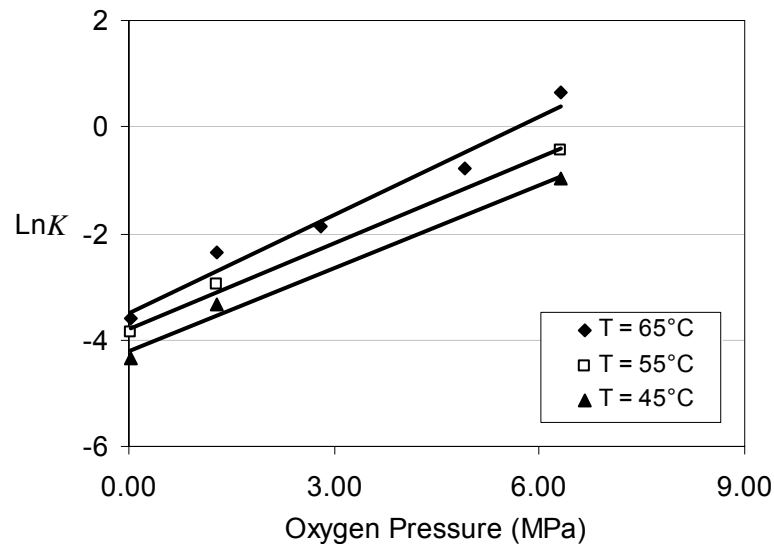


Figure 3.12 – Relationship between reaction rate and oxygen pressure

However, such an exponential relationship was not observed by other researchers in determining the effects of pressure on the oxidation degradation of polyolefins. Billingham and Walker (1975) and Boss and Chien (1966) studied the oxygen degradation of unstabilized polyolefins under very low oxygen pressures (0.0067 to 0.154 MPa). Both papers state that the oxidation reaction rate is linearly related to the oxygen pressure and is controlled by the oxygen diffusion rate at a specific temperature and pressure condition. Vink and Fontijn (2000) evaluated the oxidation of PP geotextiles under oxygen pressures from 0.007 to 0.05 MPa, and their results indicated a linear relationship between the induction time and reciprocal oxygen pressure at incubation temperatures of 140° and 150°C. Schroeder *et al.* (2000) assessed the oxidation of PP nonwoven geotextile in an aqueous solution of 0.01M NaHCO₃ under pressures of 0.1, 0.05 and 0.021 MPa. The reaction rate (reciprocal of time to 90% residual tensile strength) increases with pressure in a downward concave curve shape. The discrepancy in the reaction rate with respect to the high and low oxygen partial pressure is probably caused by the change of reaction mechanism. The exponential relationship between antioxidant depletion rate and oxygen partial pressure found in this study suggests that the reaction is not a diffusion limiting mechanism but a rate controlling mechanism. The reaction mechanism probably changes from diffusion limiting at low oxygen pressures to rate controlling at high pressures.

Effects of Pressure on Lifetime Prediction of Antioxidants

The predicted lifetimes of this particular antioxidant package at temperatures from 5° to 35°C under constant oxygen partial pressure of 0.02 MPa (1 atmosphere of air) are calculated and given in Table 3.5. The lifetime increases exponentially as the temperature decreases, according to Eq. (3-11). On the other hand, Table 3.6 shows no change in the predicted lifetime of the antioxidants when the oxygen partial pressure decreases from 0.02 to 0.005 MPa at a constant temperature. This observation does not agree with the experimental results obtained from Elias *et al.* (1999). They found that the HP-OIT depletion rate is much slower in the 0.008 MPa stagnant P_{O_2} condition than in the 0.02 MPa circulating P_{O_2} condition. However, the difference in air movement may have made some contribution to the difference in HP-OIT depletion rates.

Because of the possible change in the antioxidant reaction mechanism from low to high oxygen pressures, Eq. (3-11) may underestimate the lifetime of the geotextile in the low oxygen pressure range. However, the data analysis indicates that the prediction seems to be applicable to 0.02 MPa for this particular PP filament.

In the next section, the antioxidant depletion at low oxygen partial pressures was evaluated, to define the boundaries of the pressure ranges corresponding to different reaction mechanisms.

3.3 Antioxidant Depletion in Elevated Temperatures and Low Pressure Incubation (Series II)

3.3.1 Test Results

In Series II, elevated temperature and low oxygen pressure incubation conditions were applied to GT-sf samples. The pressure cells were filled with a N₂/O₂ gas mixture in which the oxygen partial pressure ranged from 0.005 to 0.1 MPa and the cell pressures were maintained at the level of 1 atmosphere (or 2 atmospheres in one case). Very high incubation oven temperatures, 95° and 105°C, were used to compensate for the low pressure decelerating effect on the oxidation process of GT-sf samples.

Due to the limited incubation time in the Series II experiment, only HP-OIT tests were performed on the samples, and the other physical properties were visually examined with no apparent degradation being observed. Figure 3.13 presents the low pressure HP-OIT trends over aging times of GT-sf samples. Similar to the HP-OIT curves for high pressure incubations (recall Figure 3.2), the low pressure HP-OIT values also decrease exponentially with the time. At very low partial oxygen pressure levels, 1atm (5% O₂) – 0.005 MPa [P_{O_2}] and 1atm (10% O₂) – 0.01 MPa [P_{O_2}], their HP-OIT trend curves are almost the same as those in the pure nitrogen incubation, which was designed to monitor only the temperature effect on antioxidant depletion. At the [P_{O_2}] levels of 0.015 MPa and 0.1 MPa, the antioxidant depletion rate increases with partial oxygen pressure.

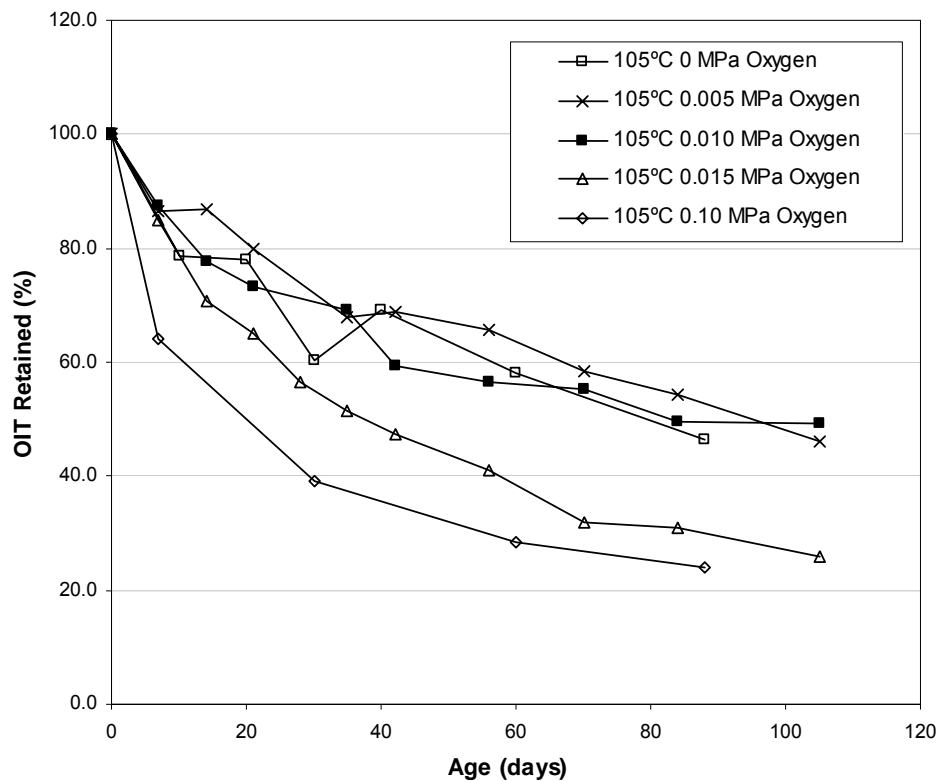


Figure 3.13 Changes in GT-sf HP-OIT retained over time at 105°C under low pressures

In the pure nitrogen incubation, there were no oxygen molecules available; the depletion of antioxidants was solely induced by the temperature volatilization. The reaction rate of this process is likely to have an Arrhenius relationship with the temperature. Recall the antioxidant lifetime prediction results in Table 3.6, which are based on Eq. (3-11). The model based on high pressure data shows that the effect of oxygen pressure level decreases exponentially and becomes almost no effect when the level approaches 1 atmosphere. This modeling prediction is inconsistent with the real experimental data shown in Figure 3.13. AO depletion data did show apparent

changes when oxygen pressure increases from 0.01 MPa to 0.015 MPa and then to 0.1 MPa.

3.3.2 Discussion

The previous section showed that antioxidant depletion rates in the PP filament were very similar in both air and oxygen when the same oxygen partial pressures were used. In this experimental series, data obtained from the 1 atm/50% oxygen incubation was compared with those obtained from the 2 atm/25% oxygen incubation which contained same oxygen partial pressure.

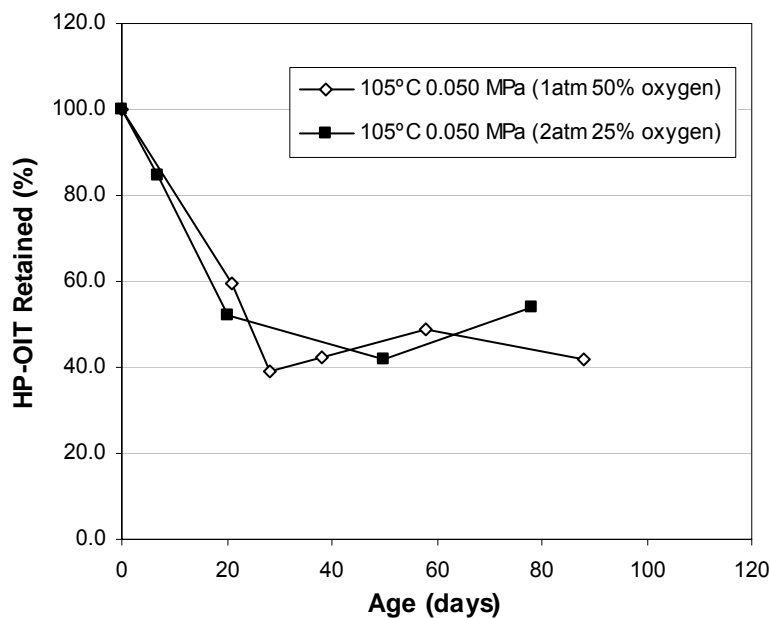


Figure 3.14 – GT-sf HP-OIT response under the same oxygen partial pressure

Figure 3.14 shows that the HP-OIT data from these two pressure cells are very similar at incubation temperatures of 105°C. Again, the results indicate that the depletion of antioxidants is controlled by the oxygen partial pressure and is not affected by the magnitude of the total pressure.

As shown in Figure 3.13, the HP-OIT retained decreases exponentially with incubation time according to Eq. (3-5), which is a first-order reaction equation for the depletion of antioxidants. Recall Eq. (3-5):

$$\ln(OIT\%) = -kt \quad (3-5)$$

where k is a reaction rate constant which is a function of the incubation temperature and the oxygen partial pressure.

Figure 3.15 and Figure 3.16 use the exponential curves from Eq. (3-5) to fit the low pressure HP-OIT data. Figure 3.15 shows that the antioxidant loss process in pure nitrogen is also related to the temperature. The antioxidant volatilization rate is higher at 105°C than at 95°C. The rate constant k values are obtained by fitting the data at each incubation condition with the exponential equation. Table 3.8 provides a comparison of low pressure AO depletion rate constant k values calculated by the Modified Arrhenius Model developed with high pressure incubation data in the last section, and the k values observed or obtained from the experimental OIT curves. It is apparent that the high pressure model is not applicable to predict low pressure rate constants, possibly because the activation energy has changed over the wide temperature range.

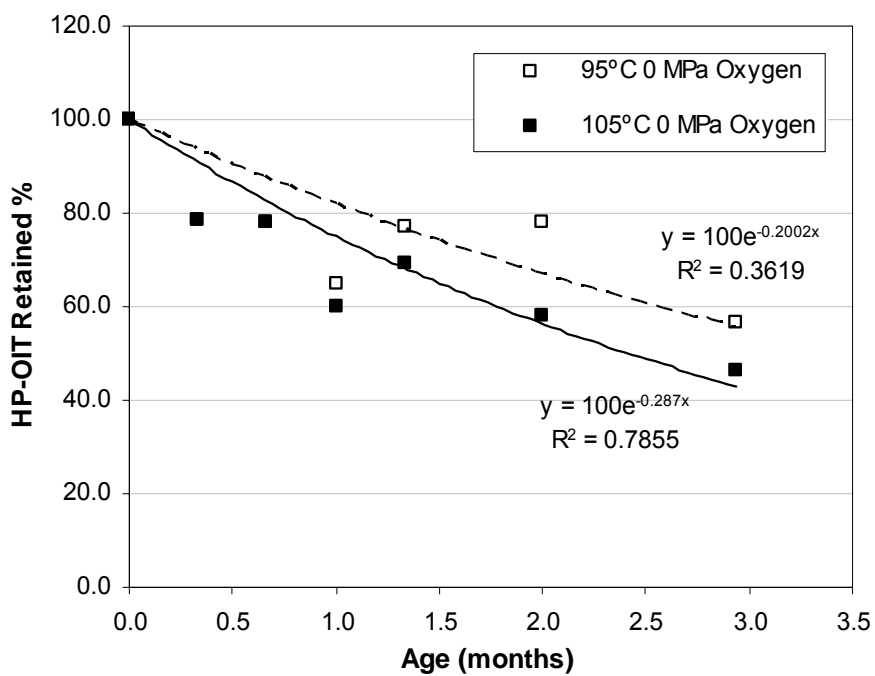


Figure 3.15 Exponential Trend Curves – OIT% vs. Time in pure Nitrogen

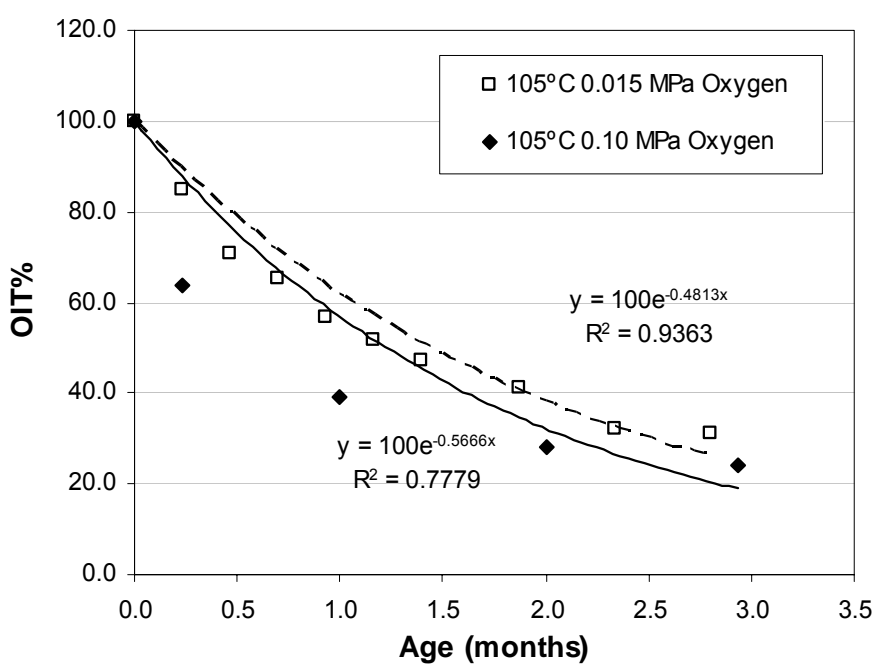


Figure 3.16 Exponential Trend Curves – OIT% vs. Time in low partial oxygen pressures

Table 3.8 – Rate Constant k Predicted values vs. Real values

Incubation Conditions	Rate Constant k Base on Eq (3-9)	Rate Constant k Experimental
95°C, 1atm (0% O ₂) – 0 MPa [P_{O_2}]	0.081	0.200
105°C, 1atm (0% O ₂) – 0 MPa [P_{O_2}]	0.108	0.287
105°C, 1atm (15% O ₂) – 0.015 MPa [P_{O_2}]	0.109	0.481
105°C, 1atm (100% O ₂) – 0.10 MPa [P_{O_2}]	0.117	0.567

3.4 Antioxidant Depletion in Elevated Temperature and Water Environment (Series IV)

In order to evaluate antioxidant extraction by surrounding liquids such as water or leachate, water incubation is carried out on the PP GT-sf samples. Figure 3.17 shows that the physical extraction process of antioxidants is also temperature sensitive. AO extraction rate increases with the temperature of the water bath, and this rate is much faster than the corresponding oven aging. But, generally, the AO depletion extraction process is faster in the early stage of water immersion than the OIT loss slow down and becomes almost constant in the second half-year.

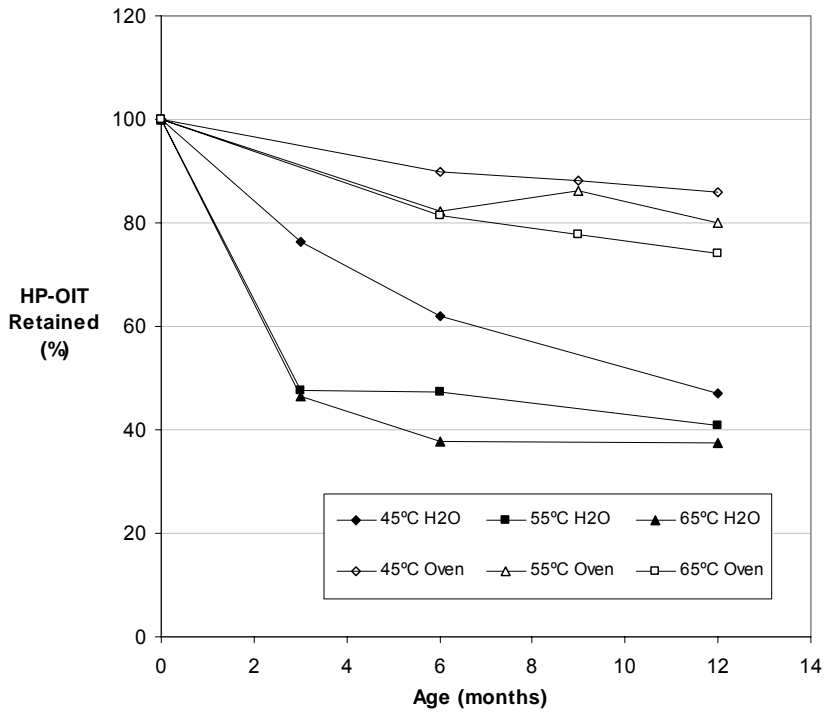


Figure 3.17 Comparisons of Antioxidant Depletion Behaviors of GT-sf in Water Environment and Regular Oven Aging

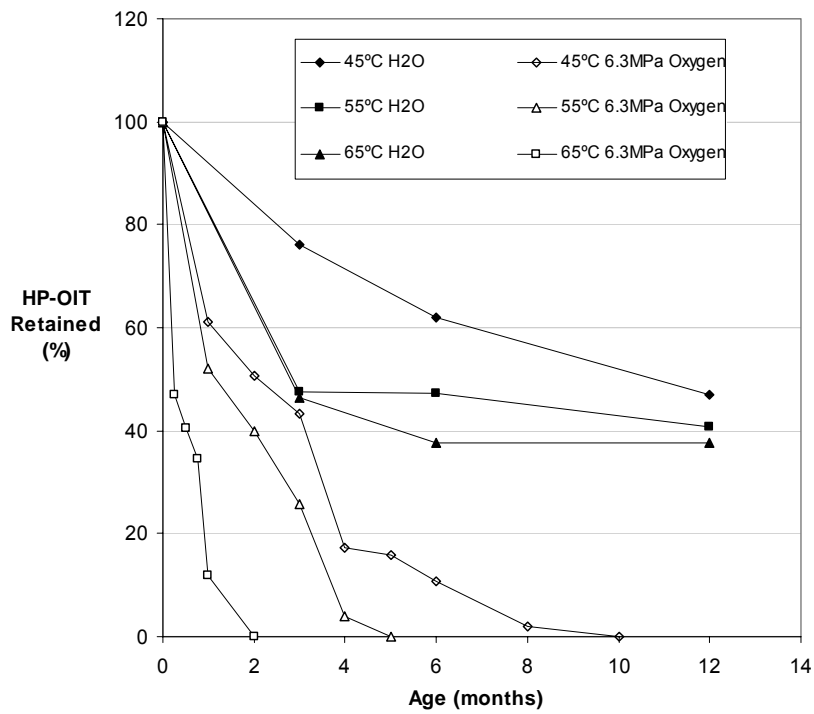


Figure 3.18 Comparisons of Antioxidant Depletion Behaviors of GT-sf in Water Environments and High-pressure Oven Aging

However, if compared with high pressure oxygen incubation, the water bath immersion process has a much slower acceleration effect on AO depletion/extraction. Oxygen concentration level makes a considerable difference in this case. Water extraction could be much faster in removing the antioxidant from the outer surface of the PP slit films in the early stage, but later on the AO needs to diffuse from the inner layers to the surface first before it can be extracted. This AO diffusion process might be a very slow one. In pressure oxygen incubation, oxygen can relatively easily diffuse into the PP slit film polymer structure to react with the polymer chain and AO. The high pressure guarantees a constant oxygen concentration gradient from the outside environment to the inside layers. This makes the oxygen pressure incubation much more effective in AO depletion than in water immersion.

3.5 Conclusions

The effects of high oxygen pressures on the depletion of antioxidants in PP GT-sf samples were evaluated by way of incubation in gas pressurized cells at temperatures of 35°, 45°, 55° and 65°C. The HP-OIT test was able to effectively monitor the depletion of the antioxidants. The HP-OIT test versus the standard OIT test was necessary since the antioxidant package contains HALS. The antioxidant depletion was governed by the partial oxygen pressure in the gas and was not affected by the total gas pressure. The test data indicate that the antioxidants ceased to function when the HP-OIT retained value reached 15% of the original value, at which point

the tensile strength started to decrease and the MI started to increase, both signaling the beginning of oxidation degradation. The Stage B “induction time of the polymer” in Figure 1.1 could not be detected under these test conditions.

An analytical model was developed to express the antioxidant reaction rate in terms of temperatures and oxygen pressures. The reaction rate increased with temperature according to the Arrhenius equation, and increased exponentially with P_{O_2} in the range of 0.02 to 6.3 MPa. The exponential relationship between the reaction rate and oxygen partial pressure indicated that the depletion of the antioxidants under the experimental conditions of this study is governed by a rate controlling mechanism which is different from other published data in the P_{O_2} range less than 0.1 MPa. By increasing the P_{O_2} in the incubation environment, the antioxidant depletion rate can be significantly modified. At a constant incubation temperature, the acceleration factor is doubled for every additional of 1 MPa of P_{O_2} .

In this chapter, the aging experiments of Series II incubation were also performed on the PP GT-sf samples applying a range of low oxygen partial pressures to assess the antioxidant depletion mechanism. At very low partial oxygen pressure levels, 0.005 MPa to 0.01 MPa [P_{O_2}], OIT trend curves are very close to those in pure nitrogen incubation, which only has temperature-induced volatilization to account for the OIT value loss over the time.

The experimental data indicate that the model to predict the lifetime of antioxidants of this particular PP tape yarn can be confidently extrapolated to 1 atmosphere of air ($0.02\text{MPa } P_{O_2}$) at site temperatures. The predicted lifetime of this particular antioxidant package at an ambient condition of 1 atmosphere and 10°C is approximately 48 years. According to the standard deviation range of OIT test values, the life prediction can be repeated using the models with regression method. The resulting AO lifetime range is from 39 years to 54 years, i.e. the average OIT data predicted value (48 years at 1 atm 10°C) plus/minus 12-16% approximately.

The prediction cannot be extended to pressures below $0.02\text{ MPa } P_{O_2}$. The low pressure data at an incubation temperature of 105°C may not have the same activation energy as the lower incubation temperatures for the AO depletion reaction, so it cannot be properly included in the modeling analysis.

AO extraction rate in water is much faster than that of regular oven aging. The AO extraction process in general is faster in the early stage of water immersion; then the loss slows down and become constant in the second half-year. However, if compared with high pressure oxygen incubation, the water bath immersion process has a much slower acceleration effect on AO depletion/extraction.

Chapter 4. Antioxidant Depletion of High Density Polyethylene Geogrids under Temperature, Pressure and Water Environments

4.1 Introduction

Geogrids have been used worldwide as reinforcement materials in walls, slopes, foundations, and base courses for more than three decades. In the past ten years, there has been a significant increase in the number of geosynthetic reinforced mechanically stabilized earth (MSE) walls. The major driving force behind such an increase is cost efficiency compared with other types of walls (Koerner & Soong, 2001). Furthermore, geosynthetic reinforced MSE walls have been integrated as critical structures into some highway systems, which require service lifetimes up to 100 years. The longevity of these geogrids is certainly being challenged. Therefore, laboratory accelerated aging is an important method to predict durability.

In a research study funded by Federal Highway Association (FHWA), the durability of a HDPE geogrid was evaluated (Elias *et al.*, 1999). However, no conclusive data was obtained regarding the lifetime of an HDPE geogrid, even after three years in forced air ovens at temperatures of 80°C and 90°C, due to the slow thermo-oxidation reaction rate of this material. The researchers also performed a preliminary study on the effect of oxygen pressure on the depletion of antioxidants. The results indicate a significant increase in the antioxidant depletion rate under a high oxygen pressure.

In this chapter, we will examine three acceleration incubation conditions which were used to evaluate the antioxidant lifetime of two high-density polyethylene (HDPE) unidirectional geogrids. Limited by the dimensions of the forced air oven and the height of the pressure cell, single rib specimens were used in the aging test, as shown in Figure 4.1. The incubation conditions of the two oven-aging series used in this study are listed in Table 4.1. All three incubation environments are briefly described as follows:

(d) Elevated temperatures and high oxygen partial pressures

Only GG-1 was assessed in Series I, in which four temperatures up to 65°C and 16 different pressure conditions were used to investigate the pressure effects. The pressure cell and pressurization system for Series I incubation were described in Chapter 2. This incubation design was identical to those described in the previous chapter on the oxidation degradation of PP slit film woven geotextiles GT-sf.

(e) Elevated oven temperature

Both HDPE geogrid products, GG-1 and GG-2, were evaluated under Series III conditions, i.e. elevated temperature oven aging. Specimens were incubated in three forced air ovens at temperatures of 55°, 65° and 75°C according to the ASTM D 5721. The geogrid specimens were fixed in position with 2.5 mm spacing between them, as shown in Figure 2.1.

(f) Elevated water temperature

GG-1 alone was assessed in the water incubation conditions, as listed in Series IV in Table 2.5. Specimens were immersed in water at temperatures of 45°, 55° and 65°C. The aging times were up to 12 months.

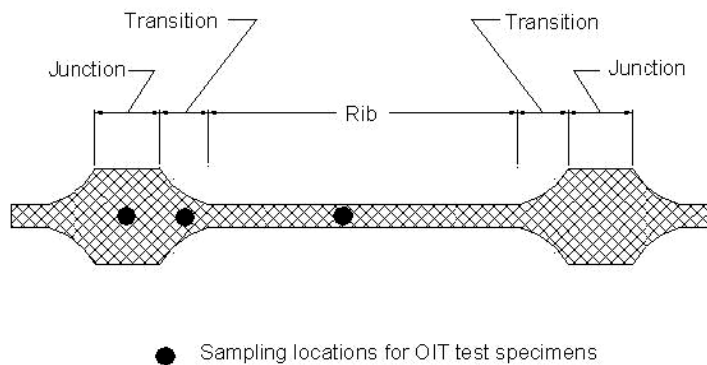


Figure 4.1 – Dimensions of single-rib geogrid specimen

Table 4.1– The different environments in two oven-aging incubation series

Condition	Series III Elevated temperature aging			Series I Elevated temperatures with high oxygen partial pressures			
	GG-1 and GG-2			GG-1			
Oven Temperature (°C)	55	65	75	35	45	55	65
Incubation Duration (month)	72	84	84	24	24	24	23
Incubation Pressure (MPa/gas)	0.1/air	0.1/air	0.1/air	0.1/air 1.3/O ₂ 2.1/air 3.5/air 4.9/air 6.3/air	0.1/air 6.3/air	0.1/air 6.3/air	0.1/air 1.3/O ₂ 2.8/O ₂ 4.9/O ₂ 6.3/O ₂ 6.3/air

Note: 0.1MPa /air means specimens were placed in ovens directly without using pressure cells.

Geogrid specimens were removed from the incubation environment at different time intervals. In Series III, the sampling intervals were 12, 24, 36, and 84 months, while in Series I and Series IV, the removal intervals varied with incubation condition, ranging from weeks to months. The retrieved specimens were evaluated for the four material properties (tensile strength, tensile break elongation, MI and OIT) described in Chapter 2, Section 2.4.

4.2 Antioxidant Depletion in Elevated Temperature Aging at Atmospheric Pressure (Series III)

4.2.1 Test Results

Figures 4.2 and Figure 4.3 show changes in the four material properties at 75°C, with incubation time for geogrids GG-1 and GG-2, respectively. Similar trends in behaviour were also observed at incubation temperatures of 55°C and 65°C. The tensile properties and MI of both geogrids remained essentially unchanged in 84 months of aging. OIT was the only property that decreased with incubation time, and the decrease rate accelerated as incubation temperature increased. After 84 months at 75°C, the OIT dropped to approximately 15% retained in both types of geogrid samples; however, the decreasing trends were significantly different between the two geogrids, indicating that their antioxidant packages are not the same. For GG-1 in Figure 4.2, the OIT exhibits a rapid initial drop and then the decreasing rate slows down. Similar OIT depletion curves were reported by Hsuan and Guan (1998) and

Mueller and Jakob (2003) in HDPE geomembranes, and Viebke and Gedde (1997) in HDPE pipes. In contrast, as shown in Figure 4.3, the OIT retained value of GG-2 decreases exponentially with incubation time, similar to those values observed in HDPE geomembranes reported by Hsuan and Koerner (1998) and Sangam and Rowe (2002). The types of antioxidants in GG-2 probably consisted of a mixture of phosphates and hindered phenols (Elias *et al.*, 1999).

For both geogrids, the OIT values in junction, transition, and rib were largely the same at all three incubation temperatures. The only exception was the rib part of GG-1 at 55°C; higher OIT retained values were consistently measured in comparison to the corresponding junction and transition regions.

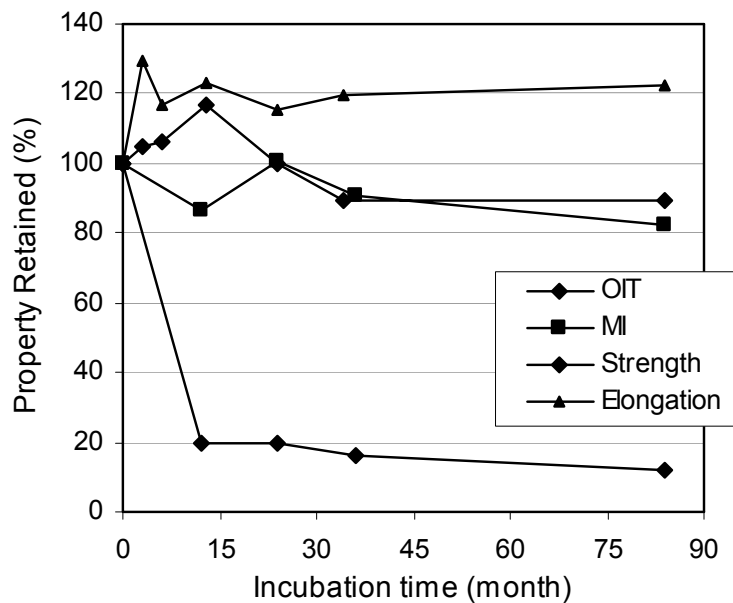


Figure 4.2 – Changes in material properties versus time for GG-1 at 75°C

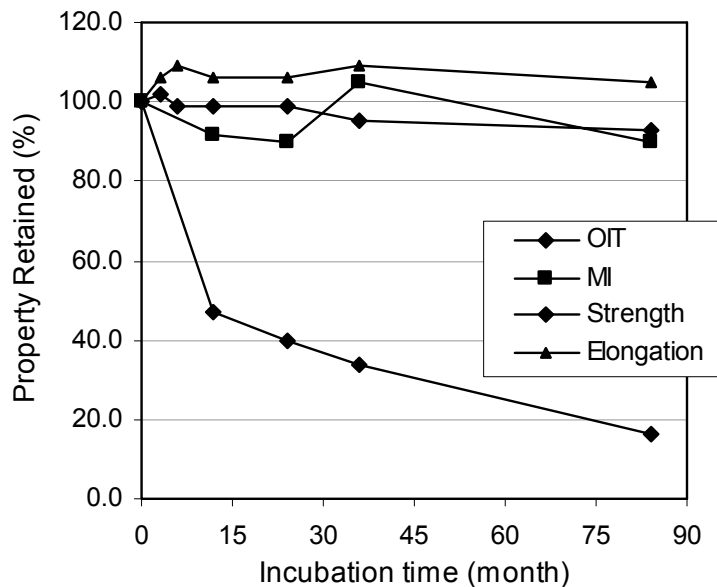


Figure 4.3 – Changes in material properties versus time for GG-2 at 75°C

4.2.2 Antioxidant Lifetime Predictions Based on Oven-Aging Data

Due to the dissimilar antioxidant depletion behaviours between GG-1 and GG-2, the methods to determine the antioxidant depletion rate (R_{AO}) must be different, while the lifetime prediction method based on the Arrhenius equation is applied to both cases. The two analytical procedures for predicting antioxidant lifetime are described as follows:

Geogrid GG-1

For GG-1, OIT data from the 1 atmosphere condition at temperatures of 35°, 45°, 55° and 65°C in Series I are incorporated into the analysis, since the exposure environments are the same, i.e., elevated temperature only. The depletion of

antioxidants in GG-1 consists of two or three regions, depending on the incubation temperature, as shown in Figure 4.4. At incubation temperatures of 65° and 75°C, two regions (Regions I and II) are observed. Region I represents the rapidly decrease in the amount of antioxidants as indicated by more than a 50% drop of the OIT value, following by a much slower decrease of the OIT value in Region II. Furthermore, the transition between Regions I and II takes place within a relatively short period of time with respect to the overall incubation duration. On the other hand, at incubation temperatures below 65°C (55°, 45° and 35°C), an “induction” region was detected prior to Regions I and II. In the induction region, the OIT value remains almost constant. The duration of the “induction” region decreases with the increasing incubation temperature.

Multiple OIT depletion rates certainly cannot be modelled by a single reaction kinetic. Viebke and Gedde (1997) utilized a bi-linear method to model similar OIT depletion behaviour in HDPE pipes at incubation temperatures of 80° and 95°C. The same method is applied to an analysis of the OIT data of GG-1 after the “induction” region. Although the number of data points in Region I at 55° and 75°C are limited, the four data points at 65°C form a good straight line. In Region II, the OIT values at all three temperatures exhibit a good straight line fit. The linear depletion rate of Region II remains unchanged until the onset of oxidation, as will be demonstrated in the aging study under high oxygen pressure in the later part of this chapter. At oxygen pressure of 6.3 MPa and 65°C, a decrease of tensile properties was detected after 23 months, at which time the average OIT retained value was 4.6% (Figure 4.8).

We estimate the critical OIT retained value to be 5%, corresponding to the onset of oxidation.

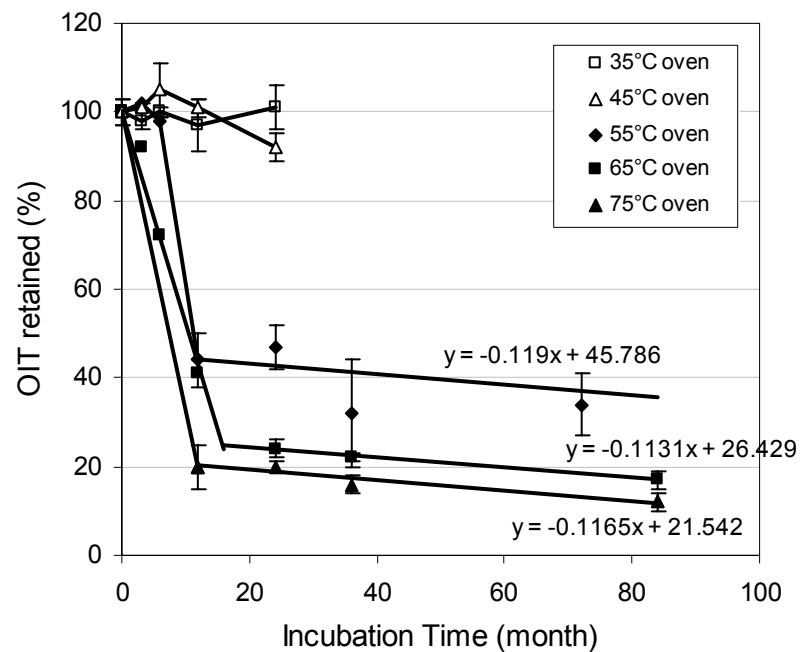


Figure 4.4 – OIT retained value versus incubation time for GG-1 in Series III at five different oven temperatures

Based on the linear equations of Region II shown in Figure 4.4, the times to reach 5% OIT retained at temperatures of 55°, 65° and 75°C are 343, 190 and 142 months, respectively. The OIT depletion rate (R_{AO}) can be calculated and then applied to the Arrhenius equation to extrapolate the OIT depletion rate at the site temperature. Figure 4.5 shows the graph by plotting $\ln(R_{AO})$ against the inverse of incubation temperature. The resulting Arrhenius equation is expressed as Eq. (4-1), which can be used to determine the reaction rate at any desired site temperature.

Knowing that the site temperatures behind three MSE walls in the northeast region of the United States range from -6°C to 20°C (Hsuan *et al.*, 2002), the maximum site temperature value of 20°C is used to extrapolate the OIT depletion rate using Eq. (4-2). The time to reach 5% OIT retained, which is defined as the lifetime of the antioxidants, is then calculated, using Eq. (4-1), to be 2,060 months (172 years).

$$R_{AO} = \frac{1}{t_{5\%OIT}} \quad (4-1)$$

$$\ln(R_{AO}) = 9.5887 - \frac{5044.9}{T} \quad (4-2)$$

Where, T = temperature (K)

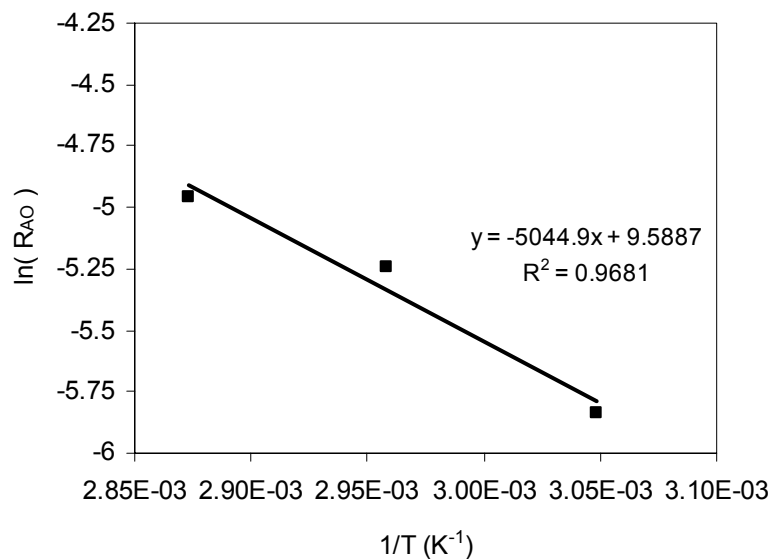


Figure 4.5 – Arrhenius plot of antioxidant reaction rate of GG-1

Geogrid GG-2

The OIT values of GG-2 decrease exponentially with incubation time at all three incubation temperatures, as shown in Figure 4.6. These behaviours are the same as those observed in the PP tape yarns, PP GT-sf (Chapter 3). Thus, the OIT depletion data can be expressed using the first order reaction, as shown in Eq. (4-3). The antioxidant depletion rate (R_{AO}) at each incubation temperature can be plotted against incubation according to the Arrhenius equation, as shown in Figure 4.7. The resulting Arrhenius equation is expressed as Eq. (4-4), which is used to extrapolate the reaction rate at 20°C and is equal to 0.0021 month⁻¹.

$$\ln(OIT\% \text{ retained}) = \ln(P) + R_{AO}t \quad (4-3)$$

Where: P = original OIT value in the product (min) = 43 minutes
 R_{AO} = OIT depletion rate (month⁻¹)
 t = incubation time (month)

$$\ln(R_{AO}) = 9.76 - \left(\frac{4664.4}{T} \right) \quad (4-4)$$

The lifetime of the antioxidants in geogrid GG-2 can be obtained by substituting the R_{AO} value of 0.0021 month⁻¹ at 20°C to Eq. (4-3). The critical OIT value at which the tensile strength starts to decrease is assumed to be the same as GG-1, at 5% retained (i.e., 43 min * 0.05 ≈ 2 minutes). The predicted lifetime of the antioxidant is therefore 1,460 months (122 years).

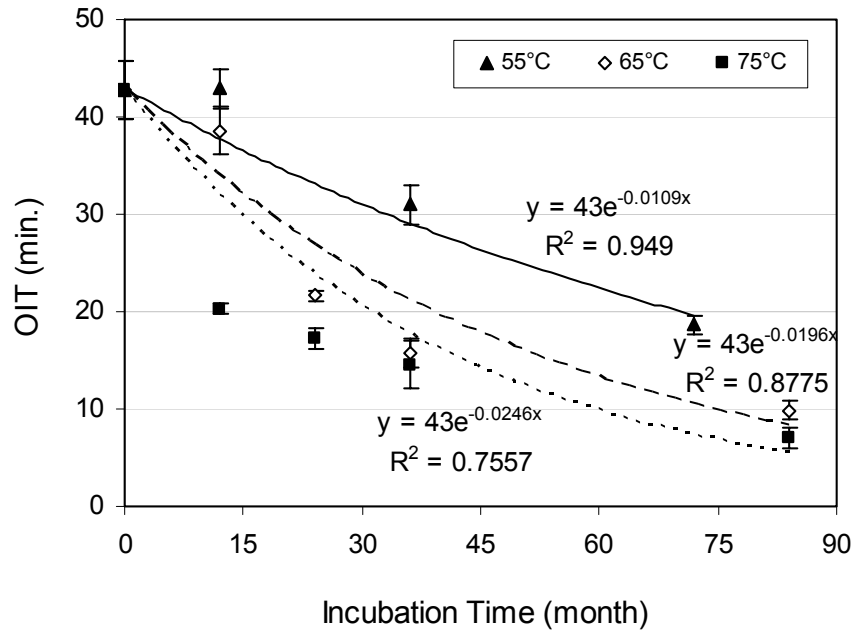


Figure 4.6 – Changes in OIT value versus incubation time for GG-2 in Series III oven aging

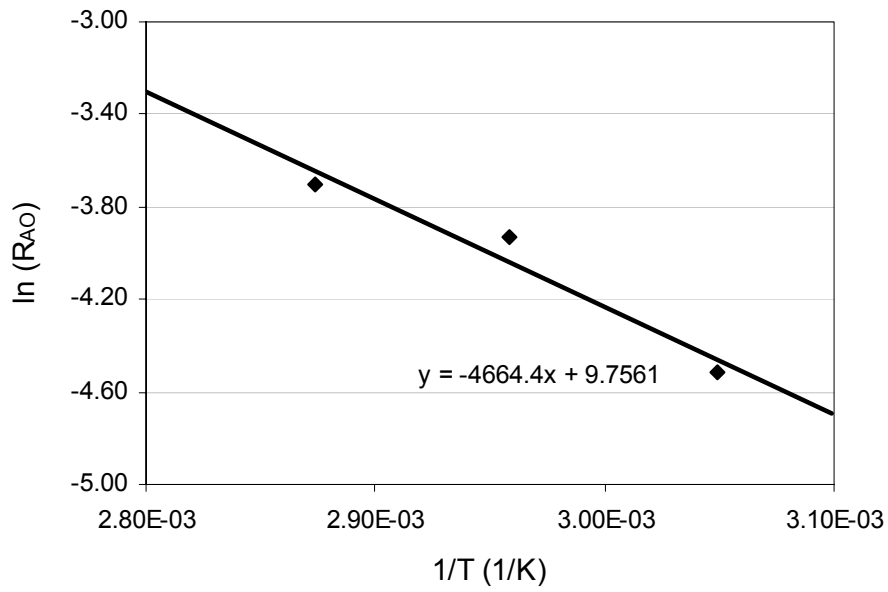


Figure 4.7 – Arrhenius plot of the OIT depletion rate of GG-2

The predicted lifetimes of antioxidants in geogrids GG-1 and GG-2 well exceeded 100 years at 20°C, which is the maximum annual average temperature behind the retaining wall. This implies that the engineering properties of both geogrids would remain unchanged for over 100 years, which is generally considered the required lifetime of most civil engineering systems.

4.3 Antioxidant Depletion in Elevated Temperatures and High Pressures (Series I)

4.3.1 Test Results

The acceleration aging study using both high pressure and elevated temperature was limited to geogrid GG-1. The incubated specimens were retrieved at different time intervals in order to monitor changes in material properties.

Figure 4.8 shows changes of four material properties versus incubation time under the most severe condition of 6.3MPa oxygen pressure at 65°C.

The MI and tensile properties remained essentially constant until 12 months, after which significant changes in these properties were detected. In the 23-month incubated specimens, the MI increased 25%, indicating that chain scissions due to oxidation had already taken place in the polymer. The oxidation degradation was also reflected by the decrease of tensile properties. The tensile strength and elongation

dropped 25% and 37%, respectively. The significant changes in MI and tensile properties signalling the onset of oxidation degradation occur between 12 and 23 months.

For the antioxidant depletion behaviour, the OIT response curves exhibited pronounced changes over time. Similar to the temperature aging, the OIT response curve consisted of two regions, Regions I and II, at this incubation condition. Region I occurred within the first three of incubation, following by Region II. After 23 months, the average OIT retained value decreased to 4.6%. Since the oxidation degradation of the geogrid took place between 12 and 23 months, the critical OIT retained is estimated to be 5%, slightly higher than 4.6%.

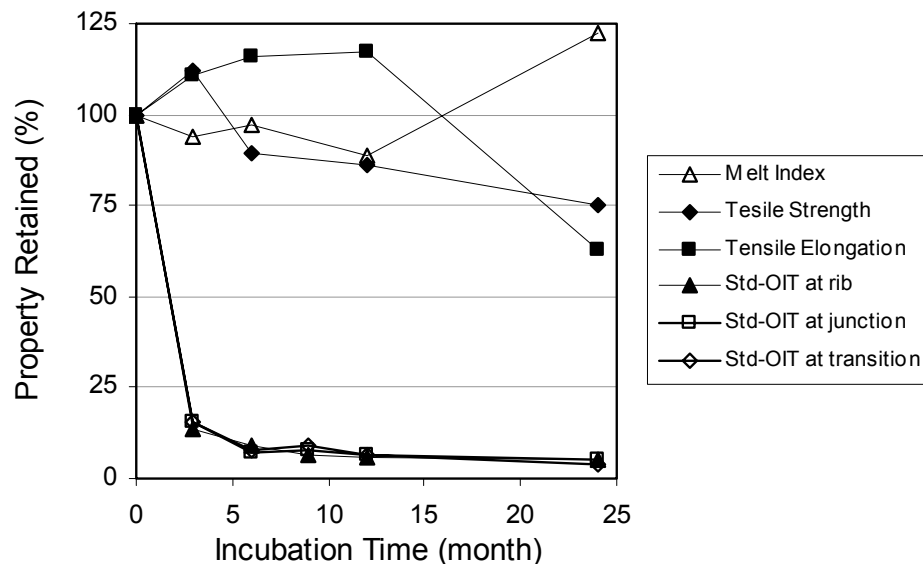


Figure 4.8 – Test results for GG-1 specimens aged at 65°C and 6.3MPa oxygen

4.3.2 Effect of oxygen pressure on OIT

In the pressure aging study of samples PP GT-sf, the OIT depletion was found to be governed by oxygen partial pressure, P_{O_2} , and not by the total pressure in the incubation cell (Chapter 3, Section 3.2.1). The same analysis was also performed on the OIT data of GG-1 by comparing OIT data between 6.3 MPa air and 1.3 MPa oxygen pressure at temperatures of 35° and 65°C, as shown in Figure 4.9. At each temperature, the OIT values are very similar under the same oxygen partial pressure but different total pressures. Therefore, for this material, all air pressures can be converted to P_{O_2} by a factor of 0.21 in the data analysis.

Figure 4.10 shows the OIT retained data under different P_{O_2} at temperatures of 35°, 45°, 55° and 65°C. Comparing these data with those obtained from oven aging at 1 atmosphere in Figure 4.4, the decrease of OIT is significantly enhanced by the oxygen pressures. The OIT retained value decreased to 20% at 45°C after 24 months under 1.3 MPa P_{O_2} , while no changes were observed in the oven aging condition. At an incubation temperature of 65°C, the decrease rate of OIT retained value increases with oxygen pressure.

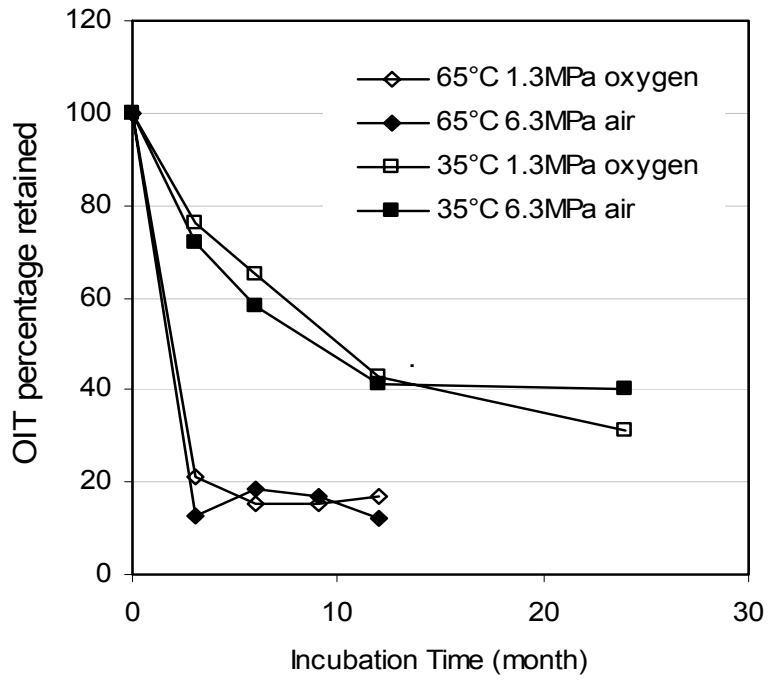


Figure 4.9 - OIT response of GG-1 at same oxygen partial pressure at 35°C & 65°C

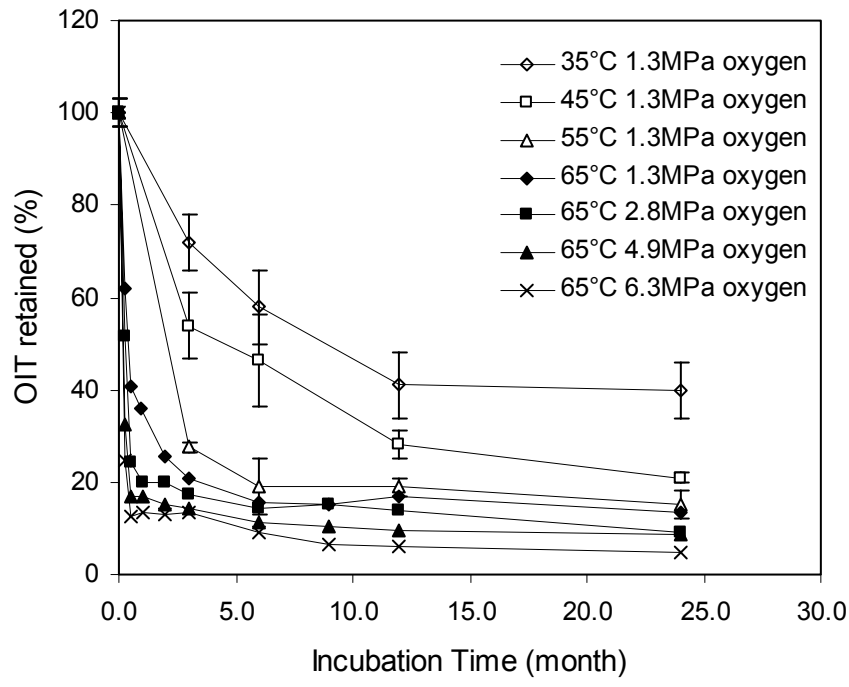


Figure 4.10 – OIT response curves of GG-1 at different temperatures and oxygen pressures

4.3.3 Antioxidant Lifetime Prediction Based on Aging Data in Elevated Temperatures and High Pressures

The OIT data of GG-1 is analyzed using the same bi-linear method as the temperature series. The model is applied to data obtained from incubation temperatures of 55° and 65°C; however, insufficient data are available to establish the slope of Region II at 35° and 45°C. Figure 4.11 shows the linear OIT retained curves of Region II at 65°C under four pressures. The linear equations at each pressure are used to calculate the time to reach OIT retained at 5%, and subsequently the R_{OA} , as shown in Table 4.2. (Note that the 0.02 MPa oxygen curve is not included in the figure but is included in the table.) The relationship between R_{OA} and oxygen pressure is shown in Figure 4.12.

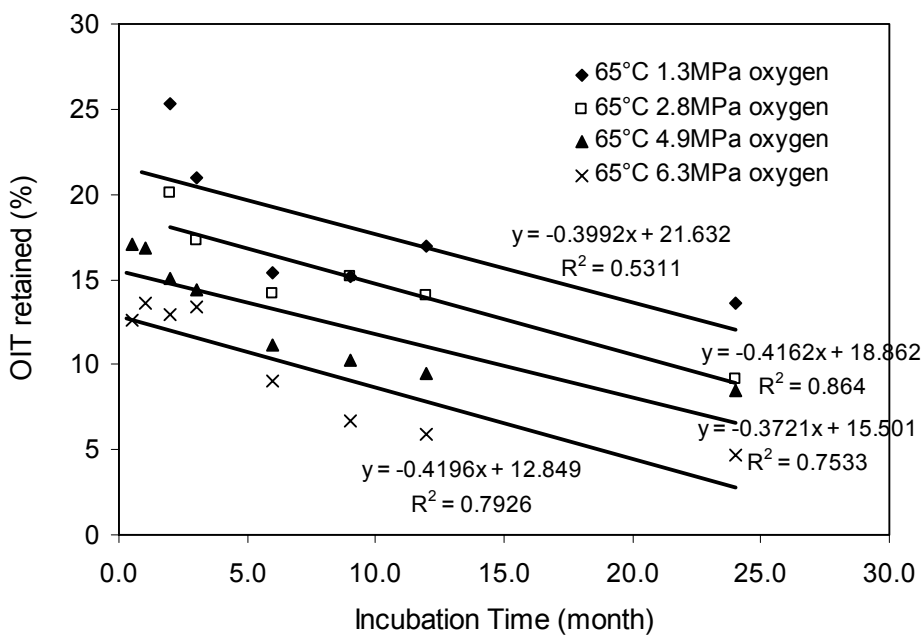


Figure 4.11 – Re-plotting Region II of the OIT curves in Figure 4.10

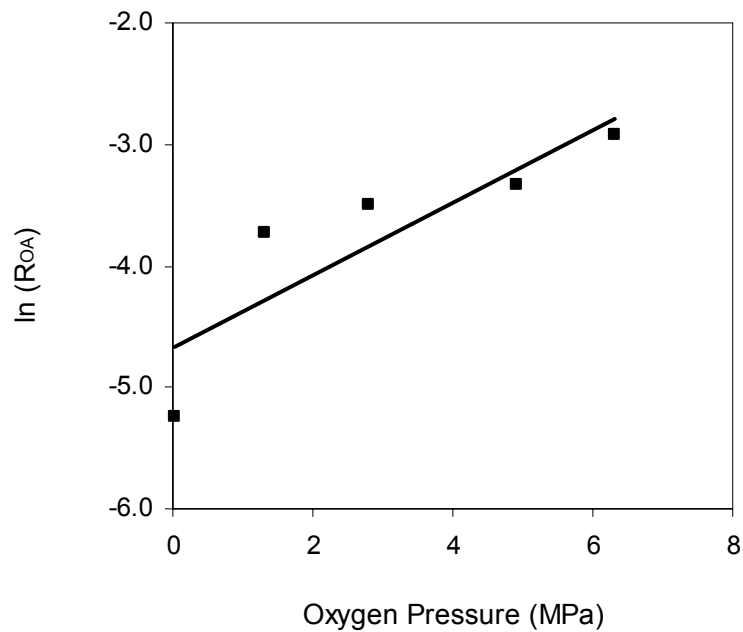


Figure 4.12 – $\ln(R_{OA})$ versus oxygen pressure at 65°C for GG-1

Table 4.2 – Data used to obtain antioxidant depletion reaction rates

Temperature (°C)	O ₂ Pressure (MPa)	Equation	t _{5%OIT} (month)	R _{OA} = 1/ t _{5%OIT}	ln(R _{OA})
65	0.02	t _{5%} = (26.4 - 5)/0.11	189.5	0.0053	-5.24
	1.3	t _{5%} = (21.6 - 5)/0.40	41.7	0.0240	-3.73
	2.8	t _{5%} = (18.9 - 5)/0.42	33.3	0.0300	-3.51
	4.9	t _{5%} = (15.5 - 5)/0.37	28.2	0.0354	-3.34
	6.3	t _{5%} = (12.9 - 5)/0.42	18.7	0.0535	-2.93

The data shown in Figure 4.12 are fitted with a straight line indicating an exponential relationship between the two parameters, as shown in Eq. (4-5).

$$R_{OA} = 0.00942 * e^{0.299 [P_{O_2}]} \quad (4-5)$$

In order to develop an equation that correlates reaction rate (R_{OA}) in terms of temperature and pressure, the relationship between the reaction rate and temperature and pressure must be evaluated. It was found in Chapter 3 that the activation energy of the Arrhenius equation is pressure dependent in PP GT-sf samples, and the reaction rate in terms of temperature and pressure is expressed by Eq. (4-6). However, the analytical procedure cannot be performed on the available data of the GG-1. The slow antioxidant depletion rates at the lower incubation temperatures could not provide sufficient changes in the OIT data to explore the interactions among activation energy, pressure, and temperature. In spite of such limitation, it is reasonable to assume that Eq. (4-6) can be applied to analyse the antioxidant reaction rate (R_{OA}), which is equal to k , since Eq. (4-5) confirms that the antioxidant depletion is a rate-controlling mechanism, the same as that in the PP GT-sf sample.

$$k = C \cdot EXP \left[-\frac{E_{ao} + \alpha P_{O_2}}{R} \cdot \frac{1}{T} + \beta P_{O_2} \right] \quad (4-6)$$

where:

- P_{O_2} = incubation partial oxygen pressure (MPa),
- R = gas constant (8.31 J/mol-K)
- T = incubation temperature in absolute value (K)
- E_{ao} = constant, Arrhenius activation energy (kJ/mol) at 1atm pressure condition (i.e., 0.02MPa of oxygen),
- C, α, β = constants which are independent of T and P_{O_2} , and determined by polymer type and antioxidant package.

The constants E_{ao} , C , α and β are deduced from seven sets of incubation data listed in Table 4.3, using a least square multi-variable linear regression method. The four constants thus obtained are as follows:

$$E_{ao} = 40.3 \text{ kJ/mol} \qquad C = 10779.5 \text{ month}^{-1}$$

$$\alpha = 1.931 \text{ m}^3/\text{mol} \qquad \beta = 0.309 \text{ MPa}^{-1}$$

Based on Eq. (4-6) and the four constants, the relationship among $t_{5\%OIT}$, temperature and pressure can be illustrated in a three-dimensional plot, as shown in Figure 4.13.

The lifetime of the antioxidant at a site temperature of 20°C and 1 atmosphere (0.02MPa oxygen partial pressure) is calculated to be 1,390 months (116 years). This predicted lifetime is slightly shorter than that predicted from the temperature alone. One possible source of error in the temperature/pressure prediction is the lack of low temperature data. Table 4.3 shows that the pressure effect relied only on data at 65°C.

Table 4.3 – Test data used to obtain four constants in Eq. (4-6)

Temp (°C)	55	75	65	65	65	65	65
Temp (K)	328	348	338	338	338	338	338
P_{O_2} (MPa)	0.02	0.02	0.02	1.3	2.8	4.9	6.3
$t_{5\%OIT}$ (month)	342.7	142.0	189.5	41.66	33.31	28.22	18.71
R_{OA} (1/month)	0.0029	0.0070	0.0053	0.0240	0.0300	0.0354	0.0535
$\ln(R_{AO})$	-5.8369	-4.9558	-5.2442	-3.7296	-3.5057	-3.3401	-2.9288

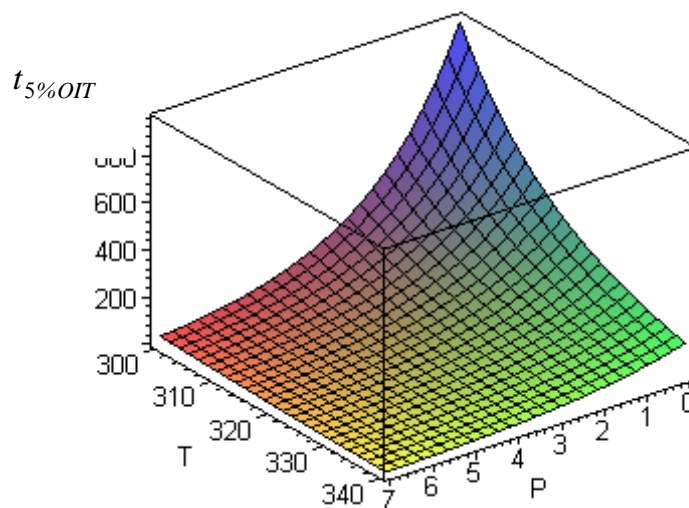


Figure 4.13 – Relationship among $t_{5\%OIT}$, temperature and pressure for GG-1

4.3.4 Discussion

The oxidation resistance of two HDPE geogrids, GG-1 and GG-2, was evaluated using two different incubation methods. Series III is a temperature aging method and Series I is temperature and pressure aging method.

In Series III, no changes in MI or tensile property were observed in either GG-1 or GG-2 after 84 months (7 years) even at the highest incubation temperature of 75°C. Temperature aging could not provide sufficient acceleration to reach oxidation degradation within the study time period. In contrast, substantial changes were detected in MI and tensile properties of GG-1 after an incubation duration of 23

months at 65°C under 6.3 MPa P_{O_2} . The combination of high P_{O_2} and elevated temperature greatly accelerates the oxidation process, and oxidation degradation could be achieved in the range of 2 to 5 years, depending on the incubation condition.

For the antioxidant depletion rate, the standard OIT test was used to determine the amount of antioxidants in the incubated specimens. The OIT response curves of GG-1 and GG-2 are significantly different, reflecting different types of antioxidants in each of the geogrids.

For GG-1, the OIT response curve consists of two or three regions, depending on the incubation condition. At low temperatures and pressures, an “induction” region is observed prior to Regions I and II. In Region I, the OIT retained value drops rapidly and then quickly converts to Region II, in which gradual changes are detected. One of the possible causes for such abrupt change is that one of the chemical compounds in the antioxidant package has a much faster reaction rate than the others and is completely consumed in the early stage of the aging. In addition, the reaction rate of this particular antioxidant compound is more sensitive to incubation temperature than to P_{O_2} . As shown in Figure 4.10, the slopes of Region I change greatly from 35° to 65°C. For Region II, the slopes of lines (OIT decreasing rates) are very similar in each set of data.

Due to the multiple depletion mechanisms of antioxidants in GG-1, the OIT data are analyzed using a bi-linear method that was described by Viebke and Gedde

(1997). The reaction rate of the antioxidant depletion is determined by the time to reach a critical OIT retained value at which the onset of oxidation begins. The oxidation degradation of the GG-1 took place between 12 and 23 months of exposure in 6.3 MPa P_{O_2} at 65°C. The onset of the oxidation was estimated to be at 5% OIT retained. Subsequently, the antioxidant reaction rates at different incubation temperatures were determined. The lifetime of antioxidants in GG-1 at a site temperature of 20°C can be predicted using Arrhenius equation, and it is 172 years.

In the Series I incubation conditions, the minor decrease in OIT retained values at temperatures of 35° and 45°C is insufficient to establish a reliable Region II; thus, data from these two temperatures are omitted from the analysis. By omitting the lower temperature data, the complete analysis to assess the relationship among reaction rate, temperature and oxygen pressure was unachievable. However, an exponential relationship was obtained between reaction rate and P_{O_2} , substantiating the applicability of Eq. (4-6) to the GG-1 data. However, the calculation of the four constants in the Eq. (4-6) relied heavily on OIT data obtained from the high incubation temperatures and P_{O_2} . As a result, the uncertainty in the lifetime prediction at 20°C and 0.02 MPa P_{O_2} increases. The predicted lifetime using Eq. (4-6) is 116 years. When we compare the predicted lifetimes of 116 years to 172 years from the oven aging, they are essentially the same, considering the overall variability in the data.

The antioxidant depletion rate of GG-1 is greatly enhanced by the increase of P_{O_2} . At 65°C temperature aging, the predicted time to reach 5% OIT retained is 210 months, which was shortened by a factor of 15 to 14 months by increasing P_{O_2} from 0.02 MPa to 6.3 MPa. Interestingly, the pressure acceleration was found to be inversely related to the temperature. An acceleration factor of 17, 15 and 12 was measured for temperatures of 55°, 65° and 75°C, respectively when P_{O_2} increases from 0.02 MPa to 6.3 MPa.

For GG-2, the OIT retained values decrease exponentially with incubation time and the depletion rate obeys the first order reaction. The critical OIT value used in the prediction is assumed to be the same as the GG-1 and is 5% OIT retained (or 2 minutes OIT value), and the predicted lifetime of antioxidants in GG-2 under elevated temperature aging is 122 years. This critical OIT% assumption seems to be reasonable, since the average OIT value of GG-2 after seven years in 75°C oven-aging is as low as 6 minutes, or 15% of the original OIT value, whereas there was still no indication of oxidation degradation in tensile or MI properties for the aged samples.

4.4 Antioxidant Depletion in Elevated Temperature and Water Environment

OIT curves for water-immersed GG-1 at different water bath temperatures are shown with solid symbols in Figure 4.14 and Figure 4.15.

By observing the OIT trend lines, it was found that the temperature effects are very much manifest, particularly for the highest temperature 65°C condition, for which the OIT% retained after 12 months dropped to 44%, while at both 45°C and 55°C, 12-month OIT% values were still around the level of 80%. A quantitative modelling AO lifetime analysis can hardly be performed on this series because the 45°C and 55°C curves are too close to each other. After six months' immersion time, the OIT curves for the two temperatures essentially overlap.

Figure 4.14 compares the water environment effect and regular oven (1 atm) environment effect on AO depletion of GG-1 at the same temperatures. At earlier age and lower temperatures, the water-immersed samples tend to have a faster AO depletion rate than the oven aging samples, while at the age of 12 months, the 55° and 65°C oven samples have OIT% values very similar to the water samples. Generally, it seems that the water extraction effects on the antioxidant are more noticeable at early ages, and after a certain time the OIT values for water samples tend to be constant with the aging time. This is shown in the 45°C and 55°C water sample OIT curves' horizontal parts beyond six months.

Although 65°C water sample OIT% values keep decreasing linearly with the aging time, there is no evidence to prove that this trend could last for longer times. Recall the water immersion aging test results for GT-sf. In Figure 3.17 the stronger water extraction effects could be observed for the thinner polypropylene materials; however, at all three temperatures the water OIT curves all tend to be horizontal with the increasing aging time.

Figure 4.15 compares the water environment effect and high pressure cell environment effect on AO depletion of GG-1 at the same temperatures. At all three temperatures, the 1.3 MPa oxygen pressure seems to be much more effective in depleting the antioxidants than the water immersion environment. It should be noted that the pressure effect is also more apparent in early stages, especially in the first three months.

The bi-linear model observed in both water and pressure samples could be explained with the antioxidant diffusion limitation and material dimensions of HDPE geogrids. Water extraction, presumably, only works for surface antioxidants just as was the case with the GT-sf. On the other hand, the pressure effect of AO depletion is induced by oxygen molecule diffusion into the geogrid HDPE polymer structure, and this diffusion process is very much limited by polymer density, crystallinity, and geometric dimensions. Thus, after the early age when the outer surface antioxidants are basically depleted, the following AO depletion process tends to be very much slower because of the limitations mentioned above for both antioxidant and oxygen.

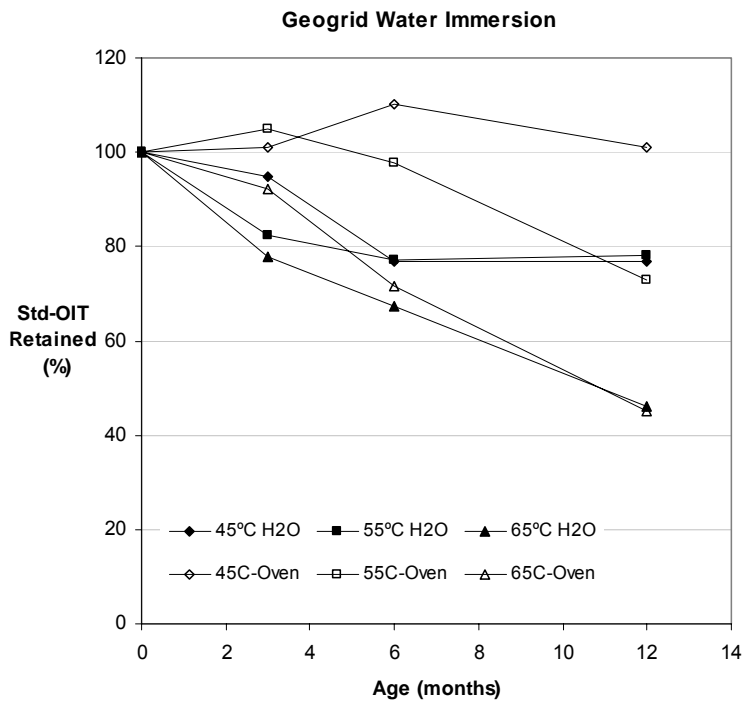


Figure 4.14 Comparisons of Antioxidant Depletion Behaviors of GG-1 in Water Environment and Regular Oven Aging

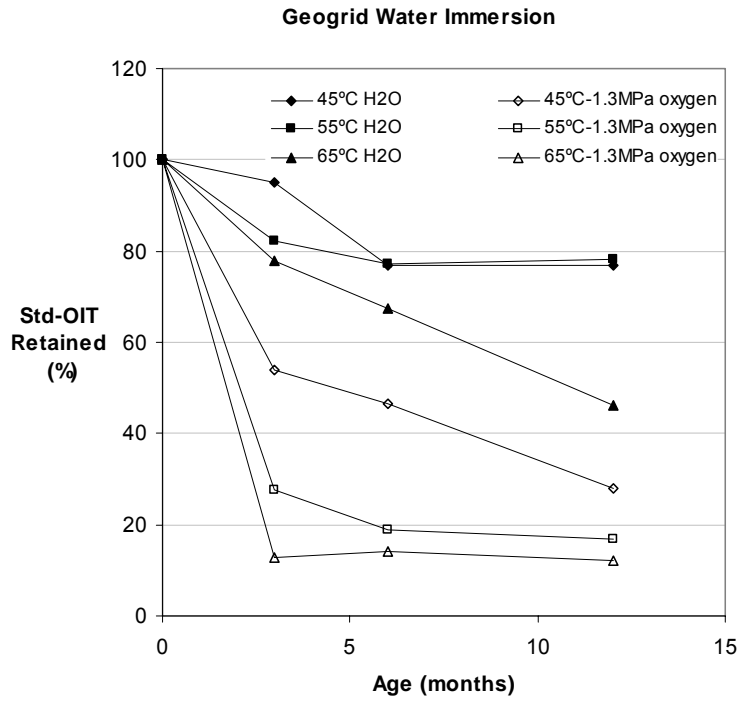


Figure 4.15 Comparisons of Antioxidant Depletion Behaviors of GG-1 in Water Environments and High-pressure Oven Aging

4.5 Conclusions

The oxidation resistance of two types of HDPE geogrids, GG-1 and GG-2, was evaluated using oven aging incubation at five elevated temperatures. In addition, GG-1 was aged under 16 incubation conditions with different combinations of elevated temperatures and high pressure. GG-1 was also immersed in water baths maintained at three different temperatures. The results concluded from the study are as follows:

1. The data confirm that the tensile properties and melt index of incubated specimens remain unchanged as long as a critical amount of antioxidants exist in the materials
2. The critical OIT retained value is 5%, after which oxidation degradation starts to take place
3. The antioxidant depletion mechanisms are not the same for GG-1 and GG-2. A bi-linear OIT depletion curve was obtained for GG-1. For GG-2, the OIT decreased according to first order of reaction
4. The Arrhenius equation was applied to predict the lifetimes of antioxidant packages based on temperature acceleration tests. The antioxidant lifetimes at 20°C site temperature are 172 and 122 years for GG-1 and GG-2, respectively.

- Both values well exceed the 100-year design life for many transportation systems. Thus, mechanical properties of the geogrids would not change during their service lifetimes
5. The predicted lifetime of antioxidants in geogrid GG-1 under the combined effects of elevated temperature and high pressure is 116 years at a site temperature of 20°C and one atmosphere. This value is essentially the same as the lifetime value obtained from temperature acceleration alone but the needed incubation time could be reduced from 7 years (oven) to 2 years (oven plus pressure cell).
 6. A high P_{O_2} can significantly accelerate the oxidation degradation of geogrid GG-1 by accelerating the antioxidant depletion rate
 7. AO depletion rates for GG-1 in water immersion conditions also increase with rising incubation temperatures. The temperature effects are manifest, particularly at the high temperature, 65°C condition
 8. Water extraction rate of GG-1 AO loss is higher than oven aging but lower than pressure incubation at 1.3 MPa oxygen and the same temperatures
 9. Water extraction effects on the antioxidant are more noticeable at early ages and, after a certain time, roughly six months, the AO depletion rate tends to slow down

and OIT curves become horizontal. Similar phenomena are also observed in pressure incubation of GG-1, possibly because AO or oxygen diffusions within the polymer are limited by high density, crystallinity, and geometric dimensions of the GG-1 HDPE polymer structure.

Chapter 5. Oxidative Behaviors of Polypropylene Nonwoven Geotextiles under Temperature, Pressure and Water Environments

5.1 Introduction

Polypropylene nonwoven geotextiles are widely used for separation, filtration, reinforcement, drainage, and erosion control in both transportation and environmental applications. Applications related to transportation include base course separation in highways and airports, reinforcement in retaining walls, filtration/separation in pavement side-drains and soil erosion protection. For environmental applications, particularly in landfill systems, nonwoven geotextiles are used in the following functions:

- Filtration: block for the liquid collection systems against clogging caused by soil or waste particles carried by the liquids.
- Cushion: The barrier systems include a thin geomembrane that must be protected from puncture.
- Bio-barrier: Impregnated with a biocide agent, geotextiles are being used to limit root penetration into the landfill system.
- Barrier: Geosynthetic clay liners (GCL) use geotextiles to confirm bentonite granules into sheets that can be used to form liners.

Long-term performance of the geotextile is required in many of the transportation and environmental applications. In the introduction section of Chapter 1, it was stated that the landfill lifetime requirement could be up to hundreds of years

whereas a design life of 100 years is commonly required in critical transportation systems.

This chapter focuses on the antioxidant (AO) depletion behaviors of the PP nonwoven geotextiles, GT-nw, under incubation conditions of elevated temperatures and high oxygen partial pressures, along with the water immersion conditions. The chemical properties of nonwoven geotextile have been found to be highly scattered with large standard deviation (Elias *et al.*, 1999). This can be caused by the variation in the degree of drawn in each fiber, poor distribution of antioxidants in the fiber(s), variation in the fiber diameters and the high specific surface area making fibers more susceptible to be attacked by oxygen. All these factors can lead to inconsistent AO depletion rates from sample to sample. Therefore, a reliable quantitative analysis can only be achieved using a large specimen size and large number of the test specimens and tests. Unfortunately, such requirements are not possible in the design of this incubation study. However, a qualitative assessment of AO depletion can still be performed and is presented in this chapter.

Nevertheless, in order to monitor the material property degradation of GT-nw, tensile properties were evaluated and data were analyzed. Melt Flow Index results are not included in our discussion because data are too variable to follow any reasonable trends. Fibrous material itself has very large original standard deviation; also nonwoven fibers cannot be placed into the MI testing barrel within two minutes,

therefore oxidation might have already happened during the pre-testing time which may lead to further variations within the test results.

The nonwoven geotextile used in this study is a polypropylene staple needle punched geotextile with unit weight of 335 g/m². Specimens with dimensions of 50 mm wide and 150mm long were incubated in Series I and Series IV conditions. The specific incubation conditions in Series I are shown in Table 5, including

(g) Elevated temperatures and high oxygen partial pressures

See Table 5.1

(h) Elevated temperature water immersion

The aging conditions for Series IV are shown in Table 2.5. Specimens were immersed in water at temperatures of 45 °C, 55 °C and 65 °C. The aging times were up to 12 months.

Table 5.1 – High Pressure Incubation environments for aging GT-nw geotextiles

	Oven Temperature (°C)			
	35	45	55	65
Incubation Pressure (MPa)	0.1 air	0.1 air	0.1 air	0.1 air
	6.3 air	6.3 air	6.3 air	6.3 air
	1.3 O ₂	--	--	1.3 O ₂
	--	--	--	2.8 O ₂
	--	--	--	4.9 O ₂
	--	6.3 O ₂	6.3 O ₂	6.3 O ₂
Incubation Duration (months)	24	24	24	up to 16

Note: 0.1 MPa air means samples were placed in ovens directly without using the pressure cells since 1atm = 0.1MPa.

5.2 Oxidative Behaviors in Elevated Temperatures and High Pressures (Series I)

Similar to other nonwoven geotextile, large standard deviations resulted in measured material properties in all incubation conditions. For the OIT test, 5 replicates were performed in each group of the incubation specimens; the majority of the coefficient of variation is in the range from 15% to 20%, and the highest value is 32% maximum. For the tensile strength and elongation, which were obtained by performing a 25 mm strip tensile test, 5 replicates were tested for each group of incubation specimens; the majority of the coefficient of variation is in the range from 25% to 30% on average, but values up to 70% was resulted in some cases. With such a large variation in the data, the reliability of the analysis is questionable. Nevertheless, it is possible to assess the changing trends of the material property in some of the incubation conditions, such as flowing air and highest oxygen concentration, to get a general sense of the oxidation degradation in this particular PP nonwoven geotextile.

5.2.1 Depletion of Antioxidants

The depletion of antioxidants in the PP GT-nw was measured using HP-OIT. The coefficient of variation for the as-received sample is as high as 17.7%, and the variation value is even higher for retrieved incubated specimens. However, no correlation was found between the variation value and incubation temperature, pressure or time.

Trend curves in Figure 5.1 and Figure 5.2 show OIT depletion over the aging time at different elevated temperatures in 1-atm circulating air and 6.3 MPa air pressure cells.

It appears that the circulating air has an apparent effect in accelerating antioxidant depletion. Although the oxygen concentration is much higher in the 6.3 MPa air pressure cells, the OIT curves in Figure 5.2 show almost no changes over 24 months of aging times when the large standard deviations are taken into account. In contrast, the OIT retained values show a gradual decrease in circulating air conditions, Figure 5.1. It is believed that the AO depletion in circulating air ovens was mainly caused by the physical extraction during the 24 months period. In addition, the physical extraction is somewhat temperature dependent.

For incubations at 65°C and different pressures, Figure 5.3, it seems that the OIT retained values were not affected by pressures below 4.9 MPa. Under 6.3 MPa oxygen (Figure 5.3), a progressive decrease in OIT retained value can be observed. The oxidative degradation under this condition will be further analyzed in the Discussion section of this chapter along with tensile data. It should be noted that this type of OIT curves, with no change or very little change over duration of age, were also observed at lower incubation temperatures of 35°C, 45°C and 55°C with different pressure conditions (not shown).

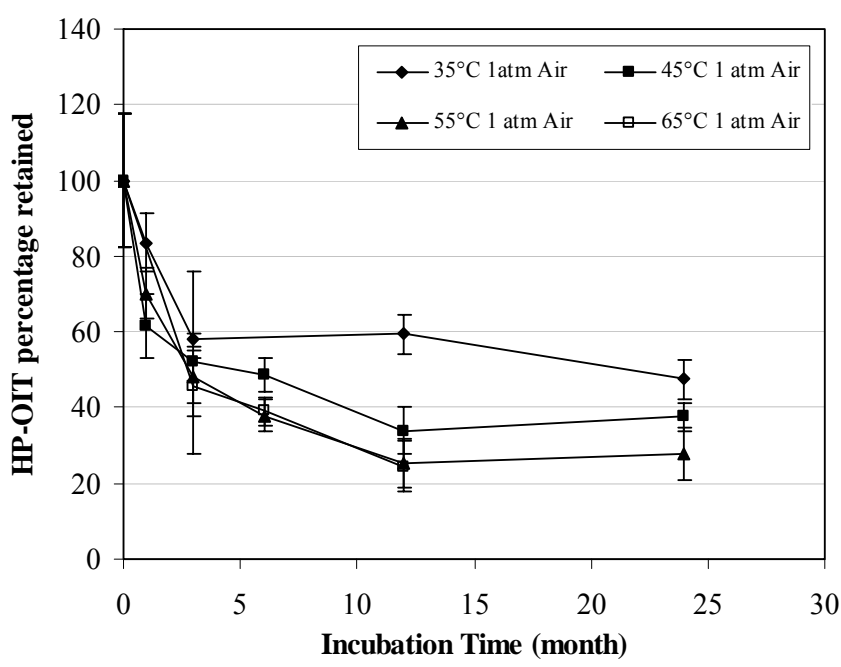


Figure 5.1 Changes in HP-OIT of GT-nw over time in 1-atm circulating air oven at different temperatures

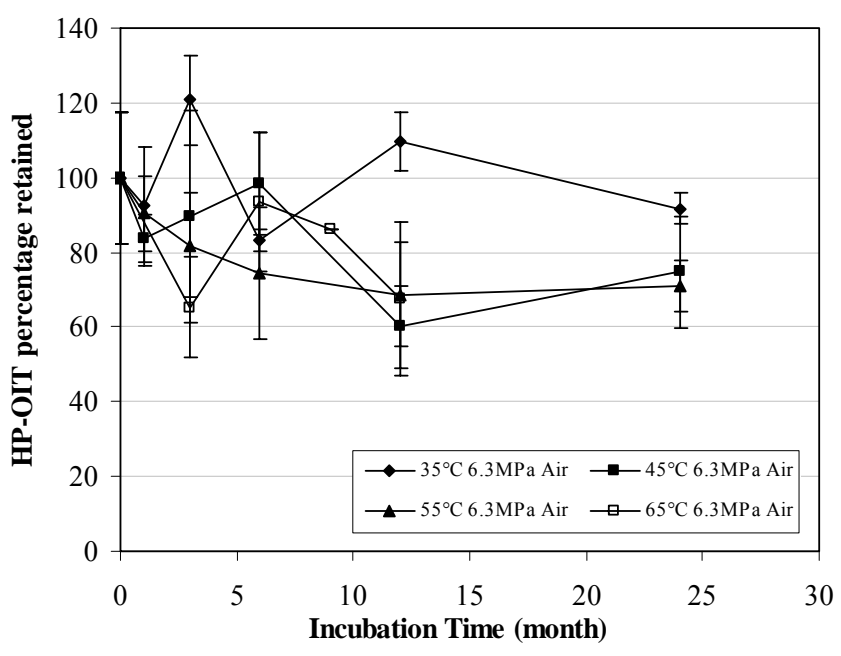


Figure 5.2 Changes in HP-OIT of GT-nw over time under 6.3 MPa air pressures at different temperatures

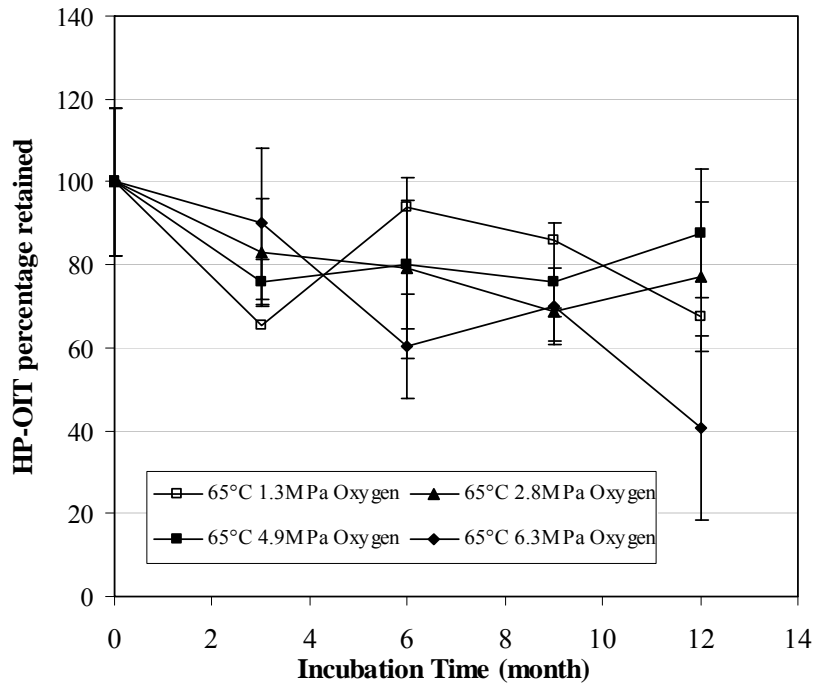


Figure 5.3 Changes in HP-OIT of GT-nw over time at 65°C under different oxygen pressures

5.2.2 Tensile Property

The GT-nw samples were exposed to four temperatures of 35, 45, 55 and 65°C in circulating air and in closed cells with various pressures. The coefficient of variation for tensile strength and elongation of as-received samples were less than 10%. However, after incubation, the coefficient of variation become much larger, i.e. 20% to 30% in average, and as high as 70% in some cases. It is believed that non-uniform fibrous structure distribution in the nonwoven textile product should be the reason for the observed large standard variation in sample tensile strength.

Typical tensile curves of 65°C at different pressure levels are shown in Figure 5.4 and Figure 5.5. The variability of tensile strength seems to be greater than that of tensile elongation. However, there is no apparent decrease in both properties. At lower temperature conditions (not shown), similar behaviors were also observed.

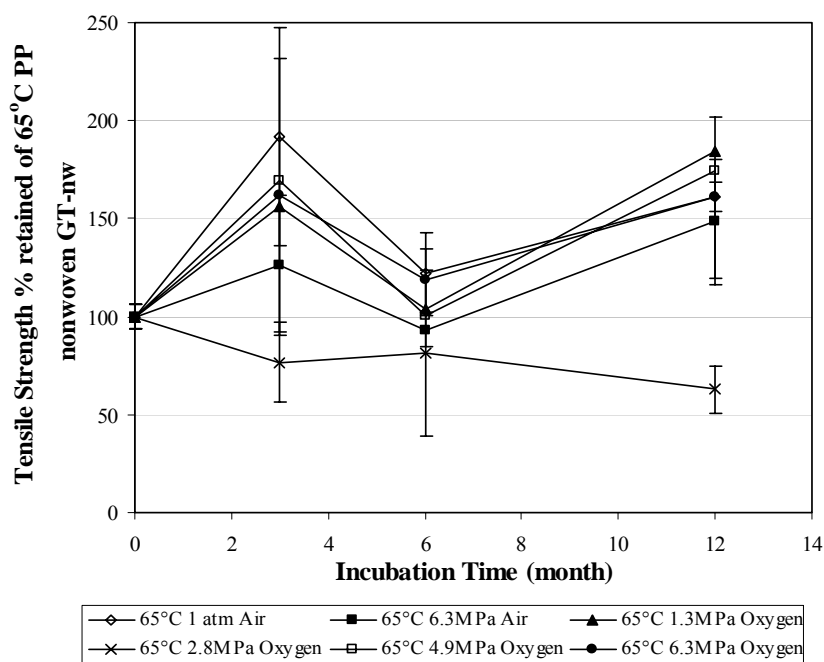


Figure 5.4 GT-nw tensile strength vs. time at 65°C under different pressures

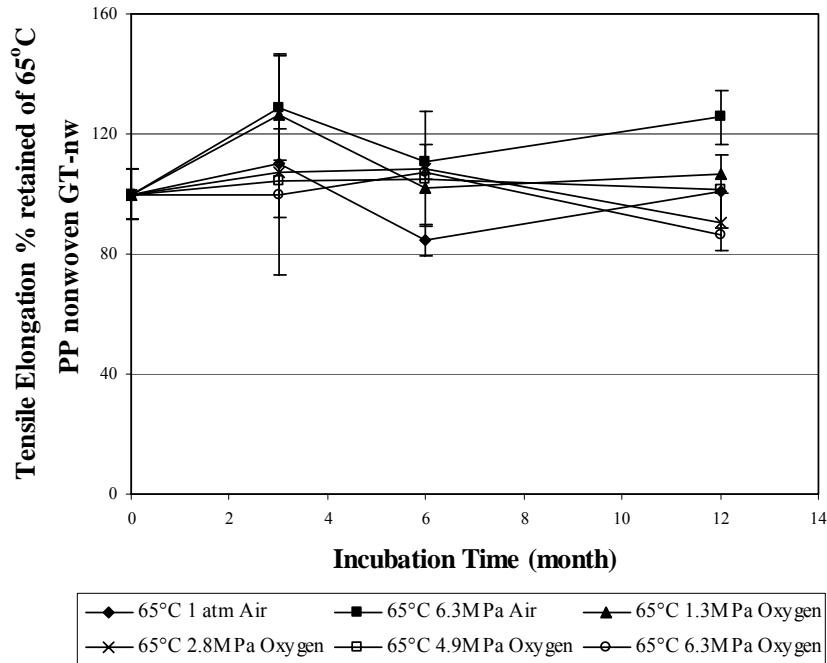


Figure 5.5 GT-nw tensile elongation vs. time at 65°C under various pressures

5.2.3 Discussion – Oxidative Degradation of GT-nw

Although OIT property over aging time shows some temperature-dependent decreasing trend in circulating air conditions, the antioxidant depletion mechanism should be a physical extraction type rather than a chemical reaction type as shown in Eqs (1-1) to (1-3) in Chapter 1. The flowing air extraction of AO is not valid for the field buried condition in which only thermo-oxidation reactions could be a concern. Therefore, it is more appropriate to correlate the degradation data of closed cell temperature/pressure incubation conditions to field conditions so as to evaluate or predict the service performance of this type of geotextile product.

Because the OIT curve shows a progressive drop in 65°C and 6.3 MPa oxygen cell, this condition was continued after one year aging, while all other cells in this temperature were terminated at the duration of 12 month. The samples were taken out and observed at fixed intervals. At the age of 16 months, the samples were tested, and degradation was observed. The complete resulting degradation curves, including all three material tests for this condition, are shown in Figure 5.6.

The OIT curve in Figure 5.6 shows that the HP-OIT value continues to decrease to a very low level at 16 month age and by that time, all other material properties are basically gone. Tensile strength and elongation were almost zero. In this condition, polymer chain degradation occurred abruptly once OIT reached below a certain level.

In the pressure cell samples' OIT curves shown in the earlier sections of this chapter, most pressure data demonstrated no change in material properties in regard to the degradation over the incubation time. The 65°C and 6.3 oxygen pressure is the most severe incubation condition for GT-nw samples, and only in this condition, were material oxidative degradations observed. This fact illustrates that oxygen pressure combined with temperature could create a very strong force in aging polypropylene nonwoven materials. To reach this observed rapid degradation rate, the pressure and temperature should be higher than an initial limitation level, below which the degradation could be hardly detected or would be very slow.

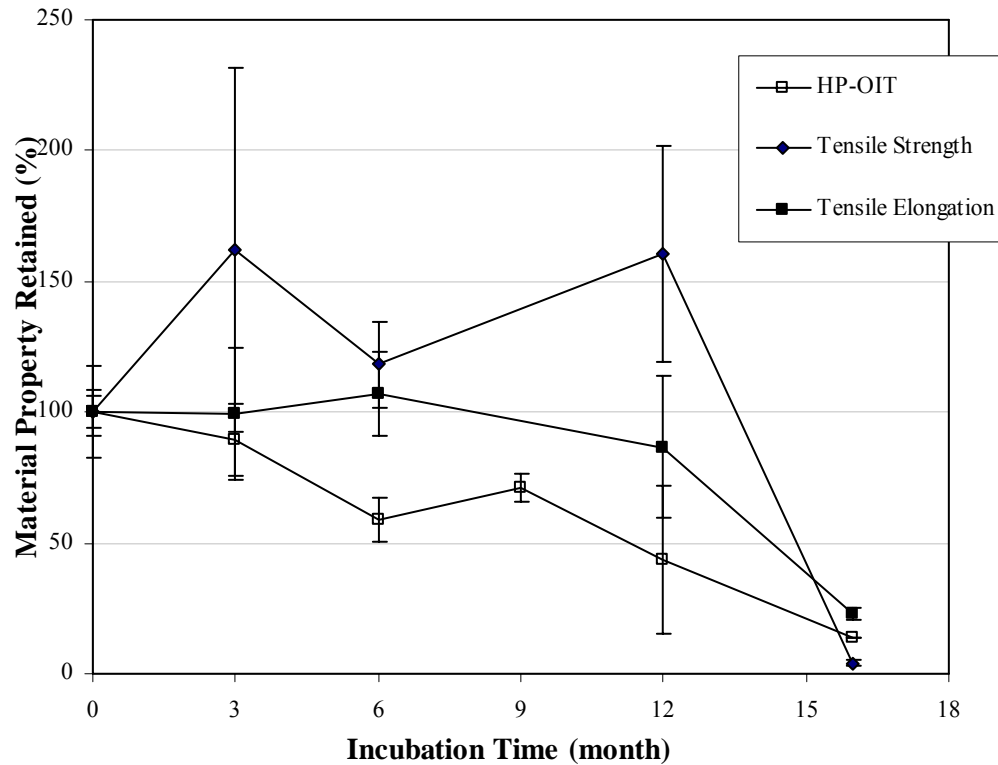


Figure 5.6 Changes in GT-nw properties over time at 65°C under 6.3 MPa oxygen pressure

The reason for the initial limitation of degradation condition remains unknown but could be due in part to the antioxidant package and polymer type used to manufacture this nonwoven product. The observation in this sample may not be representative for all nonwoven polypropylene geotextiles.

5.3 Antioxidant Depletion in Elevated Temperature and Water Environment (Series IV)

OIT curves for water-immersed GT-nw samples at three different water bath temperatures are shown in Figure 5.7. Temperature effects are not very noticeable on GT-nw AO depletion behaviours, as observed in Figure 5.2 under both oven and pressure conditions, especially for temperatures higher or equal to 55°C. This is also the fact for water immersion data of this material. Figure 5.7 shows that the 55°C water-immersed samples even have lower retained OIT values than the 65°C samples, although both of them have a much higher OIT decreasing rate than the lower temperature data at 45°C.

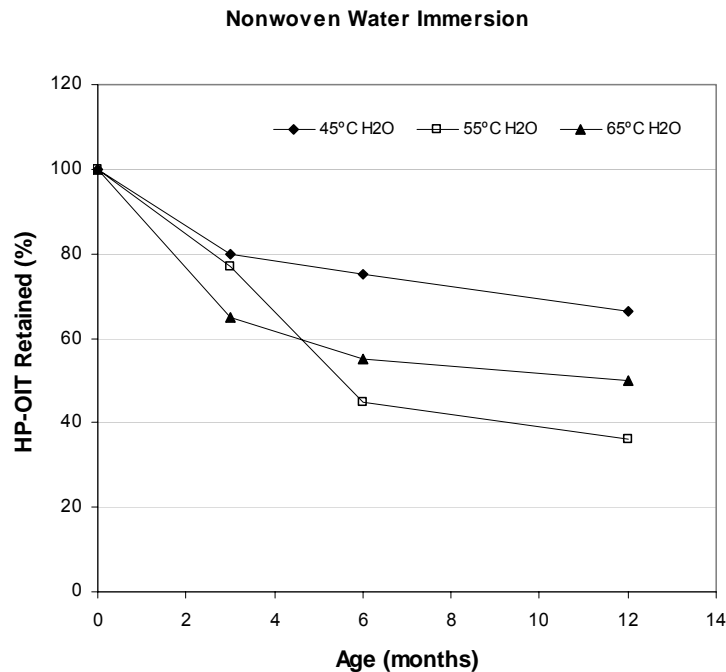


Figure 5.7 Changes in HP-OIT of GT-nw in Water environments at different temperatures

At all three temperatures the OIT values keep decreasing steadily with the aging time. Therefore, we can separate the OIT behaviours of GT-nw at the three temperatures. At each temperature, the OIT data of three aging conditions were compared in order to see the differences of three incubation environments acting on AO depletion from the GT-nw samples.

As shown in Figure 5.8, Figure 5.9 and Figure 5.10, the forced air oven has the strongest effect in extracting antioxidants out of the GT-nw samples. At each temperature, oven curves always have the fastest AO depletion rate. The water immersion environment has less manifest effect but it is much more effective than the pressure cell incubation, which has very slow AO depletion trend at each temperature. If the aforementioned large standard deviations (up to 20%) of this material in OIT tests are taken into account, the pressure data basically shows little change over the aging duration.

Again, the water extraction of antioxidant is supposed to be a physical process similar to the flowing air, but not as effectual. At a relatively low temperature, this physical process is accelerated when the temperature is raised. However, once a limiting rate has been reached, the water extraction rate of AO tends to be stable and even reversed when the water temperature continues to be increased.

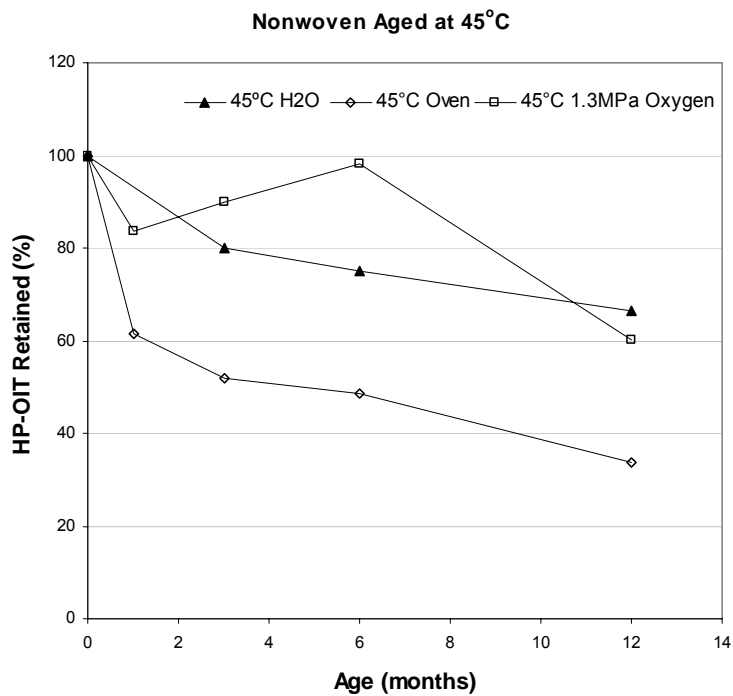


Figure 5.8 Changes in GT-nw HP-OIT at 45°C with different aging conditions

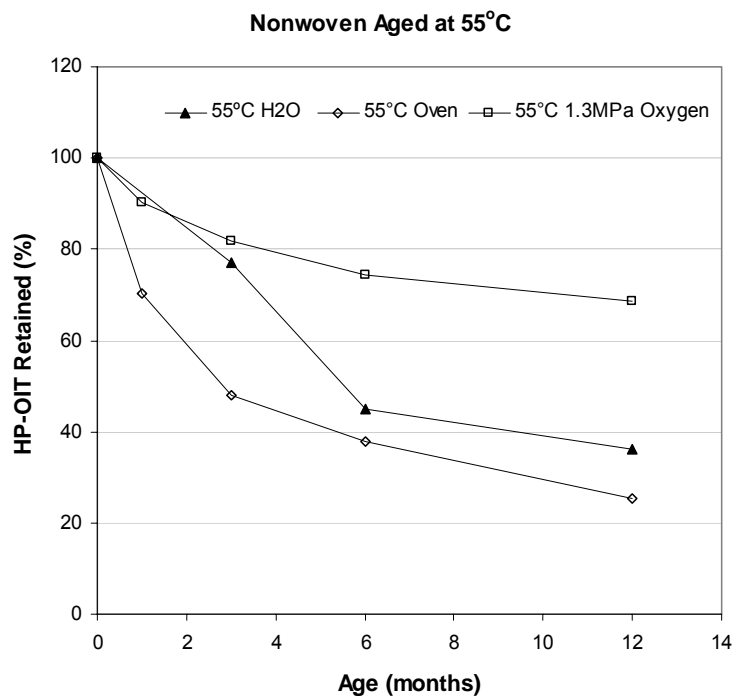


Figure 5.9 Changes in GT-nw HP-OIT at 55°C with different aging conditions

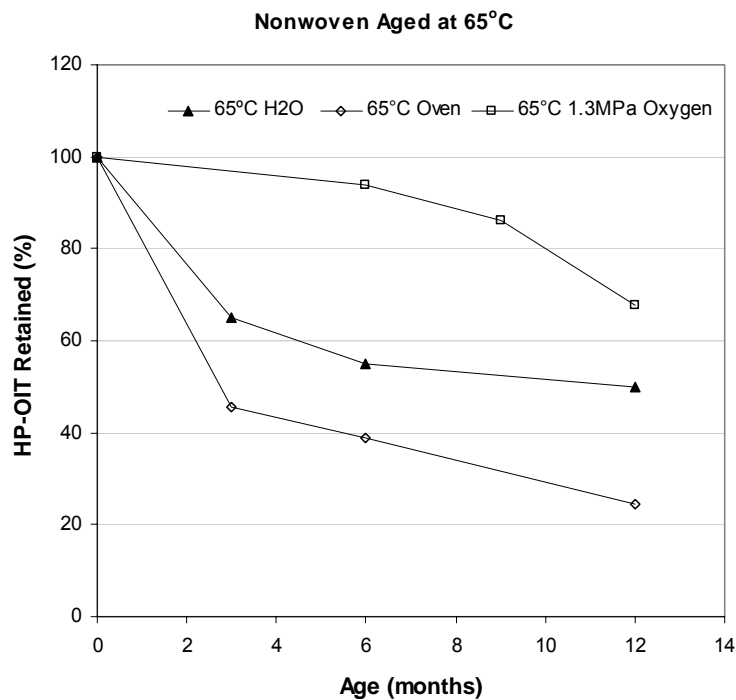


Figure 5.10 Changes in GT-nw HP-OIT at 65°C with different aging conditions

5.4 Conclusions

Given the above analysis and discussion of the material test results, the following conclusions could be reached regarding temperature and/or pressure effects on degradation:

1. Due to the small amount and poor distribution of antioxidants within the finished GT-nw product, the depletion of the antioxidants, as monitored by HP-OIT, shows very large variability for different samples under the same aging condition.

2. 1 atm circulating air has a significant effect in accelerating the antioxidant depletion of GT-nw. Water immersion is also effective in this regard but not as strong as flowing air. Both mechanisms are believed to represent the physical extraction of flowing air or simulate a water environment; this process is temperature dependent when temperatures are below a certain level, above which temperature effects are not as evident.
3. There is no evidence that pressure and temperature can accelerate the antioxidant depletion for the closed cell incubated sample except under the most intense condition, i.e. 65°C and 6.3 MPa. Therefore, it could be assumed that the pressure plus temperature condition should be higher than an initial limitation level, below which the degradation could be very slow.
4. No Arrhenius Log relationship between AO depletion and temperature were observed over the aging time for all three incubation conditions applied to this nonwoven geotextile product GT-nw: Traditional Forced Air Oven, High Pressure Cell and Water Bath.
5. The test data indicate that the antioxidants ceased to function when the HP-OIT retained value reached a certain low percentage of the original value at which point the tensile strength started to decrease very quickly, both signaling abrupt oxidation degradations.

Chapter 6. Service Lifetime Prediction of Polypropylene Slit Film Geotextiles Utilizing an Accelerated Aging Test Based on Temperature and Pressure

6.1 Introduction

As shown in Figure 1.1, the complete oxidative degradation progression of polyolefins normally comprises three stages:

Stage A: antioxidant depletion period, no property changes take place

Stage B: the induction time of oxidation with slow property changes

Stage C: oxidative degradation period with significant property changes

The discussions in this chapter will be focused on Stage C degradation analysis, which is the continuation and extension of the former studies of antioxidant depletion behaviors (Stage A/B degradation) of polyolefin geosynthetic materials. Considering the limited incubation time and cell space, only PP slit film geotextile, GT-sf, samples were used in this study.

In the preceding chapters of this thesis, the antioxidant depletion behavior of GT-sf was analyzed and a Modified Arrhenius Model was developed to correlate the antioxidant depletion rate with the surrounding pressure and temperature conditions.

However, in order to predict the AO lifetime with this method, it was necessary to pre-determine the critical OIT percentage, i.e. the critical antioxidant level at which the AO package would stop functioning, the polymer would start to be

oxidized and material property would start to reduce consequently. It has been proven that predicted AO lifetimes are very sensitive to the critical OIT%. In Chapter 3, critical OIT percentage was estimated to be 15% of the original OIT value, which is based on limited degradation data in aging conditions of 65°C with 2.8 MPa, 4.9 MPa and 6.3 MPa oxygen pressures. Only under these conditions were Stage C polymer degradation onsets and tensile property reductions observed for the GT-sf samples after a certain time of incubation.

To precisely determine the critical OIT%, more enhanced incubation conditions were utilized to allow the GT-sf specimens to reach Stage C oxidation. Accordingly, the stage C degradation curves that correspond to changes of tensile properties in GT-sf, at each of these conditions could be established, and the onset points of the oxidation degradation could then be determined, i.e. the down turn point of the curve for property percentage retained as shown in Figure 6.1. The detailed experimental plan of enhanced temperature plus pressure conditions are introduced in next section of this chapter.

With the established stage C curves at these different pressure and temperature levels, it is intended to predict the performance of the GT-sf at service. For this reason, in this chapter, a new Time-Temperature-Superposition (TTS) plus Time-Pressure-Superposition (TPS) method is introduced to generate a degradation master curve at the geotextile service condition (10°C, 1 atm). Thus, with this

technique, it will be possible to calculate the total time for the material to reach 50% property reduction, i.e. the service lifetime, or half-life of the materials.

As a widely accepted concept in the polymer degradation research area, oxidation of polyolefins is normally an auto-accelerating process, i.e. the oxidation rate is slow and even negligible at first but gradually accelerates, often at a constant value. The auto-accelerating induction time (equivalent to Stage B in Figure 1.1) could be well extended by the antioxidants and stabilizers (equivalent to Stage A in Figure 1.1). In our discussion, the constant-rate of oxidation actually takes place in Stage C.

In efforts to simplify the calculation of the total service lifetime of the material, some assumptions and definitions need to be made in advance:

- In State A, it is assumed that no polymer oxidation reaction occurs and tensile properties remain at 100% level while antioxidant depletion takes place following a first-order reaction rate law, so OIT% retained is an exponential function of the aging time. See Figure 6.1.
- In Stage C, antioxidants stop functioning completely and degradation becomes a pure oxidation process at a constant reaction rate, which is essentially a zero-order chemical reaction within the polymer structure;

thus, tensile property percentage retained is a linear function of the aging time.

- Stage B is a transition stage which is relatively short and hardly detectable in the case of polypropylene oxidation. We can neglect stage B by defining the onset of stage C as the intersection point of the horizontal line at 100% property level and the extended stage C straight line. Thus, the total service lifetime of the PP GT-sf can be expressed in Eq. 6-1.

Total Service lifetime =

Stage A/B time for zero property change (t_{AO}) + Stage C half-life ($t_{C-50\%}$)

(6-1)

t_{AO} and $t_{C-50\%}$ are defined in the Figure 6.1 below, and critical OIT% is defined as the percentage retained value corresponding to the onset of Stage C. It should be noted that the Stage A/B time is denoted by t_{AO} here, which is actually equivalent to the AO lifetime in the Chapter 3.

The slope of Stage C degradation straight line is defined as oxidation rate R_C (unit: %/day, i.e. the property percentage loss per day):

$$R_C = \frac{50\%}{t_{C-50\%}} \quad (6-2)$$

Figure 6.1 shows that material property doesn't change until critical OIT% value has been reached, which means the AO amount remaining within the polymer are above the critical level. After that the tensile property of material decreases linearly with the aging time. Invariably in each of incubation conditions of GT-sf in this study, degradation data points fit well in the Simplified Model although we need to take the large standard deviations into consideration. Tensile strength and elongation of GT-sf specimens exhibited similar trend curves in most incubation conditions. However tensile strength has a relatively smaller standard deviation statistically; thus, it is more appropriately to be used for the data analysis.

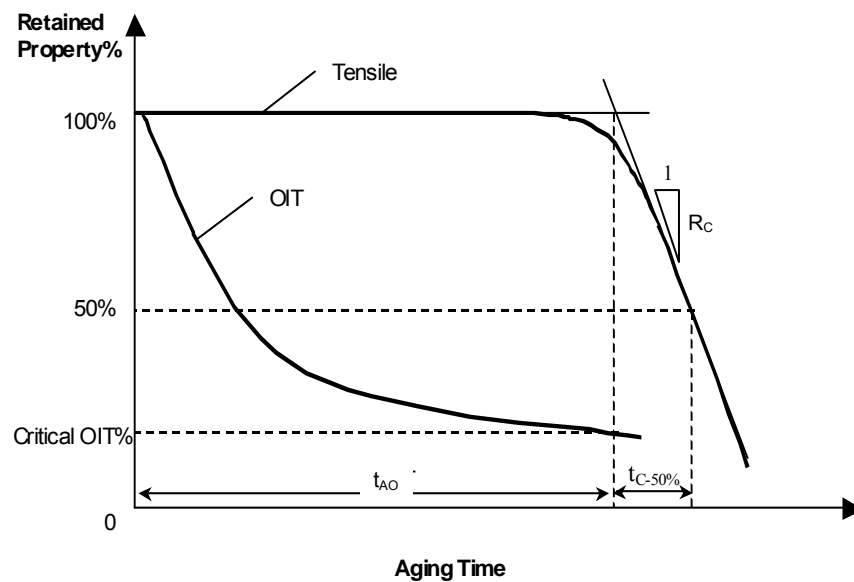


Figure 6.1 Typical oxidative degradation curves of PP yarn geotextiles

6.2 Experimental – Enhanced Elevated Temperatures & High Pressures (Series I)

With the same high pressure cell device setup and sampling procedures as described in the preceding chapters, a total of 14 enhanced pressure/temperature incubation conditions were applied in this study, as listed in Table 6.1. The cells were pressurized by pure oxygen, so the partial oxygen pressures [P_{O_2}] were equal to the cell pressures. The incubation temperatures were elevated to 85°C and 105°C so that the degradation of the GT-sf samples could be achieved in relatively short durations. The incubation in a 65°C oven and 1.3 MPa oxygen cell was continued up to approximately two years so as to reach degradation Stage C. Aging tests in 45°C and 55°C with very high oxygen pressure at a level of 6.3MPa were also included to evaluate the temperature effects on the degradation reaction rate.

Table 6.1 Incubation Conditions

[P_{O_2}] (MPa)	T (°C)				
	45	55	65	85	105
1.3	N/A	N/A	√	√	√
2.8	N/A	N/A	√	√	√
4.9	N/A	N/A	√	√	√
6.3	√	√	√	√	√

√ -- already done; N/A – this condition is not available

In order to obtain sufficient tensile strength data to confidently establish Stage C straight lines, the OIT values were monitored until a value close to 25% were observed, and then the sampling interval was decreased for tensile test. In the most

intense condition of 105°C and 6.3 MPa oxygen, this sampling interval was shortened to a few hours because of the rapid oxidation rate, while in 65°C and 1.3 MPa oxygen, the sampling interval was one or two months.

6.3 Results and Data Analysis

6.3.1 Establishing of Stage C Straight Lines and Calculation of Relevant Parameters

The degradation curves (tensile strength vs. time) for samples incubated in 1.3 MPa oxygen at three different temperatures are shown in Figure 6.2. Note the time scales are in logarithm for the comparison of the three conditions. For each temperature, to separate Stage C from Stage A/B, Stage C data points could be defined as the ones with an evident decrease in tensile strength. More specifically, for each Stage C data point, its tensile strength percentage retained value with the whole error bar range (Strength% \pm Standard Deviation) should be lower than 100% level. On the other hand, points in Stage A/B are the ones around 100% strength, which means their strength decreases are within the error bar range and are negligible.

For further data analysis only points falling into Stage C will be needed to establish the Stage C straight lines. Thus, Figure 6.2 can be replotted as only Stage C lines with linear equations in Figure 6.3.

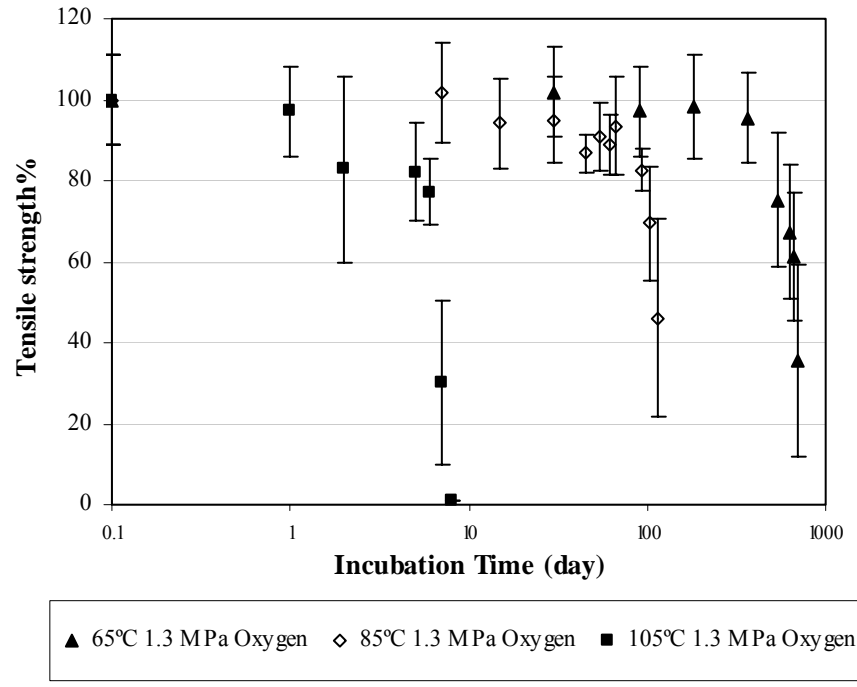


Figure 6.2 Tensile property changes with the incubation time in 1.3MPa incubation

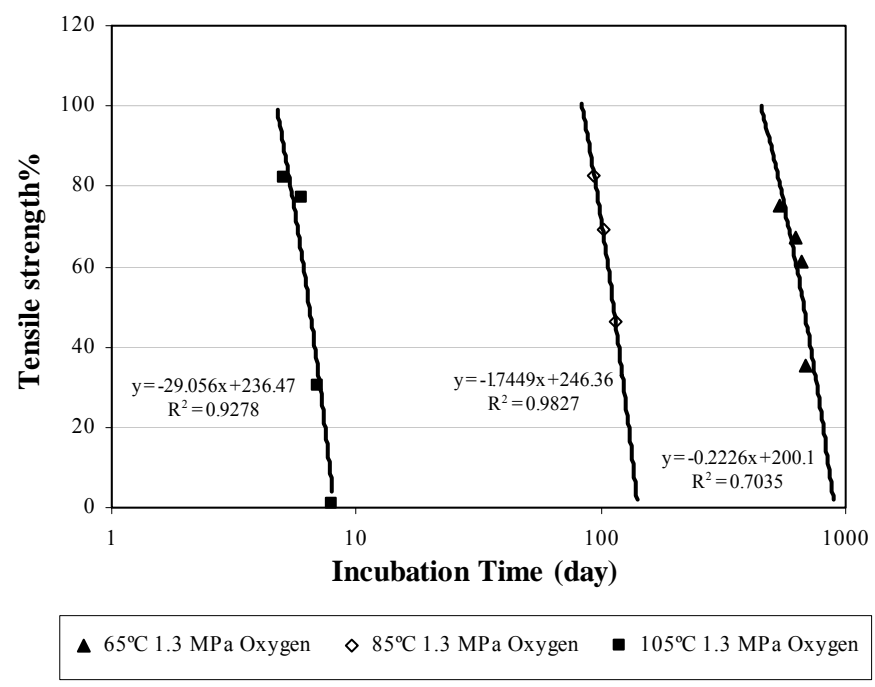


Figure 6.3 Stage C degradation straight lines in 1.3MPa incubation

It should be noted that the Stage C lines seem to parallel each other in the logarithm coordinate scale, but this is not the case in the linear coordinate scale. The reaction rates (R_c) for tensile strength degradation in 1.3 MPa oxygen are the slopes of the three Stage C straight lines, and they are 0.22%/day, 1.75%/day, and 29.06%/day for incubation temperatures of 65°C, 85°C, and 105°C, respectively.

Subsequently, we can directly calculate $t_{C-50\%}$ and t_{AO} using Stage C straight line equations. Critical OIT% can also be obtained with the calculated t_{AO} value and the OIT exponential curves that are modeled by the first-order reaction rate law. Take the condition of 105°C and 1.3 MPa as an example, as shown in Figure 6.4.

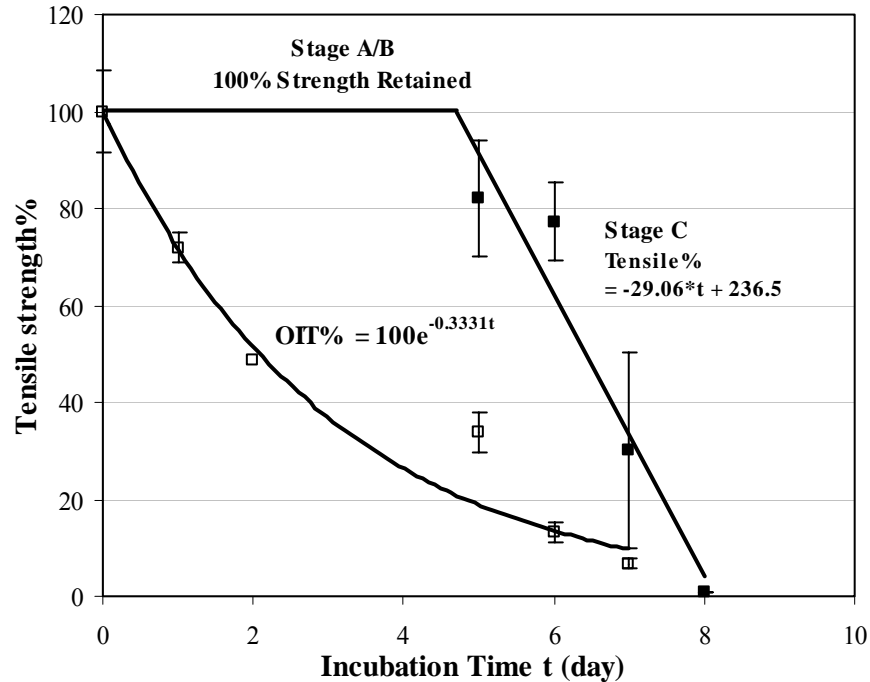


Figure 6.4 GT-sf degradation curves in 105°C, 1.3MPa oxygen incubation

Using the definitions of parameters in Fig 6.1 in the Introduction section of this chapter, for 105°C, 1.3MPa oxygen in Figure 6.4, the Stage C oxidation rate R_C can be found as the slope value of the Stage C straight line,

$$R_C = 29.06 \text{ \%/day}$$

With Equation (6-2), Stage C Half-life, $t_{C-50\%}$, can be easily obtained

$$t_{C-50\%} = 50\% / R_C = 50 / 29.06 = 1.7 \text{ days}$$

It takes 1.7 days to reach 50% retained property after the polymer oxidative degradation starts. The Stage A/B time for zero property change, t_{AO} , can be obtained by locating the starting point of the Stage C straight line, at which the tensile strength level is still 100% and just about to drop. So, at this point:

$$\text{Strength \%retained} = -29.06 \cdot t_{AO} + 236.47 = 100 \text{ (\%)}$$

$$t_{AO} = (236.47 - 100) / 29.06 = 4.7 \text{ days}$$

With the OIT curve, at this time point where $t = t_{AO} = 4.7$ days, we have

$$\text{Critical OIT \%} = 100\% \cdot e^{-0.3331 \cdot t_{AO}} = 20.8\%$$

For all 14 conditions in Table 6.1, the tensile strength degradation curve and OIT trend curve were established. With the same procedures as presented above, the parameters previously discussed could be calculated for each condition, as listed in Table 6.2, Table 6.3, Table 6.4 and Table 6.5.

Table 6.2 Stage C Oxidation Rate R_C (%/day)

[P_{O_2}] (MPa)	T (°C)				
	45	55	65	85	105
1.3	N/A	N/A	0.22	1.74	29.06
2.8	N/A	N/A	0.28	2.88	35.43
4.9	N/A	N/A	0.96	5.41	95.74
6.3	0.46	1.02	1.47	9.88	154.00

Table 6.3 Stage C Half-life $t_{C-50\%}$ (days)

[P_{O_2}] (MPa)	T (°C)				
	45	55	65	85	105
1.3	N/A	N/A	224.6	28.7	1.7
2.8	N/A	N/A	176.1	17.3	1.4
4.9	N/A	N/A	52.1	9.3	0.5
6.3	107.9	49.1	34.0	5.1	0.3

Table 6.4 Stage A/B time for zero property change t_{AO} (days)

[P_{O_2}] (MPa)	T (°C)				
	45	55	65	85	105
1.3	N/A	N/A	358.1	60.9	4.7
2.8	N/A	N/A	141.0	19.6	2.3
4.9	N/A	N/A	117.7	11.8	1.0
6.3	179.2	85.1	37.6	12.0	0.6

Table 6.5 Critical OIT%

[P_{O_2}] (MPa)	T (°C)				
	45	55	65	85	105
1.3	N/A	N/A	24.4%	13.5%	20.8%
2.8	N/A	N/A	15.2%	21.2%	18.8%
4.9	N/A	N/A	17.0%	18.3%	25.1%
6.3	10.7%	16.0%	9.2%	12.2%	17.7%

With the Eq. (6-1) and the demonstration in Figure 6.1, Table 6.3 – Stage C Half-life $t_{C-50\%}$ and Table 6.4 – t_{AO} could be combined to obtain the total lifetime of this material at each incubation conditions. The time fraction of Stage C, $t_{C-50\%}$, varies from 25% to 50% of the total service life. On average, Stage C takes up approximately 40% of total lifetime of GT-sf while the other 60% belongs to t_{AO} or antioxidant depletion processes. Unexpectedly, no clear evidence was found in this study to show that the $t_{C-50\%}$ percentage tends to follow any functional trend pertaining to temperature and oxygen pressure.

Stage C Half-life $t_{C-50\%}$, however, is still an essential part of the material performance and it needs to be evaluated properly. In the next sections, an analytical model will be presented to predict the total service life of GT-sf with the Stage C data obtained from the incubation study of this Chapter. t_{AO} and $t_{C-50\%}$ will be treated as two independent processes and evaluated separately with two models.

6.3.2 Discussion of Enhanced Pressure and Temperature Effects on AO Depletion and Polyolefin Oxidation Reactions

Stage A/B – Antioxidant Depletion Reaction

The Modified Arrhenius Model in Chapter 3 is used to predict t_{AO} duration, i.e. the time for GT-sf to reach the critical OIT value. In Table 6.5, it should be noted that critical OIT% values show very large variations from condition to condition and again, are not in any clear relationship with temperature or pressure. The critical OIT% varies randomly from 9% to 25%. However, the average value of all conditions is around 15%. The same value was used in Chapter 3 to calculate the AO lifetime at the service condition (10°C, 1 atm) with a predicted AO lifetime of 570 months or 48 years.

The Modified Arrhenius Model was developed based on the 35°C, 45°C, 55°C and 65°C oven and pressure data. In this chapter, OIT data at higher temperatures was also obtained. However, as indicated by a number of published research studies, very high temperatures were not recommended to be applied in the oven aging of polyolefin geosynthetics. Reportedly, it was observed that the polypropylene structure was altered and the activation energy, E_a , of the mechanism changed accordingly when temperature exceeded a certain level. This critical level, as reported for oven aging of polyolefins, ranges from 50°C to 85°C and is product-specific.

The phenomenon of activation energy transition was also observed in our elevated temperature and high pressure incubation data. At a certain pressure level, here using 6.3 MPa as an illustration, we can plot in logarithm coordinate the reaction rate constant k against the inverse of absolute temperature for incubation. The reaction rate constant k is the governing parameter for the first-order AO depletion reaction and could be determined with Equation (3-5). An Arrhenius linear relationship was expected for the plot in the studied temperature range. Apparently this was not the case, as revealed in Figure 6.5.

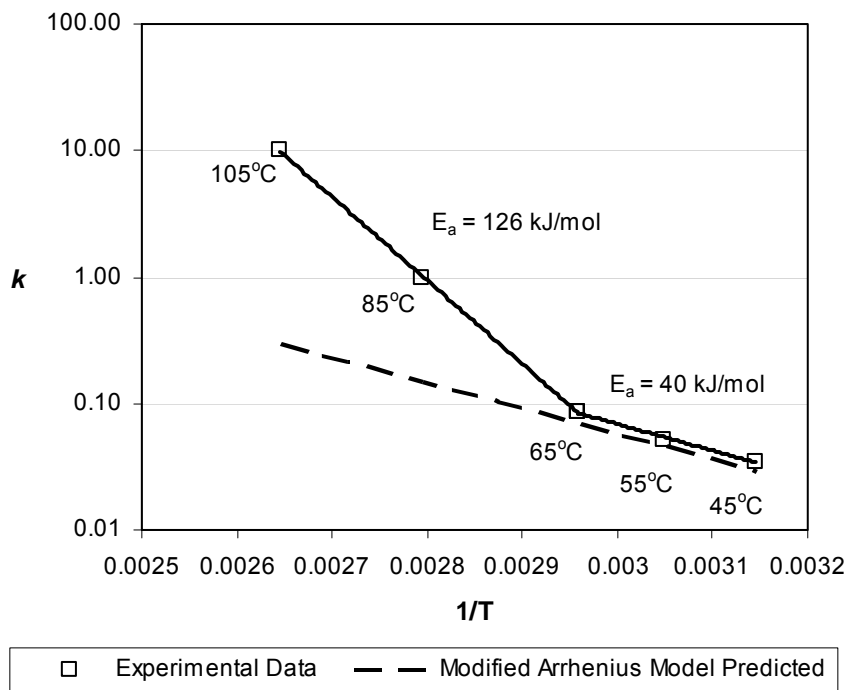


**Figure 6.5 AO Depletion Activation Energy Change
for GT-sf in 6.3MPa oxygen incubation**

A bi-linear model provided a better fit on data points in the $\ln(k)$ versus inversed temperature plot with changes of the slope at 65°C. The activation energy values are obtained for the two segments over two temperature sub-ranges: 40 kJ/mol for 45°C to 65°C segment and 126 kJ/mol for 65°C to 105°C segment. Activation energy was greatly increased by high incubation temperature.

The Modified Arrhenius model in Chapter 3, however, assumes that a linear relationship exists over the whole temperature range down to the service condition, but if we extrapolate this model back to 105°C, the high temperature end, the huge difference in Modeled k and Experimental k is shown in Fig 6.5. Conversely, if the 125 kJ/mol is used to extrapolate the k value to the lower service temperature, it would significantly overestimate the service lifetime of the material.

Figure 3.6 and Figure 3.7 indicate that the activation energy (E_a) for AO depletion in GT-sf at incubation temperatures lower than 65°C also change linearly with the pressure level applied. This linear relationship was used in the development of the Modified Arrhenius Model in Chapter 3. However, in the higher temperature data of this chapter, no functional dependence of E_a on oxygen pressure has been observed. Again, we believe the high temperature may alter the polymer behavior and AO depletion mechanism. The Chapter 3 Model should only be applied to the AO depletion data in temperatures equal to 65°C or lower.

Based on these findings, OIT data of 85°C and 105°C are not included in the t_{AO} or AO lifetime prediction. The relatively low temperature incubation data (\leq

65°C, one year incubation duration) are more appropriate and more reliable for the t_{AO} evaluation. The next section of the discussion will show that, with the proper analytical method, the degradation data for the 85°C and 105°C are very useful in Stage C lifetime prediction.

Stage C – Polymer Oxidative Degradation Reaction

The Stage C, polymer oxidation reaction has been determined to be a zero-order chemical reaction. Therefore, the oxidation rate R_C , is anticipated to have an Arrhenius relationship with temperature. This relationship can be established by plotting Stage C oxidation rate R_C values in Table 6.2 against the inversed temperature ($1/T$) at different oxygen pressures in a semi-log scale, Figure 6.6.

Over the high temperature range 65°C to 105°C, the four Arrhenius lines at four different pressure levels are roughly parallel to each other, which indicate that activation energy doesn't change with oxygen pressure. This behavior of Stage C oxidation is different from that of the AO depletion reaction whose activation energy either increases linearly with oxygen pressure for low temperatures or vary randomly with oxygen pressure for high temperatures.

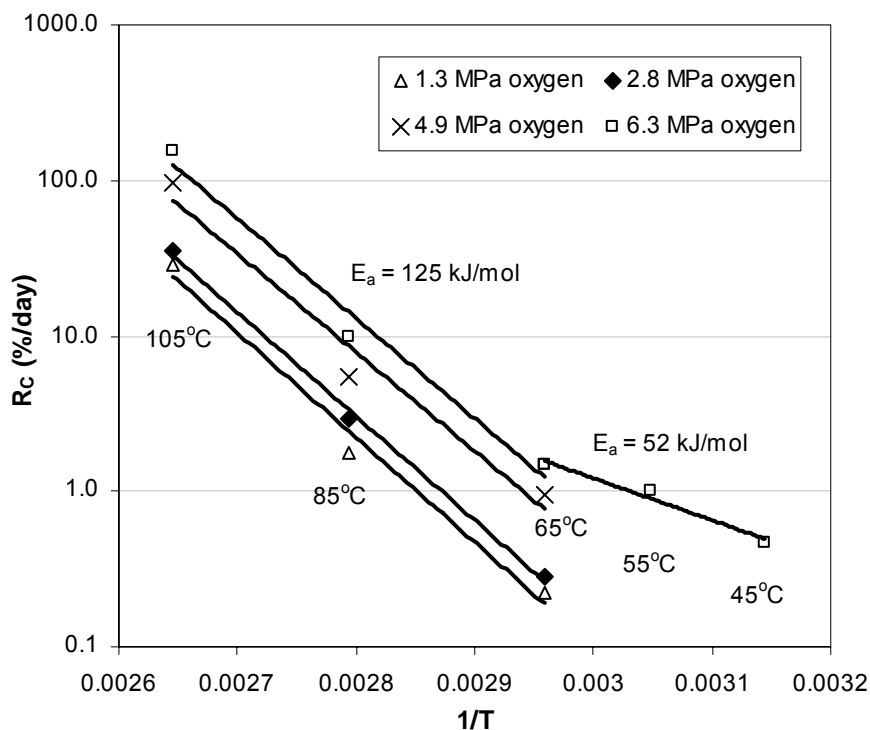


Figure 6.6 Arrhenius Plots for R_C vs. $1/T$ at different oxygen pressures

Under the 6.3MPa pressure condition, Stage C degradation data was obtained at incubation temperatures from 45°C up to 105°C. It was observed that activation energy is sensitive to incubation temperature; there is an apparent curvature in 6.3MPa Arrhenius plot in Figure 6.6. If we use the bi-linear model, the turning point is approximated at 65°C, the same as the earlier AO depletion reaction. Using the Arrhenius equation, two activation energies for oxidation degradation of GT-sf (E_{ox}) can be calculated separately for the two segments of this model:

$$R_C \propto \exp\left(-\frac{E_a}{RT}\right) \quad (6-3)$$

Where, gas constant $R = 8.31$ kJ/mol-K

For the high temperatures range [from 65°C to 105°C]

$$E_{\text{ox1}} \approx 125 \text{ kJ/mol, for all four pressure levels}$$

For the low temperature range [from 45°C to 65°C]

$$E_{\text{ox2}} \approx 52 \text{ kJ/mol, at 6.3 MPa oxygen pressure}$$

The large difference of the activation energy between two different temperature ranges implies that the high temperature incubation data cannot be extrapolated to the low temperature service conditions using the Arrhenius equation. With 65°C as the transition point, different activation energy values should be used due to the fact that this bi-linear model of GT-sf Stage C oxidation could fit well with the experimental degradation data.

In Figure 6.7, the oxidation rate R_C is plotted against oxygen pressure P at different temperature levels in a semi-log scale. The logarithm of R_C is linearly related to oxygen pressure over the pressure range from 1.3 MPa to 6.3 MPa. It is assumed that this relationship will continue to be valid up to service pressure as low as 0.02MPa oxygen, or 1 atm. There is little temperature interference in the pressure effect on the reaction rate. In contrast, there is also little pressure interference in the temperature effect on the reaction rate, as shown in Figure 6.6. Thus, for Stage C oxidative degradation reactions, temperature and pressure are working independently on accelerating polymer oxidation rates such that their effects could be evaluated separately. This phenomenon makes possible to apply Time-temperature

Superposition and Time-pressure Superposition Methods to predict the Stage C of GT-sf.

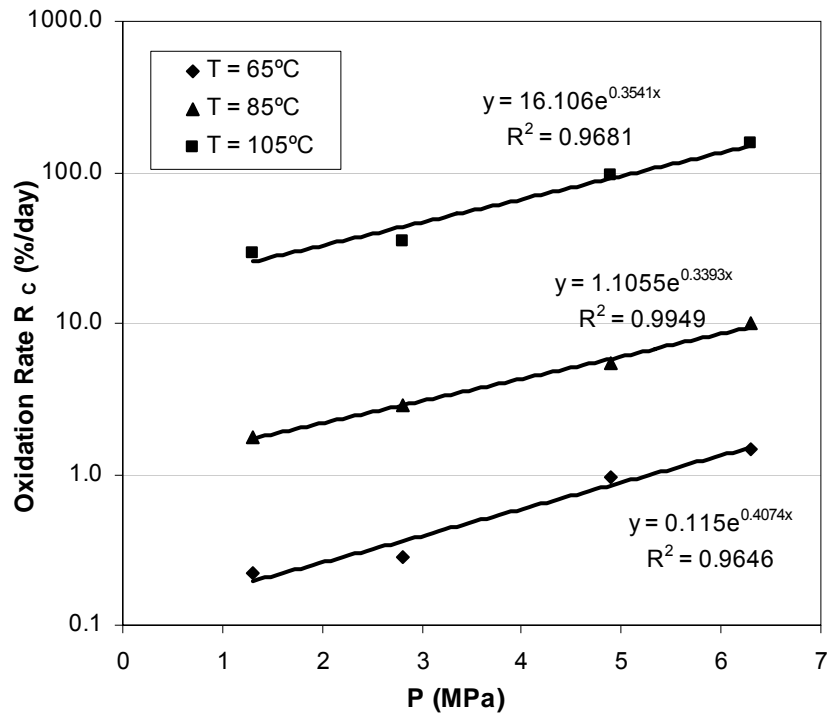


Figure 6.7 R_c vs. Oxygen Pressure at different temperatures

6.3.3 Prediction of GT-sf Stage C Half-life at Service Condition

The theoretical background and relevant studies of time-temperature superposition for polyolefin materials' thermal aging data were been reviewed in Chapter one, Section 1.2.1. The new methodology presented in this section is based on an expansion of the traditional time-temperature superposition procedures; it can

extrapolate data obtained from the high pressure-thermal accelerated degradation to a longer time at much lower temperatures and pressures. This method will be referred to as the TTS-TPS Method in the following analysis and derivations. The temperature shift factor a_T and pressure shift factor a_P shall be used to horizontally shift experimental degradation data along the log-time axis so as to establish a Master Degradation Curve of this material at service condition (10°C, 1 atm).

With the information provided in the earlier discussion, the following TTS-TPS procedure is proposed.

Reconstruction of Stage C degradation curves as a function of Stage C Age t'

The principle of the TTS-TPS method is its reciprocal independence of temperature and pressure effects on accelerating the GT-sf degradation. This, however, is only valid for the Stage C part of the degradation curve shown in Figure 6.1. For Stage A/B or the AO depletion stage, the Modified Arrhenius Model takes into account interactive temperature-pressure effects on AO depletion and yields a more reasonable AO lifetime prediction. Thus, from each degradation curve at all fourteen incubation conditions, Stage A/B needs to be excluded so that Stage C can be identified and analyzed by the TTS-TPS method. In order to make this possible, we should define Stage C duration (t')

$$t' = t - t_{AO} \quad (6-4)$$

Where, t is total incubation time used in all Figures prior to this section;

t_{AO} is the specific value for each particular incubation condition.

Equation (6-5) shows the generic form of equation for Stage C straight lines subsequent to Stage A/B, e.g. curves shown in Figure 6.3.

$$\text{Tensile strength \% retained} = C - R_C \cdot t \quad (6-5)$$

Where, C is a constant which is different at each incubation condition.

Recall the calculation of t_{AO} , which is the start time point of Stage C with 100% strength retained, i.e.

$$100\% = C - R_C \cdot t_{AO} \quad (6-6)$$

So we have,

$$t_{AO} = (C - 100\%) / R_C \quad (6-7)$$

Combine (6-4) and (6-7), it shows that

$$t = t' + t_{AO} = t' + (C - 100\%) / R_C \quad (6-8)$$

Substitute (6-8) into (6-5), we have Stage C line equation with t' as an age variable,

$$\text{Tensile strength \% retained} = 100\% - R_C \cdot t' \quad (6-9)$$

Next, the stage C curves of Tensile strength %retained are replotted against time t' . Equation (6-9) is utilized to horizontally shift stage C straight lines making

them intersect the y-axis (tensile strength retained) at 100%. It should be noted that the R_C values after this shifting are still same as the ones calculated in Table 6.2.

Using Figure 6.3 (1.3 MPa oxygen at three temperatures) as an example, after this reconstruction, the Stage C straight lines become the typical zero-order reaction linear curves shown in Figure 6.8. It is clear that temperature makes a huge difference in degradation rates. In order to apply the TTS-TPS method for horizontal shift, we replot Figure 6.8 using a semi-log coordinate system as shown in Figure 6.9.

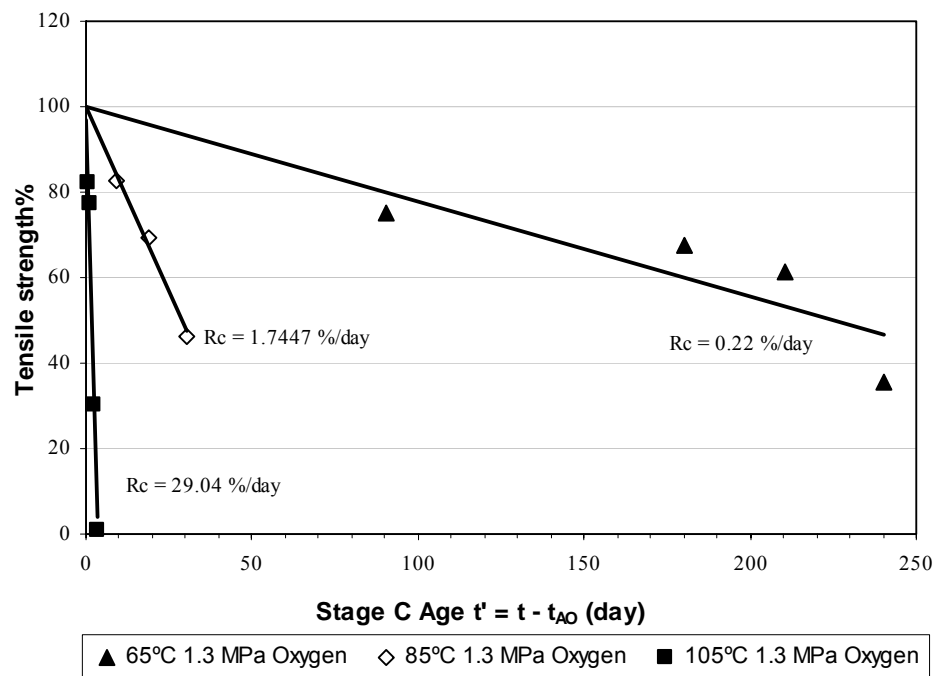


Figure 6.8 Stage C straight lines plotted against Stage C Age $t' = t - t_{A0}$ (Linear Coordinate Scale)

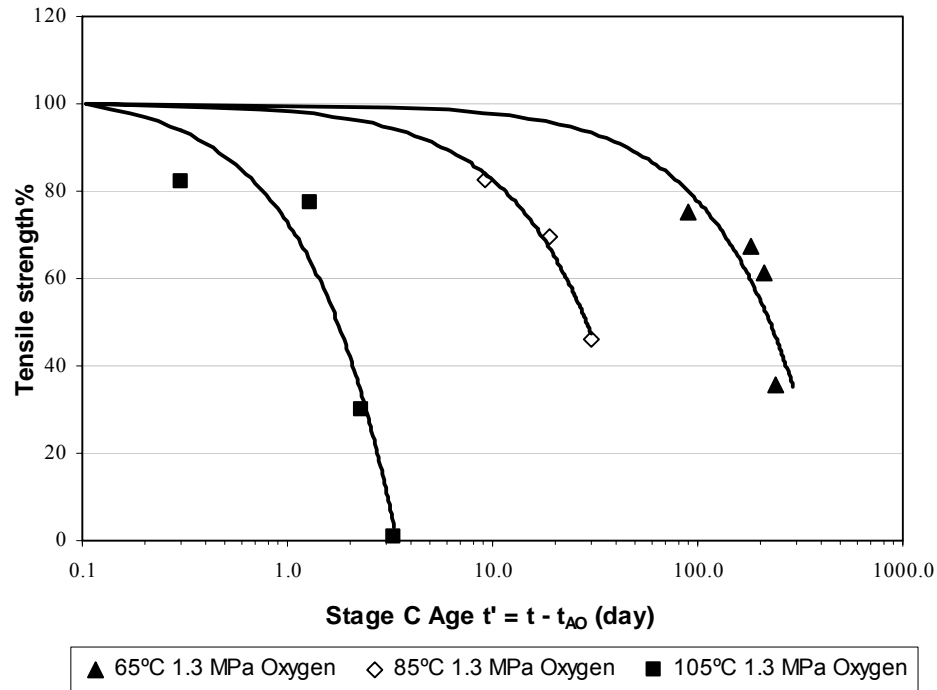


Figure 6.9 Stage C straight lines plotted against Stage C Age $t' = t - t_{A0}$ (Semi-Log Coordinate Scale)

Two-step Time-temperature superposition

The TTS approach is used to shift all degradation data to the reference temperature T_{ref} at which a master degradation curve could be formulated as desired. Over the temperature range [from 65°C to 105°C], a constant thermal acceleration is expected because a constant activation energy value has been obtained over this temperature range as shown in Figure 6.6. According to the chemical reaction rate law, the temperature shift factor should have the same Arrhenius temperature dependence as the reaction rate, i.e.

$$a_T \propto \exp\left(-\frac{E_a}{RT}\right) \quad (6-10)$$

Using the reference temperature $T_{ref} = 65^\circ\text{C} = 338\text{ K}$, data in Fig 6.9 can now be shifted from a higher temperature to 65°C by multiplying the times appropriate to each aging temperature, T (in K), by

$$a_T = \exp\left[\frac{E_a}{R}\left(\frac{1}{T_{ref}} - \frac{1}{T}\right)\right] \quad (6-11)$$

The result is shown as Master Curve I – 65°C and 1.3 MPa oxygen in Figure 6.10, which include all data points for 1.3 MPa incubations. This First-step TTS shifting procedure applied $E_a = 125\text{ kJ/mol}$.

In our next step, the 65°C master curve to the service temperature 10°C or 283 K will be shifted. However, due to the bilinear behavior in the Arrhenius plot shown in Figure 6.6, a different activation energy value ($E_a = 52\text{ kJ/mol}$) was obtained over the temperature range from 45°C to 65°C . Although this E_a value is for 6.3 MPa oxygen data only, it is assumed the value is applicable for all other pressure levels because E_a values are basically the same at all four pressures within the high temperature range [65°C to 105°C].

With the $E_a = 52\text{ kJ/mol}$, the result of the Second-step TTS shifting is shown as Curve II – 10°C and 1.3 MPa oxygen in Figure 6.10. In similar way, the Stage C master curves at 10°C for 2.8 MPa, 4.9 MPa and 6.3 MPa are depicted in Figure 6.11.

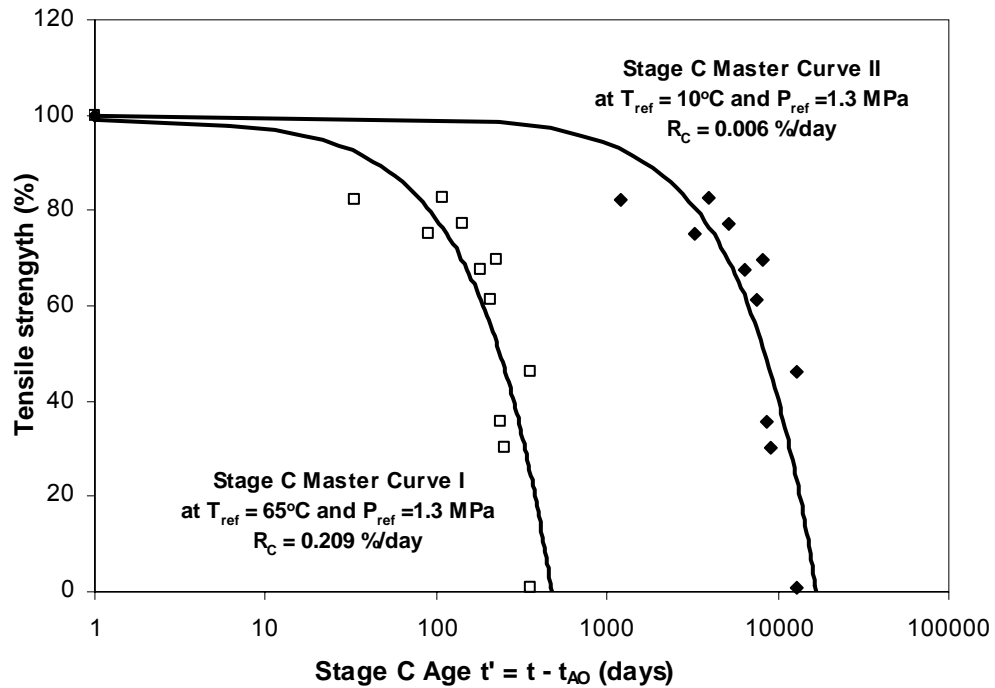


Figure 6.10 Stage C Master Curve Generated by Two-Step TTS Method
(For 1.3 MPa oxygen incubation data)

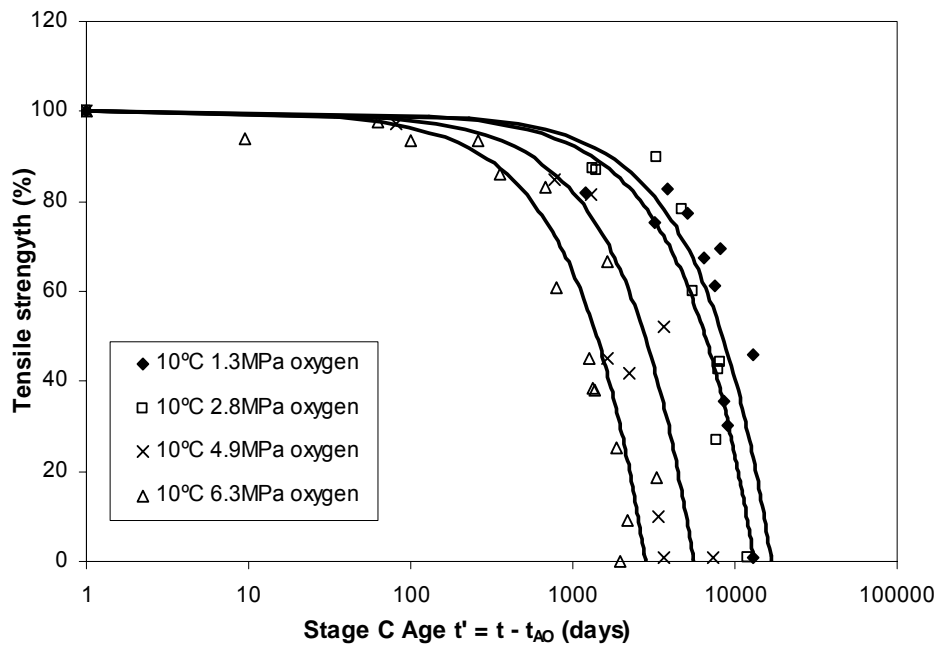


Figure 6.11 Stage C Master Curves at reference temperature 10°C

for various incubation oxygen pressures

Time-pressure superposition

Figure 6.7 indicates that a Stage C oxidation degradation rate, R_C , also has an exponential dependence on the incubation oxygen pressure P . At all three temperatures 65°C, 85°C and 105°C, $\log(R_C)$ exhibited a linear function with P and their slopes are approximately equal. The relationship between the oxidation degradation rate and pressure can be expressed in Eq. 6-12.

$$R_C \propto \exp(\beta \cdot P) \quad (6-12)$$

The β is equal to 0.37 MPa^{-1} , the average slope of the three roughly parallel trendlines in Figure 6.7. It can be assumed that this exponential dependence of reaction rate R_C on oxygen pressure P will continue to be valid with the constant slope for the lower pressures and lower temperatures. Accordingly, we can define the pressure shift factor a_p to unify all high pressure aging data to a reference pressure P_{ref} :

$$a_p \propto \exp(\beta \cdot P) \quad (6-13)$$

$$a_p = \exp(\beta(P - P_{ref})) \quad (6-14)$$

Taking the site oxygen pressure (1 atm, or 0.02 MPa [P_{O_2}]) as the reference pressure, $P_{ref} = 0.02$ MPa, the pressure shift factors for different incubation pressure aging data can be calculated with Equation (6-14) as shown in Table 6.6.

**Table 6.6 Pressure shift factors to $P_{ref} = 0.02$ MPa
for Aging Data at High Incubation Pressures**

Incubation oxygen pressure (MPa)	a_p
1.3	1.68
2.8	3.10
4.9	7.30
6.3	12.91

The Time-Pressure-Superposition, TPS method, can now be used to shift the four 10°C master curves at high pressure conditions to generate the Stage C Master Curve at service conditions. With this procedure, the aging data of all fourteen incubation conditions as listed in Table 6.1 are utilized to determine the degradation rate at service, i.e. $R_C = 0.0032$ %/day.

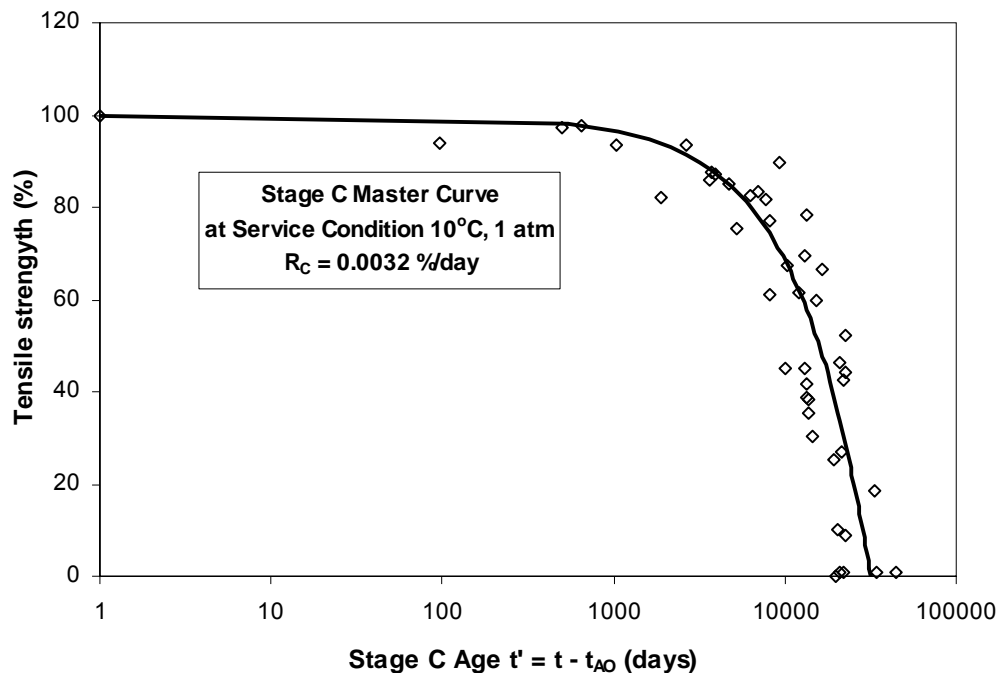


Figure 6.12 Stage C Master Curves at Service Condition

At the 10°C, 1 atm, field condition, with the master curve shown in Figure 6.12, the GT-sf Stage C Half-life

$$t_{C-50\%} = 50\% / R_C = 15625 \text{ days} \approx 43 \text{ years}$$

Recall AO lifetime (or t_{AO}) \approx 48 years, at the same condition (in Chapter 3), and Equation (6-1)

Total Service Lifetime of GT-sf

= Stage A/B time for zero property change (t_{AO}) + Stage C Half-life ($t_{C-50\%}$)

\approx 91 years

6.4 Conclusions

The GT-sf samples were incubated in enhanced high pressure and elevated temperature conditions so as to reach the Stage C oxidation degradation in each incubation condition. The proposed Bilinear – t_{AO} plus $t_{C-50\%}$ Model fits well with all aging data obtained. A TTS-TPS methodology was derived for extrapolating combined pressure-thermal aging data to long-time, experimentally-inaccessible service conditions. To summarize the discussions in this chapter, the following conclusions could be reached:

1. For the tensile strength degradation data in most conditions a clear and separate Stage C segment could be observed. This stage takes place after the antioxidant

stops functioning. Critical OIT% signifying this state show very large variations from condition to condition and are not in any clear relationship with temperature or pressure. The average Critical OIT% of fourteen conditions is still 15%, the same as the estimation in Chapter 3.

2. Oxidation degradation proceeds, following a zero order reaction, as indicated by a linear reduction of tensile strength with incubation time. The time to reach 50% strength retained, Stage C half-life, for each condition has been proven to be an essential part of the material's total life time.
3. Over the wide temperature range from 45°C to 105°C in this study, changes of activation energy were observed in both Stage A/B – Antioxidant Depletion Reaction and Stage C – Polymer Oxidative Degradation Reaction. To account for the abrupt slope change in the Arrhenius plots, a two-step Time-temperature superposition method is proposed for Stage C data.
4. At different temperatures, an exponential relationship could be observed between the Stage C reaction rate and incubation pressure. This observation is the basis of the Time-Pressure Superposition method.
5. The parallel iso-thermal curves and iso-pressure curves of the Stage C reaction rate indicate that temperature and pressure work to accelerate polymer oxidation rates independently so their effects could be evaluated separately by the derived

TTS-TPS method. This method cannot be used for Stage A/B to predict t_{AO} or AO lifetime because OIT data shows a strong interactive between temperature and pressure; the model expressed in Chapter 3 is more appropriate.

It should be noted that the cell pressures used in this part of the study were based on the initial pressure values that were introduced at room temperature as per test procedures described in Chapter 2 – Section 2.3.2. After the pressurized cell being placed into elevated temperature ovens, the cell pressures would be increased. The difference can be estimated theoretically with the Ideal Gas equation $PV = nRT$. At the 85°C and 105°C, cell pressures were actually increased by 15% to 25% from room temperature to oven temperature. The oxygen reaction activity may also increase with the total pressure of closed system. The effects of such pressure increases in the oxidation are uncertain. Therefore, it is recommended to repeat the 85°C and 105°C section of the incubation tests to adjust the pressures at room temperature so as to make the cell pressures in oven exactly at the desired level. Relatively lower pressures will be used in this new test, and test results can be compared with this Chapter to evaluate the pressure induced reaction activity.

Chapter 7. Closing Conclusions and Future Study

7.1 Summary and Conclusions

The focus of this study was to investigate the effects of elevated temperature and/or pressure incubation environments on the oxidative reactions of four types of commercial polyolefin geosynthetic products; two HDPE geogrids, one PP needle-punched nonwoven geotextile, and one PP slit film woven geotextile. A total of four experimental series in which 39 different incubation conditions includes traditional temperature aging, water immersion aging, and a newly designed temperature/pressure aging test utilizing both oven and pressure cells (high/low), were applied for durations ranging from few days to several years.

For the antioxidant (AO) lifetime of GT-sf, a new Modified Arrhenius Model was established to account for both temperature and pressure acceleration effects. The predicted AO lifetime of GT-sf is 48 years at service conditions (1 atm and 10°C). In addition, the Stage C degradation of GT-sf after the complete depletion of AO was assessed using a new TTS-TPS method.. The Stage C half-life, the time in Stage C to reach 50% retained property, was calculated to be 43 years. Thus, the overall lifetime for GT-sf is 91 years. The Modified Arrhenius Model was also applied to determine the lifetime of the AO of GG-1 and was predicted to be 116 years at the service conditions (1 atm and 10°C). This result is close to the value

predicted by the Arrhenius model (172 years). However, the incubation time was significantly reduced, from 7 years (temperature aging) to 2 years (temperature/pressure aging).

The aging tests were also performed on two other geosynthetics, GT-nw and GG-2. For GG-2, the lifetime of AO was evaluated using the temperature aging test and was predicted to be 122 years at the service condition. However the large scattering of OIT data in the GT-nw materials makes the AO lifetime prediction unfeasible to obtain. Nevertheless, the GT-nw OIT data at incubation condition of 65°C/6.3 MPa O₂ showed that the duration of Stage A/B is estimated to be 10 to 12 months. Compared with GT-sf's Stage A/B time of 37.6 days (Table 6.4), the AO lifetime and Stage C life of GT-nw could be expected to be longer than that of GT-sf. The lifetime estimations of the four materials in this research are summarized in Table 7.1.

Table 7.1 Service lifetime estimation of the four materials based on temperature/pressure incubation test data (unit: years)

Materials	Stage A/B	Stage C	Total Lifetime
GT-sf	48	43	91
GT-nw	48+	43+	91+
GG-1	116	43+	159+
GG-2	122	43+	165+

For a comparison purpose, water immersed aging data of each material was included in this study to evaluate water environment accelerating effect on the oxidative degradation of polyolefin. The OIT test data in this series show that AO depletion in water is faster than that in oven aging but slower than that in pressure cell incubation for GG-1 and GT-sf at the same temperatures.

The general conclusions are listed as following:

1. The antioxidant depletion was governed by the partial oxygen pressure in the gas and not by the total gas pressure.
2. For all four tested geosynthetics, data indicated that the antioxidants ceased to function when the retained OIT reached a critical percentage of the original value, at which point the tensile strength started to decrease and the MI started to increase, both signaling the beginning of oxidation degradation. The critical OIT% value is material-specific due to the fact that the specific surface areas, antioxidant dispersions, and geometric dimensions of the four test materials are different.
3. For GG-1 and GT-sf, the high P_{O_2} can significantly accelerate the AO depletion rate. This reaction rate increased with temperature according to the Arrhenius equation, and increased exponentially with P_{O_2} in the range from 0.02 MPa (1

- atm) to 6.3 MPa. AO loss rate in water bath is higher than that in oven aging but lower than that in pressure cell incubation at the same temperatures.
4. Analytical models were developed to express the AO depletion rate of GG-1 and GT-sf in terms of temperatures and oxygen pressures. The model indicates an interactive relationship between these two acceleration factors because the AO activation energy of GT-sf is linearly dependent on the oxygen partial pressure applied in incubation tests.
 5. In order to assess the antioxidant depletion mechanism in a range of low oxygen partial pressures, the aging experiments of oven incubation with oxygen pressure lower than one atmosphere were also performed on the GT-sf samples. In partial oxygen pressures ranging from 0.005 MPa to 0.01 MPa [P_{O_2}], OIT trend curves are very close to those in pure nitrogen incubation, which means that only temperature-induced volatilizations account for the OIT value loss in those conditions. Nevertheless, AO depletion data did show apparent increases when oxygen pressure were elevated from 0.01 MPa to 0.015 MPa and then to 0.1 MPa.
 6. The Stage C oxidation degradation of GT-sf was determined in enhanced high pressure and elevated temperature conditions. No evident material property degradations were observed in Stage A/B until AO level followed a first order reaction law and reached a critical percentage. Afterward, Stage C oxidative

- degradation proceeds following a zero order reaction as indicated by the linear reduction of tensile strength with incubation time.
7. For GT-sf, activation energy is not constant throughout the incubation temperature range from 45 to 105°C. A bi-linear behavior was observed and the change took place at 65°C for both the AO depletion mechanism and oxidation degradation mechanism.
 8. In Stage C, oxidation degradation, the oxidation rate is exponentially related to oxygen partial pressure, indicating that the oxidative degradation of GT-sf under the experimental conditions of this study was governed by a rate controlling mechanism. This phenomenon was different from other published diffusion-controlling data of polyolefin oxidation rate in the P_{O_2} range less than 0.1 MPa (Chapter 1, Section 1.2.3). The diffusion-limited saturation of oxidation reported or assumed in the studies of other researchers (Gillen et al., 1999; Boss and Chien, 1966) was not observed in high pressure range of this study.
 9. In the oxidation degradation stage, Stage C, of GT-sf, the temperature and pressure are independent of each other, thus, their effects could be evaluated separately by the derived TTS-TPS method. With this method, it has been confirmed that the Stage C half life is an essential part of the total service life of GT-sf at site conditions.

7.2 Future Study

Interesting topics for future research could include:

1. Aging tests with low pressure cells (below 1 atm/0.02 MPa P_{O_2}) were only performed at the temperature of 105°C due to the limited experimental time and facilities. In the future, similar pressure incubation tests at different temperatures will be a necessary in order to establish a reliable functional temperature dependence of the AO depletion rate at those low pressure levels. As a result, activation energy could be obtained. Following that, the low pressure data could be incorporated into the analysis and then the effectiveness of Chapter 3 Modified Arrhenius Model could be verified at the low pressures, which is more representative of the service conditions.
2. The Modified Arrhenius Model for AO lifetime prediction is only valid for the oxygen pressure higher than 1 atm (or 0.02 MPa O_2) and temperature higher than 65°C. To estimate the AO lifetime at low pressures (e.g. 0.25 atm, 0.5 atm) with aging data at temperatures equal to or lower than 65°C, the test time will be too long to be reached in lab. To solve this problem, the incubation tests can be performed on the special-produced GT-sf materials which have the specific AO% at manufacture. The materials shall have the pre-determined AO% from 20%, 30% ... up to 100% of normal product AO content. The reaction rate of AO depletion could then be determined based on 10% reduction in OIT value instead of complete depletion, i.e., 100% reduction. This approach can significantly shorten the testing time. Temperature pressure effects on AO depletion at

pressures < 1 atm could be evaluated accordingly with the step-wise OIT% results.

3. The TTS-TPS approach to shifting the high pressure data to service ambient pressure is based on an assumption that the exponential relationship between the Stage C rate and oxygen pressure be valid down to 1 atm. This needs be confirmed with Stage C data from conventional oven aging for the same material.
4. The similar setup of the enhanced temperature and pressure aging tests as those used in Chapter 6 could be performed on the thicker and bulkier polymer products, such as PE geomembranes and geogrids, to explore the service lifetime beyond their effective AO lifetimes. Using the TTS-TPS model, the incubation cycle for this purpose could be reasonably estimated to be around three to four years or less.
5. The enhanced high temperature/pressure incubation conditions (85°C and 105°C) will be repeated with new test procedures. To avoid temperature-induced cell pressure increase and the oxygen reaction activity increase, before the pressurized cell being placed into elevated temperature ovens, the cell pressures can be adjusted at room temperature so as to make the cell pressures in oven exactly at the desired level. The difference can be estimated theoretically with the Ideal Gas equation $PV = nRT$. At the 85°C and 105°C, cell pressures were actually increased by 15% to 25% from room temperature to oven temperature. The results will be incorporated into TTS-TPS analysis again to compare the difference of the predicted lifetimes.

List of References

1. Achimsky, L., and Audouin, L., 1997. "On a transition at 80oC in polypropylene oxidation kinetics" *Polymer Degradation and Stability*, 58, pp. 283-289.
2. Atkins, P. W., 1986. *Physical Chemistry*. Third edition, Oxford University Press, 1986, pgs. 857.
3. Billingham, N. C., and Walker, T. J., 1975. "Autoxidation of poly-4-methylpentene-1. I. The role of diffusion in autoxidation kinetics", *Journal of Polymer Science*, Polymer Chemistry Edition, Vol. 13, No. 5, May, pp. 1209-1222.
4. Billingham, N. C., & Calvert, P. D., 1980. Chapter 5: The physical chemistry of oxidation and stabilization of polyolefins. In *Developments in Polymer Stabilization -- 3*, ed. G. Scott, Applied Science Publishers, London, P.139.
5. Blaine, R. L., Lundgren, C. J., and Harris, M. B., 1997. "Oxidative Induction Time – A Review of DSC Experimental Effects" *Oxidative Behavior of Materials by Thermal Analytical Techniques*. Eds. By Riga, A. T., Potterson, G. H., STP 1326, ASTM
6. Boss, C.R., Chien, C. W., 1966. "Oxygen diffusion limitation in autooxidation of polypropylene." *Journal of Polymer Science: Part A-1*, Vol.4, pp.1543-1551.
7. Bright, Donald G., 1993 "Problems with current methodology in using the Arrhenius equation to predict the long-term behavior of polymeric materials in geotechnical environments" *ASTM Special Technical Publication*, n 1211, pp. 236-247
8. Budrugaec, P. 1995. "Accelerated Thermal Aging of Nitrile-butadiene Rubber under Air Pressure" *Polymer Degradation and Stability*, 47, pp. 129-132.
9. Budrugaec, P. 2001. "The Effect of Oxygen Pressure on the Rate of Non-isothermal-oxidation of Low Density Polyethylene" *Journal of Materials Science*, 36, pp. 2999-3001.
10. Ding, S., et al., 2001. "Activation Energies of Polymer Degradation" In: *Plastics Failure - Analysis and Prevention*, Edited by John Moalli, William Andrew Publishing/Plastics Design Library, pp. 219-225.
11. Elias, V., Salman, A., Juran, I., Pearce, E., and Lu, S. 1999. "Testing Protocols for Oxidation and Hydrolysis of Geosynthetics", FHWA-RD-97-144. pgs.,200.

12. Ezrin, M., Zepke, A., Helwig, John., Lavigne, G. and Dudley, M. 2003. "Plastics Failure Due to Oxidative Degradation in Processing and Service" *Plastics Failure - Analysis and Prevention*, Edited by Moalli, J. William Andrew
13. Ferry, J.D., 1980. *Viscoelastic Properties of Polymers*. 3rd ed., Wiley, New York
14. Gray, R. L., 1990. "Accelerated testing methods for evaluating polyolefin stability" *Conference Proc. of Geosynthetic Testing for Waste Containment Applications*, Jan 23 1990, Las Vegas, NV, USA, *ASTM Special Technical Publication*, n 1081, pp. 57-74
15. Gillen, K.T., and Clough, R.L. 1991. "Accelerated Aging Methods for Predicting Long-Term Mechanical Performance of Polymers", *Irradiation Effects on Polymers*, Eds by Clegg, D.W. and Collyer, A.A., Elsevier Applied Science, London. Chapter 4.
16. Gillen, K.T., and Clough, R.L., 1989. "Time-Temperature-Dose Rate Superposition: A Methodology for Extrapolating Accelerated Radiation Aging Data to Low Dose Rate Conditions" *Polymer Degradation and Stability*, 47, pp. 137-168.
17. Gillen, K.T., Clough, R.L., and Wise, J., 1996. "Prediction of Elastomer Lifetimes from Accelerated Thermal-Aging Experiments" *Polymer Durability*, 1999, ACS, pp.557-575.
18. Gillen, K.T., Wise, J., and Clough, R.L., 1999. "General Solution for the Basic Autoxidation Scheme" *Polymer Degradation and Stability*, 47, pp. 149-132.
19. Grassie, N., and Scott, G., 1985. *Polymer Degradation and Stabilisation*. Cambridge University Press, England, pages.222
20. Gugumus, F., "Effect of temperature on the lifetime of stabilized and unstabilized PP films" *Polymer Degradation and Stability*, v 63, n 1, pp. 41-52
21. Hsuan, Y.G. and Guan, Z. 1998, "Antioxidant Depletion during Thermal Oxidation of High Density Polyethylene Geomembranes." Sixth International Conference on Geosynthetics Proc. Atlanta, Georgia, USA, pp. 375-380.
22. Hsuan, Y.G., Koerner, R.M., 1998. "Antioxidant depletion lifetime in high density polyethylene geomembranes." *Journal of Geotechnical and Geoenvironmental Engineering*, ASCE, Vol.124, No.6, pp.532 - 541.

23. Hsuan, Y. G., and Li, M., 2005. "Temperature and Pressure Effects on the Oxidation of High-Density Polyethylene Geogrids" *Geotextiles and Geomembranes*, Vol. 23, No. 1, pp. 55-75.
24. Horrocks, A.R., ValinejadJohn, K. S., and Crighton, S., 1994. "The influence of fibre production history and stress on the durability of polypropylene." *Polymer Degradation and Stability*, Volume 43, Issue 1, pp.81-91
25. Horrocks, A.R., Mwila, J., and Liu, M., 1997. "The Use of Thermal Analysis to Assess Oxidative Damage in Polyolefins." *Oxidative behavior of materials by thermal analytical techniques*. Eds. By Riga, A. T. and Potterson, G. H., STP 1326, ASTM
26. Koerner, R. M., 1998. *Designing with Geosynthetics*. 4th edition, Prentice Hall, 1998, pgs. 761.
27. Koerner, R. M., Lord, A. E. Jr. and Hsuan, Y. H., 1993, "Arrhenius modeling to predict geosynthetic degradation." *Geotextiles and Geomembranes*, Vol. 11, No. 2, pp. 151-183.
28. Koerner, R. M. and Soong, T.Y. 2001, "Geosynthetic Reinforced Segmental Retaining Walls." *Geotextiles and Geomembranes*, Vol. 19, No. 6, pp. 359-386.
29. Kramer, E. and Koppelman, J. 1986, "Measurement of oxidation stability of polyolefins by thermal analysis." *Polymer Degradation and Stability*, Vol. 16, Issue 3, pp. 261-275.
30. Li, M., and Hsuan, Y. G., 2003. "Pressure Effects on the Oxidation of High Density Polyethylene Geogrids" Proceedings of 56th Canadian Geotechnical Conference, Winnipeg, Manitoba, Canada, September, 2003
31. Li, M., and Hsuan, Y. G., 2004. "Temperature and pressure effects on the degradation of polypropylene tape yarns - Depletion of antioxidants" *Geotextiles and Geomembranes*, Vol. 22, No. 6, pp. 511-530.
32. Ling, M. T. K., Ding, S. Y., Khare, A., and Woo, L., 2001. "Shelf Life Failure Prediction Considerations for Irradiated Polypropylene Medical Devices" In: *Plastics Failure - Analysis and Prevention*, Edited by John Moalli, William Andrew Publishing/Plastics Design Library, pp. 201-208
33. Lord, A.E. Jr., Hsuan, Y.G., and Koerner, R.M., 1993. "Time-temperature superposition in mechanical durability testing of polyethylene geomembranes" *Geotechnical Testing Journal*, v 16, n 2, Jun, 1993, pp. 259-262
34. Montanelli, F., and Rimoldi, P., 1995. "Thermo-Oxidation Resistance of Polyolefin Geogrids" Proceedings of Geosynthetics' 95, pp.1003-1015

35. Morrison, R.T., Boyd, R.N., 1992. Organic Chemistry 6th Edition, Allyn and Bacon, Inc., Boston 1992
36. Muller, W., Buettgenbach, B., Jakob, I., and Mann Heidemarie, 2003. "Comparison of the oxidative resistance of various polyolefin geotextiles." *Geotextiles and Geomembranes*, Volume 21, Issue 5, pp. 289-315
37. Mueller, W., and Jakob, I., 2002. "Oxidative resistance of high-density polyethylene geomembranes" *Polymer Degradation and Stability*, Volume 79, Issue 1, Pages 161-172
38. Pospisil, J., and Billingham, N. C., 2003, "Influence of testing conditions on the performance and durability of polymer stabilisers in thermal oxidation." *Polymer Degradation and Stability*, Volume 82, pp. 145-162
39. Rapoport, N.Y., Livanova, N.M., and Miller, V.B., 1977. "On the influence of internal stress on the kinetics of oxidation of oriented polypropylene." *Vysokomol. Soyed. A18 : 9*, 1976, pp. 2045-2049 (Translated in *Poly. Sci. USSR*, 18, 1977, pp. 2336-2341)
40. Reddy D. V. and Butul. B., 1999. "A Comprehensive Literature Review of Liner Failures and Longevity" A Technical Report to Florida Center for Solid and Hazardous Waste Management, University of Florida
41. Rosa et al, 2000, "A Study of Parameters Interfering in OIT Results Obtained by Differential Scanning Calorimetry in Polyolefin." *Polymer Testing*, 19, pp. 523-531
42. Row, K., and Sangam, H. P., 2002 "Durability of HDPE geomembranes" *Geotextiles and Geomembranes*, 20, pp. 77-95.
43. Salman, A., Elias, V., DiMillio, A., 1998. "The effect of oxygen pressure, temperature and manufacturing process on laboratory degradation of polypropylene geosynthetics." *Sixth International Conference on Geosynthetics Proc.* Atlanta, Georgia, USA, pp. 683- 690.
44. Sangam, H. P., and Row, K., 2002 "Effects of exposure conditions on the depletion of antioxidants from high-density polyethylene (HDPE) geomembranes" *Canadian Geotechnical Journal*, v 39, n 6, pp. 1221-1230
45. Schroeder, H. F., Bahr, H., Herrmann, P., Kneip, G. Lorenz, E. and Schmuecking, I., 2000. "Durability of polyolefin geosynthetics under elevated oxygen pressure in aqueous liquids." *Proc. 2nd European Geosynthetics Conference (EuroGeo 2)*, Italy, pp. 459-464.

46. Tikuisis, T., Lam, P., and Cossar, M., 1992. "High pressure oxidative inductive time analysis by differential scanning calorimetry." MQC/MQA and CQC/CQA of Geosynthetics, edited by Koerner, R.M. and Hsuan, Y.G., 6th GRI Conference, Philadelphia, pp. 191-201.
47. Truttman, R., Schiano, K., and Riesen, R., 1997. "Oxidative Induction Time (OIT) Determination of Polyethylenes: Influences of Temperature, Pressure, and Crucible Materials on the Result" *Oxidative behavior of materials by thermal analytical techniques*. Eds. By Riga, A. T. and Potterson, G. H., STP 1326, ASTM
48. Vink, P., Fontijn, H.F.N., 2000. "Testing the resistance to oxidation of polypropylene geotextiles at enhanced oxygen pressures." *Geotextiles and Geomembranes*, 18, pp. 333-343.
49. Woo, L., Ding, S. Y., Ling, M. T. K., and Westphal, S. P., 1997. "Further Studies on Oxidative Induction Test on Medical Polymers" *Oxidative behavior of materials by thermal analytical techniques*. Eds. By Riga, A. T. and Potterson, G. H., STP 1326, ASTM

Appendix A. List of Symbols

α	Material constant
β	Material constants
ρ	Oxidation rate, oxygen amount absorbed during unit time
a_p	Pressure shift factor
a_T	Temperature shift factor
A	Pre-exponential factor, usually considered as a constant
C	Material constant
C_o	oxygen concentration, i.e. the partial oxygen pressure
DIT	Degradation Induction Time, equivalent to AO lifetime;
E_a	Activation Energy
E_{ao}	Constant equal to the activation energy at 1 atm
GG-1	HDPE Uniaxial geogrid Type 1
GG-2	HDPE Uniaxial geogrid Type 2
GT-nw	Polypropylene Needle-punched nonwoven geotextile
GT-sf	Slit film polypropylene woven geotextile
HDPE	High density polyethylene
HP-OIT	High Pressure OIT
k	Reaction rate constant
MI	Melt Flow Index
OIT	Oxidative Inductive Time
P	Incubation pressure

$[P_{O_2}]$	Oxygen partial pressure
PP	Polypropylene
P_{ref}	Reference pressure
R	ideal gas constant, 8.31 kJ/mol-K
R_C	Stage C Oxidation Rate
R_{AO}	Antioxidant depletion rate
Std-OIT	Standard OIT
t	Total age time
t'	Stage C age time
t_T	aging time at experimental temperature T
$t_{T_{ref}}$	aging time at reference temperature T_{ref} ,
t_{AO}	Stage A/B time for zero property change
$t_{c-50\%}$	Stage C Half-life
T	absolute temperature (K)
T_g	Glass transition temperature
TPS	Time-temperature superposition
T_{ref}	reference temperature (in K)
TTS	Time-pressure superposition

Vita

Mengjia Li

Education

PhD, Civil/Geotechnical Engineering, 2005, Drexel University, Philadelphia, PA

M.S., Geotechnical Engineering, 1999, Tongji University, Shanghai, P.R.China

B.S., Geotechnical Engineering, 1995, Tongji University, Shanghai, P.R.China

Current Research

Experimental research of durability of geosynthetics, i.e. antioxidant depletion mechanisms and degradation mechanisms in polyolefin geosynthetic materials; development of a new laboratory accelerating oven-aging method with elevated oxygen pressure to study the degradation and stabilization of polymeric geosynthetics.

Publications

- [1] Y. Grace Hsuan, Mengjia Li and Robert M. Koerner, (2005) "Stage 'C' Lifetime Prediction of HDPE Geomembrane Using Acceleration Tests with Elevated Temperature and High Pressure" *Proceedings of GRI-18 & ASCE Geo-Frontiers Conference* (2005).
- [2] Mengjia Li and Y. Grace Hsuan, (2005) "Temperature and Pressure Effects on the Antioxidant Depletion of Polypropylene Tape Yarns" *The Journal of Geotextiles and Geomembranes*, Jan, 2005.
- [3] Y. Grace Hsuan and Mengjia Li, (2004) "Temperature and Pressure Effects on the Oxidation of HDPE Geogrids" *The Journal of Geotextiles and Geomembranes*, Nov, 2004.
- [4] Y. Grace Hsuan and Mengjia Li, (2003) "Pressure Effects on the Oxidation of High Density Polyethylene Geogrids" *Proceedings of GRI-17 Conference "Hot topics in Geosynthetics – IV"* GII Publications, Folsom, PA 2003 (*Note:* This paper is the continuation of research work in [5])
- [5] Mengjia Li and Y. Grace Hsuan, (2003) "Pressure Effects on the Oxidation of High Density Polyethylene Geogrids" *Proceedings of 56th Canadian Geotechnical Conference*, Winnipeg, Manitoba, Canada, September, 2003
- [6] Dexing Zhang and Mengjia Li, (2000) "Calculation of Thermal Stress of Concrete Structures on Foundations with Bi-directional Restriction" (in Chinese), *Structural Engineers*, Sep, 2000
- [7] Dexing Zhang and Mengjia Li, (1999) "Calculation of Thermal Stress of Concrete Slabs on Subsoil with Bi-linear Method" (in Chinese), *Structural Engineers*, No.3, Sep, 1999

Organization Membership

American Society of Civil Engineers (ASCE) -- Student member

North American Geosynthetics Society (NAGS) -- Student member